Advances in Experimental Medicine and Biology 1052

Rameshwar Adhikari
Santosh Thapa *Editors*

Infectious Diseases and Nanomedicine III

Second International Conference (ICIDN - 2015), Dec. 15–18, 2015, Kathmandu, Nepal

Springer

Advances in Experimental Medicine and Biology

Volume 1052

More information about this series at http://www.springer.com/series/5584

Rameshwar Adhikari · Santosh Thapa
Editors

Infectious Diseases and Nanomedicine III

Second International Conference (ICIDN - 2015), Dec. 15–18, 2015, Kathmandu, Nepal

Springer

Editors
Rameshwar Adhikari
Research Center for Applied Science and Technology (RECAST)
Tribhuvan University
Kathmandu
Nepal

Santosh Thapa
Department of Microbiology, Immunology and Genetics, Graduate School of Biomedical Sciences
University of North Texas Health Science Center
Fort Worth, TX
USA

ISSN 0065-2598 ISSN 2214-8019 (electronic)
Advances in Experimental Medicine and Biology
ISBN 978-981-10-7571-1 ISBN 978-981-10-7572-8 (eBook)
https://doi.org/10.1007/978-981-10-7572-8

Library of Congress Control Number: 2018935847

Printed on acid-free paper

This Springer imprint is published by the registered company Springer Nature Singapore Pte Ltd.
part of Springer Nature
The registered company address is: 152 Beach Road, #21-01/04 Gateway East, Singapore 189721, Singapore

Preface

The book—*Infectious Diseases and Nanomedicine III*—is a peer-reviewed special issue of the Springer's book series *Advances in Experimental Medicine and Biology*, comprising papers in broader fields of infectious diseases and nanomedicine. A wide variety of topics presented in this book offers readers global perspectives on different disciplines, including virology, bacteriology, clinical microbiology, infectious diseases, antimicrobials and resistance, genomics, nanomaterials, Ayurvedic drugs, and applications of nanotechnology in the management of infectious diseases.

This is a compilation of original researches, review articles, and opinions from the experts who presented their findings at the Second International Conference on Infectious Diseases and Nanomedicine (ICIDN) held during December 15–18, 2015, in Park Village Hotel and Resort, Budhanilkantha, Kathmandu, Nepal. The ICIDN-2015, a triennial conference series, was jointly organized by the Nepalese Forum for Medical Microbiology, Nepal Polymer Institute, and the CAS-TWAS Centre of Excellence for Biotechnology (CoEBio) of the Chinese Academy of Sciences, in association with the Kathmandu University, the Nepal Academy of Science and Technology, with support from the American Society for Microbiology, and the European Society of Clinical Microbiology and Infectious Diseases. The conference was also accompanied by a pre-conference workshop on the current trends of researches in infectious diseases and nanomedicine. Attended by more than 200 participants, including a dozen of eminent scientists, from 20 counties across the globe, ICIDN-2015 had the motto of "*Interdisciplinary Collaborative Education for Research & Innovation in Biomedical Sciences*."

It is expected that this book provides resources for interested readers and those actively working in the related fields of infectious diseases and nanomedicine.

Kathmandu, Nepal — Rameshwar Adhikari
Fort Worth, TX, USA — Santosh Thapa

Acknowledgements

This book in its current format is only possible due to contributions of many esteemed delegates presented at the Second International Conference on Infectious Diseases and Nanomedicine (ICIDN)-2015. We are thankful to all the participants and delegates of ICIDN-2015, including Prof. Geoffrey L. Smith (University of Cambridge, UK), Past President of the International Union of Microbiological Societies; Prof. Ananda Mohan Chakrabarty (University of Illinois, Chicago, USA); Prof. Muhammad G. Morshed (University of British Columbia, Vancouver, Canada); Prof. Robert Bragg (University of the Free State, Bloemfontein, South Africa); Prof. Abdul Haque (The University of Faisalabad, Pakistan); Prof. Buddha Basnyat (Patan Academy of Health Sciences, Kathmandu, Nepal) for their contributions and support. We extend our special thanks to Prof. Jiba Raj Pokhrel (Vice-Chancellor of the Nepal Academy of Science and Technology) for his support and contribution to the conference. Generous support from the American Society for Microbiology, the European Society of Clinical Microbiology and Infectious Diseases, the University Grant Commission (Bhaktapur, Nepal), the Kathmandu University, and the Nepal Academy of Science and Technology has highly been acknowledged. We further extend our sincere thanks to the Nanotechnology Now (USA) and BREC Solutions (UK) for the media partnership and several national and international news agencies and journalists for the coverage of the information and news of the meeting. Special thanks to the members of the national and international advisory boards for their feedback and support and the organizing committee members for their efforts to make the ICIDN-2015 a grand success.

We are thankful to the authors for their contributions, without whom this publication is impossible. We sincerely thank all the reviewers for their constructive feedbacks and timely submission of the reports.

We are grateful to Mr. Aninda Bose and Ms. Kamiya Khatter at the Springer Nature for their continued interest and cordial support in bringing this special issue out to the readers.

Lastly, the cooperation and support from Ms. Sushmita Adhikari, Ms. Pooja Sharma, and our family and friends is highly appreciated.

Rameshwar Adhikari
Santosh Thapa

Reviewers

Bhagirath S. Bhadoria
Department of Physics, Bundelkhand University, Jhansi, UP, India

Sven Henning
Fraunhofer Institute for Microstructure of Materials and Systems, Halle/Saale, Germany

Sajjad Karim
Center of Excellence in Genomic Medicine Research, King Abdulaziz University, Jeddah, Saudi Arabia

Sanjit Kumar
Centre for Bio-separation Technology, VIT University, Vellore, India

Nereide Stela Santos-Magalhães
Keizo-Asami Immunopathology Laboratory, Federal University of Pernambuco, Recife-PE, Brazil

Sher Bahadur Pun
Sukraraj Tropical and Infectious Disease Hospital, Kathmandu, Nepal

Manoj Rajaure
Center for Cancer Research, National Institutes of Health, Bethesda, MD, USA

Shardulendra Prasad Sherchand
Department of Microbiology, Parasitology and Immunology, Louisiana State University Health Sciences Center, New Orleans, LA, USA

Sikandar Khan Sherwani
Department of Microbiology Federal Urdu University of Arts, Science and Technology, Karachi, Pakistan

Jakub Sirc
Institute of Macromolecular Chemistry, Academy of Science of Czech Republic Prague, Czech Republic

Sabu Thomas
Cholera and Biofilm Research Laboratory, Rajiv Gandhi Center for Biotechnology, Thiruvananthapuram, India

Contents

Editors and Contributors

About the Editors

Dr. Rameshwar Adhikari is a Professor of Chemistry and currently serving as Executive Director of the Research Center for Applied Science and Technology (RECAST), Tribhuvan University, Kathmandu, Nepal. He has been an Invited Professor at Rouen University (France), Mahatma Gandhi University (India), and Tokyo Institute of Technology (Japan). He was General Secretary of the Nepal Chemical Society and German Engineers Society. He has been bestowed several awards including the Alexander von Humboldt Foundation's Ambassador Scientist Award, Fellowship of International Union of Pure and Applied Chemistry (IUPAC), and POLYCHAR World Forum International Materials Science Prize. He is the Founder President of the Nepal Polymer Institute and has convened several international congresses, symposia, and workshops. His research areas include biopolymers, nanostructured polymers, block copolymers, polymer microscopy, and bionics. He has authored over 120 research papers in peer-reviewed journals, co-authored four textbooks, and edited four books. He was an Editorial Board Member of the Journal of Applied Polymer Science, Wiley InterScience, from 2011 to 2015 and is currently an expert reviewer for several international journals.

Dr. Santosh Thapa received his M.Sc. (Microbiology) from Tribhuvan University, Kathmandu, Nepal, in 2005 and taught related courses for undergraduate and graduate students at various colleges in Kathmandu, including Tri-Chandra College, and the Central Department of Microbiology. He is a Member of the American Society for Microbiology, European Society of Clinical Microbiology and Infectious Diseases (ESCMID), Society for Applied Microbiology (SfAM) and is associated with the International Union of Microbiological Societies (IUMS). He has received several awards, including the Asian Productivity Organization Travel Award (2011), SfAM Bursary Award (2013), SfAM Public Engagement Workshop Grant Award (2015), Phylogenomics Symposium Travel Award (2016), ESCMID/ECDC (European Center for Disease Prevention and Control) Observership (2016), SfAMPresident Award (2017), the University of North Texas Health Science Center's Graduate Student Association (GSA) Scholarship (2017), GSA Travel Award (2017), GSA Professional Development Award (2017). He has organized several international conferences and workshops and has authored five research papers in peer-reviewed journals and edited two books. Currently, he works at the Graduate School of Biomedical Sciences, University of North Texas Health Science Center, Fort Worth, Texas, USA, where he is pursuing his Ph.D.

Contributors

Rameshwar Adhikari Research Centre for Applied Science and Technology (RECAST), Tribhuvan University, Kathmandu, Kirtipur, Nepal

Hans-Peter Beck Swiss Tropical and Public Health Institute, University of Basel, Basel, Switzerland

Tika Ram Bhandari Research Centre for Applied Science and Technology (RECAST), Tribhuvan University, Kathmandu, Kirtipur, Nepal

R R Bragg Department of Microbial, Biochemical and Food Microbiology, Faculty of Natural and Agricultural Sciences, University of the Free State, Bloemfontein, Republic of South Africa

M Coetzee Department of Microbial, Biochemical and Food Microbiology, Faculty of Natural and Agricultural Sciences, University of the Free State, Bloemfontein, Republic of South Africa

Chayanika Deka Department of Chemistry, Gauhati University, Guwahati, Assam, India

Nirmala Devi Department of Science & Humanities, National Institute of Technology Nagaland, Dimapur, Nagaland, India

Abdul Haque Postgraduate Research Laboratory, Health Sciences Campus, The University of Faisalabad, Faisalabad, Pakistan

Dilip Kumar Kakati Department of Chemistry, Gauhati University, Guwahati, Assam, India

Arti Kapil Department of Microbiology, All India Institute of Medical Sciences, New Delhi, India

Punit Kaur Department of Biophysics, All India Institute of Medical Sciences, New Delhi, India

Umay Kulsum Department of Biophysics, All India Institute of Medical Sciences, New Delhi, India

Bidit Lamsal Research Centre for Applied Science and Technology (RECAST), Tribhuvan University, Kathmandu, Kirtipur, Nepal

J-Y Lee Department of Microbial, Biochemical and Food Microbiology, Faculty of Natural and Agricultural Sciences, University of the Free State, Bloemfontein, Republic of South Africa

Wolfgang Meier Department of Chemistry, University of Basel, Basel, Switzerland

C M Meyburgh Department of Microbial, Biochemical and Food Microbiology, Faculty of Natural and Agricultural Sciences, University of the Free State, Bloemfontein, Republic of South Africa

Adrian Najer Department of Chemistry, University of Basel, Basel, SwitzerlandSwiss Tropical and Public Health Institute, University of Basel, Basel, Switzerland

Prajnya Nath Department of Chemistry, Gauhati University, Guwahati, Assam, India

Cornelia G. Palivan Department of Chemistry, University of Basel, Basel, Switzerland

Prasamsha Panta Research Centre for Applied Science and Technology (RECAST), Tribhuvan University, Kathmandu, Kirtipur, Nepal

Shiba Kumar Rai Nepal Medical College, Kathmandu, NepalNational Institute of Tropical Medicine and Public Health Research, ShiGan International College of Science and Technology, Narayangopal Chok, Kathmandu, Nepal

Harpreet Singh Indian Council of Medical Research, New Delhi, India

Mahi R. Singh Department of Physics and Astronomy, The University of Western Ontario, London, ON, Canada

Geoffrey L. Smith Department of Pathology, University of Cambridge, Cambridge, UK

Vaccinia Virus Protein C6: A Multifunctional Interferon Antagonist

Geoffrey L. Smith

Abstract

Vaccinia virus (VACV) is the prototypic member of the *Orthopoxvirus* genus of the *Poxviridae*. It is also the live vaccine that was used to eradicate smallpox. Like other poxviruses, VACV replicates in the cytoplasm and has a large double-stranded (ds)DNA genome and a complex virion. Approximately, half of the VACV genes are nonessential for virus replication in cell culture but encode a remarkable array of immunomodulators that antagonise the innate immune response to virus infection. This short review concerns one such protein, C6, that is a multifunctional inhibitor of interferon. C6 can both diminish the production of interferon and inhibit interferon-induced signalling and thereby the expression of interferon-stimulated genes.

Keywords

Vaccinia virus · Immune evasion · Interferon IRF3 · JAK–STAT pathway · STAT2 Vaccines

G. L. Smith (✉)
Department of Pathology, University of Cambridge, Tennis Court Road, Cambridge CB2 1QP, UK
e-mail: gls37@cam.ac.uk

Introduction

Vaccinia virus (VAV) is the live vaccine used to eradicate smallpox [1] but its origin and natural host remain unknown [2]. It is the most intensively studied poxvirus and is a member of the orthopoxvirus genus that also includes variola virus (the cause of smallpox), cowpox virus (the vaccine used by Edward Jenner in 1796 to prevent smallpox), monkeypox virus, camelpox virus and ectromelia virus [3]. These viruses are morphologically indistinguishable and antigenically cross-reactive such that infection with any member of the genus provides protection against all other members of this genus. The widespread use of VACV as a live vaccine led to the eradication of smallpox. The last naturally occurring case was in Somalia in 1977 and after a further 2 years of surveillance the World Health Organization certified that eradication was complete. Smallpox and rinderpest remain the only virus diseases to have been eradicated.

VACV strain Copenhagen was the first VACV strain to be sequenced and has a 191-kbp dsDNA genome encoding about 200 genes [4]. Analysis of the arrangement of these genes and their conservation shows that genes in the central 100 kb are highly conserved between different strains of VACV and other orthopoxviruses, but genes toward either terminus are more variable and are mostly nonessential for virus replication [5, 6] (Fig. 1). These latter genes encode proteins

R. Adhikari and S. Thapa (eds.), *Infectious Diseases and Nanomedicine III*,
Advances in Experimental Medicine and Biology 1052, https://doi.org/10.1007/978-981-10-7572-8_1

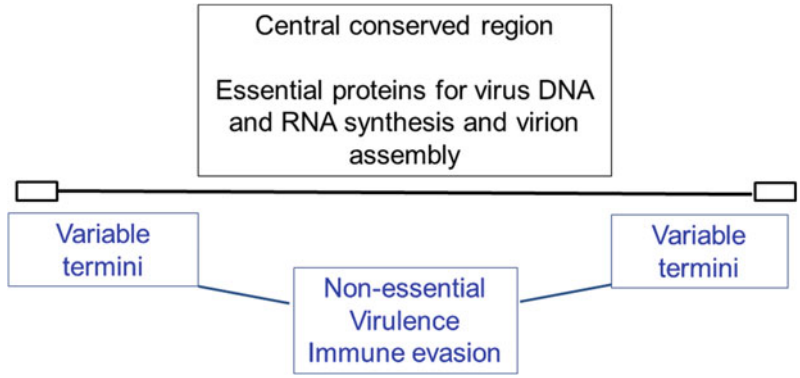

Fig. 1 Diagram illustrating the VACV genome and the functions of genes present in the central conserved region and the terminal variable regions. The linear dsDNA genome of ~190 kbp encoding about 200 genes is shown as a horizontal line. The open boxes at each end represent the inverted terminal repeats in which DNA at one end is also present at the opposite end in inverted orientation Adapted from [10]

that influence the virulence and host range of the virus and many of them function by interfering with the host response to infection. The number and variety of these immunomodulatory proteins is remarkable and a notable feature is that VACV encodes several proteins that target the same cellular pathway, for review see [7]. For instance, there are multiple proteins that inhibit induction of programmed cell death [8], or the activation of the transcription factors interferon regulatory factor (IRF)3, nuclear factor kappa B (NF-κB), or the Janus kinase (JAK)/signal transducer and activator of transcription (STAT) pathway [9]. Despite having multiple proteins that target each of these pathways, the functions of the individual VACV proteins are nonredundant because deletion of any one protein causes a change to the virulence or immunogenicity of the virus in vivo [7]. This short article concerns protein C6 that is a multifunctional inhibitor of interferon (IFN).

Interferons

IFNs are species-specific glycoproteins that induce an antiviral state in cells bearing the appropriate receptors [11, 12]. There are three types of IFN. Type I IFNs include IFNα and IFNβ and several others, and these bind to the type I IFN receptor (IFNR) that is expressed ubiquitously. IFNγ is the only type II IFN, and this binds to a type II IFNγR that also has widespread distribution [13]. Type III IFNs, or IFN lambdas, were discovered more recently, and include IFNλ1-4. These bind to type III IFNλR that is expressed in epithelial tissue. As well as inducing an antiviral state in cells, IFNs contribute to the inflammatory response to infection and IFNγ is particularly important for the development of cell-mediated immunity, such as cytotoxic T cells, that are responsible for recognition and lysis of virus-infected cells.

The induction of IFN expression is illustrated with IFNβ (Fig. 2). Virus infection is sensed by detection of pathogen-associated molecular patterns (PAMPs) by pathogen recognition receptors (PRRs) and this activates signalling pathways that culminate in the activation of transcription factors such as IRF3, NF-κB and AP-1. These transcription factors then migrate to the nucleus and, collectively, form the enhanceosome that activates transcription from the IFNβ promoter [14, 15]. IFNβ mRNA is then translated in the cytoplasm and IFNβ is secreted from the cell. To activate an antiviral response, IFNβ and other type I IFNs bind to the type I IFNR to induce a signalling cascade that culminates in the expression of IFN-stimulated genes (ISGs). It is these ISG products that mediate antiviral activity.

Type I and III IFNs induce phosphorylation of STAT1 and STAT2 that enables the formation of STAT1–STAT2 heterodimers. These then

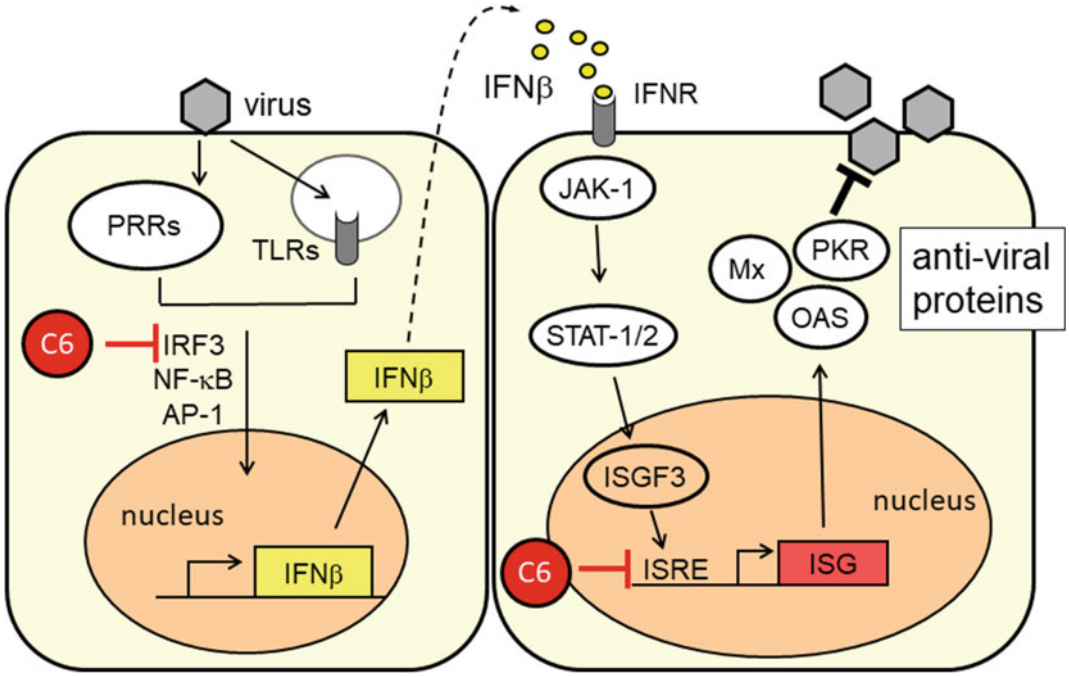

Fig. 2 Diagram showing a simplified scheme for the induction and action of IFNβ. Toll-like receptors (TLRs) or other pattern recognition receptors (PRRs) recognise virus PAMPs and activate the transcription factors NF-κB, IRF3 and AP-1. These translocate into the nucleus and drive transcription from the IFNβ gene. IFNβ is secreted from the cell and binds to the type I IFNR to activate the JAK–STAT pathway and transcription of IFN-stimulated genes (ISGs) bearing the IFN-stimulated response element (ISRE). ISG products such as Mx, protein kinase R (PKR) and 2′5′-oligoadenylate synthetase (OAS) function in the cytoplasm to block virus replication. The positions at which protein C6 (red circles) interferes with these pathways are illustrated

associate with IRF9 to form the ISGF3 complex, which translocates into the nucleus and binds to promoters bearing the IFN-stimulated response element (ISRE). This causes the expression of hundreds of different ISGs. Type II IFN (IFNγ) induces a different signalling pathway that involves the phosphorylation of STAT1, the formation of STAT1 homodimers and their translocation into the nucleus where they bind to promoters bearing the IFNγ-associated sequence (GAS). This also induces the expression of many ISGs, some of which are also induced by type I and III IFNs, but others are only induced by IFNγ. The signalling pathways leading to the induction of IFN expression and the expression of ISGs are summarised in Fig. 2. These pathways provide viruses with the opportunity to intervene at multiple stages to block the production of IFNs, the binding of IFNs to IFNRs, JAK–STAT signalling or the antiviral activity of specific ISGs. For a review of the IFNs and virus countermeasures, see [16] and for details of proteins expressed by VACV that antagonise the IFN system, see [9].

Protein C6

Protein C6 was first identified in a screen of VACV proteins for inhibitors of activation of the IFNβ promoter [17]. Cells transfected with a plasmid containing the IFNβ promoter linked to a luciferase reporter gene were stimulated by transfection with poly I:C or poly dA:dT, or by infection with Sendai virus to induce expression of luciferase. In parallel, cells treated in this way were also transfected with a plasmid expressing protein C6, and this inhibited IFNβ-promoter

activation by all these stimuli. The IFNβ promoter contains binding sites for the transcription factors NF-κB, IRF3 and AP-1 and to test which transcription factors C6 inhibited, reporter plasmids expressing luciferase driven by NF-κB or IRF3 responsive promoters were stimulated in the presence or absence of C6. This showed that C6 was an inhibitor of IRF3, but not NF-κB, activation. Mechanistically, C6 prevented the activation of TANK-binding kinase 1 (TBK1) and IKKε by interacting with the scaffold proteins TANK, SINTBAD and NAP1. Consequently, IRF3 was not phosphorylated or translocated into the nucleus [17] (Fig. 2).

During VACV infection, protein C6 is expressed early, before virus DNA replication, so that it is able to inhibit the induction of IFNβ expression quickly. Immunofluorescence and biochemical fractionation of cells showed that C6 is present in both the cytoplasm and nucleus [17]. Sequence comparisons had showed that C6 shared amino acid similarity with several other small VACV proteins [4, 18]. Subsequently, these were shown to also be expressed early during infection and are now known to be members of a B-cell lymphoma protein 2 (Bcl-2) family [19]. This similarity was recognised only when the three-dimensional structure of members of this virus protein family was determined by X-ray crystallography or nuclear magnetic resonance, because there is little similarity in primary amino acid sequence. The structures of the virus proteins had a close structural relationship with cellular Bcl-2 family proteins, which regulate the induction of programmed cell death (apoptosis). VACV Bcl-2 family members for which structures have been determined include N1 [20, 21], B14 [22], A52 [22], K7 [23], A46 [24, 25], F1 [26] and A49 [27]. Other members of this family are predicted by virtue of amino acid similarity to members whose structure has been determined [19].

The importance of C6 for virus virulence was investigated using a VACV mutant engineered to lack the *C6L* gene (vΔC6), or in which the *C6L* gene was not expressed due to mutation of the translation initiation codon (vC6-FS). Compared to wild-type and a revertant virus (formed by reinsertion of the *C6L* gene into vΔC6 at its natural locus), both vΔC6 and vC6-FS were less virulent [17]. This was shown in two mouse models of infection. The first was an intranasal model in which animals develop a respiratory infection and the virus can spread to other organs depending on the dose of virus administered. Outcome is measured by body mass and by development of signs of illness [28, 29]. The second is an intradermal infection of the ear pinna that induces only a local infection and mimics dermal vaccination [30, 31]. In this case, outcome is measured by the size of local lesion and there are no systemic signs of illness. In both models, viruses lacking C6 were less virulent than controls [17]. Despite this, immunisation with vΔC6 induced better immunological memory so that vaccinated mice were better protected against intranasal infection with wild-type virus 1 month after vaccination [32]. However, when C6 was deleted together with either the *N1L* gene or *K7L* gene, or both genes, the double or triple deletion mutant viruses were less potent vaccines than viruses in which only a single gene was deleted [33]. This was likely attributable to the progressive attenuation caused by deletion of each additional gene [33]. A study using the modified virus Ankara (MVA) strain of VACV in which the *C6L* gene was deleted also showed an enhanced immune response, in this case against foreign antigen expressed by this recombinant virus [34].

Further study of the C6 showed another function in blocking type I IFN-induced signalling via the JAK–STAT pathway [35]. Surprisingly, expression of C6 in cells treated with IFNβ inhibited expression of luciferase from a plasmid in which luciferase was driven by the ISRE promoter. This effect of C6 was confirmed by measuring the level of transcription of endogenous ISGs following IFN stimulation in the presence or absence of C6, and by measurement of the level of expression of ISG products by ELISA and immunofluorescence.

How C6 inhibits the pathway was investigated by determining the stage at which the pathway was blocked by C6. After addition of type I IFN, phosphorylation of both STAT1 and STAT2 was normal in the presence of C6, while in parallel

this was blocked by other viral inhibitors such as the parainfluenza virus V5 protein. Further, in the presence of C6, the STAT1 and STAT2 proteins could dimerise, and assemble with ISG3 to form the ISGF3 complex that translocated into the nucleus. This complex was also able to bind ISRE-containing DNA. Nonetheless, in the presence of C6, transcription was blocked [35]. This indicated that C6 was acting very late in the pathway within the nucleus, and is somehow perturbing the assembly or function of the transcriptional machinery on promoters bearing the ISRE (Fig. 2). Exactly, how this occurs remains unclear, but an unbiased proteomic screen for cellular proteins that co-purify with C6 showed that STAT2 was co-purified with C6 [35]. Further mapping of the region of STAT2 needed for this interaction identified the transactivation domain (TAD) at the C terminus as necessary for this interaction. Transfer of the C-terminal 104 amino acids of STAT2 to IRF9 enabled the IRF9-STAT2 fusion protein to co-precipitate with C6. Whether there is a direct interaction between C6 and STAT2, or whether this is via another protein(s), is unknown. Mechanistically, it is possible that C6 blocks the interactions of the STAT2 TAD with other factors and these interactions are needed for activation of transcription. However, confirmation of this will require further work to investigate if interactions between the STAT2 TAD and other factors are perturbed by C6. Additionally, structural determination of C6 in complex with cellular binding partners is needed, as is the isolation of a mutant C6 protein that no longer co-precipitates with STAT2 and has lost the ability to inhibit the JAK–STAT pathway, while retaining other biological activity, such as inhibition of IRF3 activation and binding to the TBK1 adaptor proteins.

Other Inhibitors of IFN Encoded by VACV

In addition to C6 and other inhibitors of activation of IRF3 or NF-κB, some other VACV-encoded IFN antagonists are mentioned here. Most VACV inhibitors act within the infected cell, either in the cytoplasm or nucleus, to block the induction of IFN expression, or the JAK–STAT signalling pathways leading to expression of ISGs. These VACV defences are effective at preventing the antiviral activity of IFN within the infected cell, but cannot combat the activity of IFNs that are produced from uninfected cells recruited to the site of infection. However, VACV also targets IFNs extracellularly by the expression of secreted proteins called B8 and B18. B8 binds IFNγ and prevents it reaching the IFNγR on cells [36–38]. Similarly, B18 binds to type I IFNs extracellularly, either in solution or on the cell surface, and so prevents signal transduction from the type I IFNR [39–42]. In addition to these extracellular antagonists, VACV has another strategy to block JAK–STAT signalling. It encodes a phosphatase, called vH1, that is packaged within virus particles [43, 44]. This protein is released into infected cells immediately after infection and virus uncoating, before even the early VACV genes are expressed, and it functions to dephosphorylate STAT1 and STAT2 to prevent signalling deriving from engagement of IFNs with IFNRs [43, 44]. Another VACV protein that is packaged within virions and can antagonise innate immunity immediately after infection is the B1 serine–threonine protein kinase [45, 46]. B1 phosphorylates the barrier to autointegration factor (BAF) and prevents BAF from binding to virus DNA to block DNA replication [46]. Thus, VACV expresses proteins that function either in the cytoplasm or nucleus or extracellularly to combat the antiviral activities of IFNs.

Summary

VACV expresses many proteins that antagonise the IFN system and these can function to block induction of IFN expression, the binding of IFNs to IFNRs, the signalling pathways that IFN induces, or the activity of ISG products. The large number of proteins that VACV devotes to interfering with interferon is testament to how potent the IFN system is in the restriction of viruses. Protein C6 is just one example and is a small intracellular protein with similarity to Bcl-2

proteins that has two different mechanisms to antagonise IFN. First, it blocks the induction of IFNβ by binding to the TBK1 adaptor proteins in the cytoplasm to inhibit activation of IRF3. Second, it co-purifies with STAT2 and functions within the nucleus to block transcription of genes bearing the ISRE.

Acknowledgements Work in the author's laboratory has been supported by grants from the UK Medical Research Council, the Lister Institute, and the Wellcome Trust. GLS is a Wellcome Trust Principal Research Fellow.

References

1. Fenner F, Anderson DA, Arita I, Jezek Z, Ladnyi ID (1988) Smallpox and its eradication. World Health Organization, Geneva
2. Baxby D (1981) Jenner's smallpox vaccine The riddle of the origin of vaccinia virus. Heinemann, London
3. Fenner F, Wittek R, Dumbell KR (1989) The Orthopoxviruses. Academic Press Ltd, London
4. Goebel SJ, Johnson GP, Perkus ME, Davis SW, Winslow JP, Paoletti E (1990) The complete DNA sequence of vaccinia virus. Virology 179(247–266):263–517
5. Gubser C, Hue S, Kellam P, Smith GL (2004) Poxvirus genomes: a phylogenetic analysis. J Gen Virol 85:105–117
6. Upton C, Slack S, Hunter AL, Ehlers A, Roper RL (2003) Poxvirus orthologous clusters: toward defining the minimum essential poxvirus genome. J Virol 77:7590–7600
7. Smith GL, Benfield CT, Maluquer de Motes C, Mazzon M, Ember SW, Ferguson BJ, Sumner RP (2013) Vaccinia virus immune evasion: mechanisms, virulence and immunogenicity. J Gen Virol 94:2367–2392
8. Veyer DL, Carrara G, Maluquer de Motes C, Smith GL (2017) Vaccinia virus evasion of regulated cell death. Immunol Lett 186:68–80
9. Smith GL, Talbot-Cooper C, Lu Y (2018) How does vaccinia virus interfere with interferon? Adv Virus Res 100:355–378
10. Smith GL, McFadden G (2002) Smallpox: anything to declare? Nat Rev Immunol 2:521–527
11. Pestka S, Krause CD, Walter MR (2004) Interferons, interferon-like cytokines, and their receptors. Immunol Rev 202:8–32
12. Platanias LC (2005) Mechanisms of type-I-and type-II-interferon-mediated signalling. Nat Rev Immunol 5:375–386
13. Farrar MA, Schreiber RD (1993) The molecular cell biology of interferon-g and its receptor. Annu Rev Immunol 11:571–611
14. Maniatis T, Falvo JV, Kim TH, Kim TK, Lin CH, Parekh BS, Wathelet MG (1998) Structure and function of the interferon-beta enhanceosome. Cold Spring Harb Symp Quant Biol 63:609–620
15. Thanos D, Maniatis T (1995) Virus induction of human IFN beta gene expression requires the assembly of an enhanceosome. Cell 83:1091–1100
16. Randall RE, Goodbourn S (2008) Interferons and viruses: an interplay between induction, signalling, antiviral responses and virus countermeasures. J Gen Virol 89:1–47
17. Unterholzner L, Sumner RP, Baran M, Ren H, Mansur DS, Bourke NM, Randow F, Smith GL, Bowie AG (2011) Vaccinia virus protein C6 is a virulence factor that binds TBK-1 adaptor proteins and inhibits activation of IRF3 and IRF7. PLoS Pathog 7:e1002247
18. Smith GL, Chan YS, Howard ST (1991) Nucleotide sequence of 42 kbp of vaccinia virus strain WR from near the right inverted terminal repeat. J Gen Virol 72:1349–1376
19. Gonzalez JM, Esteban M (2010) A poxvirus Bcl-2-like gene family involved in regulation of host immune response: sequence similarity and evolutionary history. Virol J 7:59
20. Aoyagi M, Zhai D, Jin C, Aleshin AE, Stec B, Reed JC, Liddington RC (2007) Vaccinia virus N1L protein resembles a B cell lymphoma-2 (Bcl-2) family protein. Protein Sci 16:118–124
21. Cooray S, Bahar MW, Abrescia NG, McVey CE, Bartlett NW, Chen RA, Stuart DI, Grimes JM, Smith GL (2007) Functional and structural studies of the vaccinia virus virulence factor N1 reveal a Bcl-2-like anti-apoptotic protein. J Gen Virol 88:1656–1666
22. Graham SC, Bahar MW, Cooray S, Chen RA, Whalen DM, Abrescia NG, Alderton D, Owens RJ, Stuart DI, Smith GL et al (2008) Vaccinia virus proteins A52 and B14 Share a Bcl-2-like fold but have evolved to inhibit NF-kappaB rather than apoptosis. PLoS Pathog 4:e1000128
23. Kalverda AP, Thompson GS, Vogel A, Schroder M, Bowie AG, Khan AR, Homans SW (2009) Poxvirus K7 protein adopts a Bcl-2 fold: biochemical mapping of its interactions with human DEAD box RNA helicase DDX3. J Mol Biol 385:843–853
24. Fedosyuk S, Bezerra GA, Radakovics K, Smith TK, Sammito M, Bobik N, Round A, Ten Eyck LF, Djinovic-Carugo K, Uson I et al (2016) Vaccinia virus immunomodulator A46: a lipid and protein-binding scaffold for sequestering host TIR-domain proteins. PLoS Pathog 12:e1006079
25. Fedosyuk S, Grishkovskaya I, de Almeida Ribeiro E, Skern T (2014) Characterization and structure of the vaccinia virus NF-kappaB antagonist A46. J Biol Chem 289:3749–3762
26. Kvansakul M, Yang H, Fairlie WD, Czabotar PE, Fischer SF, Perugini MA, Huang DC, Colman PM (2008) Vaccinia virus anti-apoptotic F1L is a novel

Bcl-2-like domain-swapped dimer that binds a highly selective subset of BH3-containing death ligands. Cell Death Differ 15:1564–1571
27. Neidel S, Maluquer de Motes C, Mansur DS, Strnadova P, Smith GL, Graham SC (2015) Vaccinia virus protein A49 is an unexpected member of the B-cell Lymphoma (Bcl)-2 protein family. J Biol Chem 290:5991–6002
28. Alcami A, Smith GL (1992) A soluble receptor for interleukin-1 beta encoded by vaccinia virus: a novel mechanism of virus modulation of the host response to infection. Cell 71:153–167
29. Williamson JD, Reith RW, Jeffrey LJ, Arrand JR, Mackett M (1990) Biological characterization of recombinant vaccinia viruses in mice infected by the respiratory route. J Gen Virol 71:2761–2767
30. Tscharke DC, Reading PC, Smith GL (2002) Dermal infection with vaccinia virus reveals roles for virus proteins not seen using other inoculation routes. J Gen Virol 83:1977–1986
31. Tscharke DC, Smith GL (1999) A model for vaccinia virus pathogenesis and immunity based on intradermal injection of mouse ear pinnae. J Gen Virol 80:2751–2755
32. Sumner RP, Ren H, Smith GL (2013) Deletion of immunomodulator C6 from vaccinia virus strain Western Reserve enhances virus immunogenicity and vaccine efficacy. J Gen Virol 94:1121–1126
33. Sumner RP, Ren H, Ferguson BJ, Smith GL (2016) Increased attenuation but decreased immunogenicity by deletion of multiple vaccinia virus immunomodulators. Vaccine 34:4827–4834
34. Garcia-Arriaza J, Najera JL, Gomez CE, Tewabe N, Sorzano CO, Calandra T, Roger T, Esteban M (2011) A candidate HIV/AIDS vaccine (MVA-B) lacking vaccinia virus gene C6L enhances memory HIV-1-specific T-cell responses. PLoS ONE 6: e24244
35. Stuart JH, Sumner RP, Lu Y, Snowden JS, Smith GL (2016) Vaccinia virus protein C6 inhibits type I IFN signalling in the nucleus and binds to the transactivation domain of STAT2. PLoS Pathog 12:e1005955
36. Alcami A, Smith GL (1995) Vaccinia, cowpox, and camelpox viruses encode soluble gamma interferon receptors with novel broad species specificity. J Virol 69:4633–4639
37. Mossman K, Upton C, Buller RM, McFadden G (1995) Species specificity of ectromelia virus and vaccinia virus interferon-gamma binding proteins. Virology 208:762–769
38. Symons JA, Tscharke DC, Price N, Smith GL (2002) A study of the vaccinia virus interferon-gamma receptor and its contribution to virus virulence. J Gen Virol 83:1953–1964
39. Alcami A, Symons JA, Smith GL (2000) The vaccinia virus soluble alpha/beta interferon (IFN) receptor binds to the cell surface and protects cells from the antiviral effects of IFN. J Virol 74:11230–11239
40. Colamonici OR, Domanski P, Sweitzer SM, Larner A, Buller RM (1995) Vaccinia virus B18R gene encodes a type I interferon-binding protein that blocks interferon alpha transmembrane signaling. J Biol Chem 270:15974–15978
41. Montanuy I, Alejo A, Alcami A (2011) Glycosaminoglycans mediate retention of the poxvirus type I interferon binding protein at the cell surface to locally block interferon antiviral responses. FASEB J 25:1960–1971
42. Symons JA, Alcami A, Smith GL (1995) Vaccinia virus encodes a soluble type I interferon receptor of novel structure and broad species specificity. Cell 81:551–560
43. Mann BA, Huang JH, Li P, Chang HC, Slee RB, O'Sullivan A, Anita M, Yeh N, Klemsz MJ, Brutkiewicz RR et al (2008) Vaccinia virus blocks Stat1-dependent and Stat1-independent gene expression induced by type I and type II interferons. J Interf Cytokine Res Off J Int Soc Interferon Cytokine Res 28:367–380
44. Najarro P, Traktman P, Lewis JA (2001) Vaccinia virus blocks gamma interferon signal transduction: viral VH1 phosphatase reverses Stat1 activation. J Virol 75:3185–3196
45. Banham AH, Smith GL (1992) Vaccinia virus gene B1R encodes a 34-kDa serine/threonine protein kinase that localizes in cytoplasmic factories and is packaged into virions. Virology 191:803–812
46. Wiebe MS, Traktman P (2007) Poxviral B1 kinase overcomes barrier to autointegration factor, a host defense against virus replication. Cell Host Microbe 1:187–197

Significance of Vi Negative Isolates of *Salmonella Enterica* Serovar Typhi

Abdul Haque

Abstract

Typhoid is a major global disease. The causative agent, *Salmonella enterica* serovar Typhi (*S*. Typhi) has a capsular antigen called Vi antigen which is traditionally considered to be the main cause of virulence. All the current vaccines are based on Vi antigen. However, the realization of the fact that there are *S*. Typhi strains which lack Vi antigen but still exist naturally and can cause disease has stirred great scientific interest. It is also interesting to note that their relative prevalence is affected by climatic conditions. Now it is established that Vi positive and Vi negative *S*. Typhi have different modes of pathogenesis; and as recent studies suggest, different structure of polysaccharide antigens. This means that current vaccines are not effective against a significant number of *S*. Typhi strains which not only affect the success of vaccination programs but also help in rapid emergence of Vi negative *S*. Typhi due to natural selection. The focus should be on vaccines based on antigens which are universally present in all *S*. Typhi. One such candidate is O-specific polysaccharides (OSPs). Successful attempts have been made to prepare conjugate vaccines based on OSPs.

Keyword

Typhoid · OSP antigen · Conjugate vaccines

Introduction

Typhoid is an acute infectious febrile illness with anorexia, headache, malaise and abdominal discomfort. Although hygienic conditions have improved generally, typhoid fever is still a significant health concern in lesser developed countries. According to WHO, there were 22 million new cases in 2004, 5% of which were fatal [1]. However in 2010, the figure had risen to 33 million cases per year [2]. Typhoid is the fourth most common cause of death in Pakistan [3].

Typhoid is caused by *Salmonella enterica* serovar Typhi (*S*. Typhi) which are gram negative bacilli belonging to family *Enterobacteriaceae*. Unlike many other *Salmonella* serovars, *S*. Typhi is restricted to human populations.

S. Typhi genome size is ~5 million base pairs with 4000 genes. *S*. Typhi isolates are highly related (clonal) and there was a single

A. Haque (✉)
Postgraduate Research Laboratory, Health Sciences Campus, The University of Faisalabad, Sargodha Road, Faisalabad, Pakistan
e-mail: ahaqnibge@gmail.com

R. Adhikari and S. Thapa (eds.), *Infectious Diseases and Nanomedicine III*,
Advances in Experimental Medicine and Biology 1052, https://doi.org/10.1007/978-981-10-7572-8_2

point of origin ~30,000–50,000 years ago. S. Typhi has acquired some genes recently including those encoding the Vi antigen [4].

Vi Antigen

Vi capsular polysaccharide was identified as the major virulence factor of *S*. Typhi in 1934 by Felix [5]. It has been focused both as an essential virulence factor and a protective antigen of *S*. Typhi. The internationally used typhoid vaccines are based on Vi polysaccharide.

Its production is controlled by Vi operon which is located on a large 134 kb pathogenicity island SPI7 with two loci *tviA* and *tviB*. Trancription is controlled by factors such as osmolarity [6]. SPI7 are unstable genetic elements [7]. These elements may be lost during in vitro passage. SPI7 may be lost entirely [8] or there may be partial excision of Vi operon [9]. The synthesis of Vi polysaccharide, is controlled by *ompR-envZ* and *rscB-rscC*, depending on level of osmolarity [10]. Size of Vi-antigen-encoding region is 15 kb as determined by recombination experiments. [11].

The *S*. Typhi Vi antigen is a glycan. A soil bacterium *Achromobacter* also has genetic locus for this antigen but it possesses a Vi antigen-specific depolymerase enzyme VexE missing in *S*. Typhi resulting in different physical properties [12].

Vi Negative *S*. Typhi

The emergence of Vi negative isolates of *S*. Typhi in recent years has sparked a lot of interest because these isolates have direct implications on future development of typhoid vaccines which are currently almost exclusively Vi polysaccharide based. The Vi negative strains of *S*. Typhi were initially reported in 1960s. During 1970s, several reports of Vi negative strains emerged from various countries including Jamaica, Indonesia, New Zealand and Malaysia. In 1999–2000, an epidemic of typhoid due to Vi negative strains of *S*. Typhi was reported from India [13]. These reports placed the efficacy of typhoid vaccines based on the Vi antigen in doubt.

The difference between Vi polysaccharide and O-antigen display (VW variation) is known since early days [14]. *rpoS* gene is considered to be responsible for this phenomenon [10]. *S*. Typhi reported from clinical laboratories may be Vi negative due to down regulation of Vi operon thus giving false negative results. Vi negativity may be due to the absence of the 134 kb SPI-7. This finding led to the proposal that SPI-7 may be able to excise from the chromosome and act in similar fashion to a conjugative transposon [15].

These studies were carried out on cultivated bacteria and in some cases, stored *S*. Typhi isolates. It raised doubts that storage might be the reason for Vi negativity and loss of SPI-7.

Naturally Occurring Vi Negative *S*. Typhi

In recent years, it has been shown that Vi negative *S*. Typhi exist naturally [9, 16].

We found *tviA* and *tviB* negativity in 15% of all *S*. Typhi isolates (2005) with absence of SPI-7 in 4%. Sixty stored isolates of *S*. Typhi from the Faisalabad region of Pakistan were explored for lack of Vi expression by PCR for *tviA* and *tviB* and SPI-7. Only two isolates were negative for SPI-7 but nine (15%) lacked both *tviA* and *tviB*. Blood samples from typhoid patients were investigated to establish natural presence of this phenomenon. Of the 48 blood samples, 42 showed *fliC* positive PCR for *S*. Typhi. Among these, *tviA* and *tviB* were not detected in four samples; and three of these (75%) were positive for SPI-7. These results demonstrated that *viaB*-negative, SPI-7-positive *S*. Typhi are naturally occurring and can be detected by PCR on the peripheral blood of typhoid patients [9] (Fig. 1).

These findings were subsequently substantiated by reports from Nepal [17]. There is a great discrepancy among reports from different parts of the world regarding the relative frequency of Vi-negative *S*. Typhi (ranging from less than 1 to 25.7%). In areas of significant occurrence they are overtaking classical Vi positive isolates with

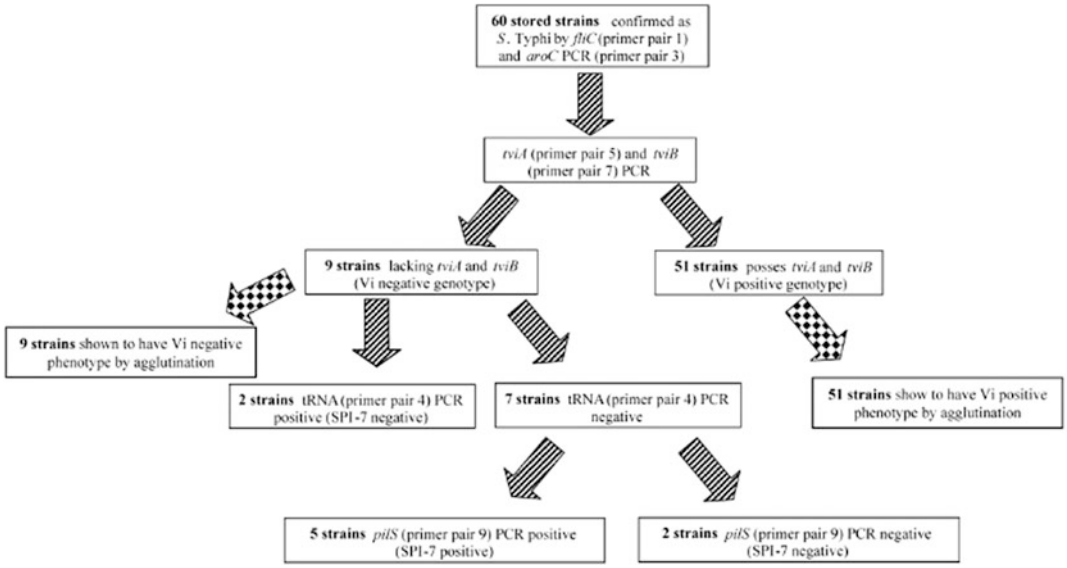

Fig. 1 Flow diagram showing the results of investigation of 60 stored isolates of *S*. Typhi from Faisalabad, Pakistan to express Vi antigen

passage of time. Why they are significantly present in some areas but not others? An explanation is required to develop a consensus because there is a danger that the importance of these emerging pathogens may get ignored due to contradictory reports.

As mentioned above, our study in 2005 [9] showed 15% isolates as Vi negative. In another study conducted in 2009, we found 21% isolates as Vi negative [18]. In 2010, Maurya et al. [19] reported 35% *S*. Typhi isolates as Vi negative. They used *tRNA–pheU* and *fliC* amplification to detect loss of SPI-7 and *viaB* operon deletion due to storage in isolates collected during 1987–2006. All 111 isolates were positive for *fliC* gene but 39 were negative for *viaB* operon. As many as 106 isolates showed presence of SPI-7. SPI-7 presence was not affected by repeated culture and long-term storage; but *viaB* operon was not so stable suggesting a role of selection pressure.

On the other hand, Wain et al. [20] found less than 1% *S*. Typhi as Vi negative in a study conducted in Karachi, Pakistan. Presence of genetic locus required for Vi expression was studied by using a multiplex PCR. Among 2,222 *S*. Typhi clinical isolates, 12 showed Vi negativity by serology, but only one was negative by PCR. This result was supported by immunofluorescence. Similarly Sur et al. [21] reported negligible number of Vi negative *S*. Typhi from Kolkata, India.

How We Can Explain This Difference in Reports?

When outside the body, bacteria pass through various stress conditions ranging from very low temperatures to scorching heat, low to very high humidity, and varying osmotic conditions to name a few. So it is logical to say that in environment where conditions remain mostly conducive for growth and replication, they do not have to fight a battle for survival and need not to shed off the excessive baggage. However in harsh conditions they either shed off the non-essential genes or make them dormant.

S. Typhi passes a considerable period of its life outside the body in feces, or soil. It is reported that it may survive up to 1 year in soil

[22]. It is during this period that it faces stress conditions and is prone to lose its Vi operon.

Now let us consider the various reports regarding occurrence of Vi negative isolates of *S*. Typhi. As shown in Table 1, significant presence of these isolates has been reported from Faisalabad, Pakistan [9, 18] as well as from Delhi, India [16]. The percentage ranges from 8 to 25. 7. On the other hand, less than 1% presence has been documented from Karachi [20] and Kolkata [21].

The annual temperatures at Faisalabad and Delhi vary from 4° to 41 °C (Table 1). This relatively wide range of temperature which borders on extremes is usually accompanied by very dry weather for most of the year. It is only for a few months that temperatures and humidity are optimum for bacterial growth.

On the other hand, in Karachi and Kolkata where Vi negative *S*. Typhi isolates are rarely found, the temperature is moderate almost throughout the year (ranging from 19 to 30.5 °C) with high humidity because of coastal area. This makes the conditions favorable for bacterial growth and they do not have to face extreme stress conditions. There is a report on an outbreak of Vi negative *S*. Typhi in Kolkata [13] but it was an epidemic of short duration which might had a source outside that area.

Another point of great importance is that in the areas where these isolates have been detected in significant number, they are replacing Vi positive isolates over time. In 2000, the % occurrence was 8% [16], which increased to 15% [9] in 2005, 25.7% [18] in 2009 and 35% in 2010 [19].

It is important to note that there have been no extended Vi vaccination programs in these areas which would have created selective pressure. It means that Vi negative isolates are outwitting Vi positive isolates in this natural battle for survival. It also means that these isolates have better adaptability as compared with Vi positive counterparts and are increasing their numbers merrily. It is an alarming situation which underlines the need to establish their importance.

Pathogenesis of Vi Positive and Vi Negative *S*. Typhi

It is well known that Vi capsule is lost during artificial storage. Storage at low temperature enforces conditions of stress in which bacteria cannot proliferate. There is minimum supply of nutrients and they are living in almost zero metabolic state. In such conditions, they shed off the unnecessary package of genes—only those are kept which are essentially required. Vi operon or even SPI7 are not essential so we find

Table 1 Effect of climatic conditions on relative occurence of Vi positive and Vi negative S. Typhi isolates

Report	Vi +ve *S*. Typhi (%)	Vi –ve *S*. Typhi (%)	Area of study	Temperature fluctuation (Average) (°C)	Humidity % (Average)
Mehta and Arya [16]	91.2	8.0	Delhi	Max: 39.0	Max: 73
				Min: 7.0	Min: 33
Wain et al. [20]	99.4	0.6	Karachi	Max: 30.5	Data N/A
				Min: 21.3	
Baker et al. [9]	85.0	15.0	Faisalabad	Max: 41.0	Data N/A
				Min: 4.8	
Ali et al. [18]	74.3	25.7	Faisalabad	Max: 41.0	Data N/A
				Min: 4.8	
Sur et al. [21]	100.0	0.0	Kolkata	Max: 30.0	Max: 83
				Min: 19.0	Min: 58

Note Weather reference from http://en.wikipedia.org/wiki/

that Vi negativity is due to lose of either whole of SPI7 or Vi operon.

So if Vi capsule is absent, what about pathogenesis of *S*. Typhi? Various studies clearly indicate that Vi negative and Vi positive *S*. Typhi have different modes of pathogenesis.

It has been shown by Hart et al. [23] that *S*. Typhimurium is more resistant to blood and serum as compared to *S*. Typhi but Vi expression improves resistance to complement and phagocytes by reducing C3 and C5b-9 deposition, and decreasing overall antibody binding.

We recently studied the comparative growth of Vi positive and Vi negative *S*. Typhi isolates in an ex vivo human whole blood model [24]. Whole blood and a control enrichment medium (Tryptic soy broth-TSB) were employed to study four isolates of each type. Capsulated (Vi positive) strains formed smooth circular colonies and had shorter lag and generation time resulting in faster growth. In blood, lag time was double in Vi negative isolates. Their number reduced up to 81% during the first 12 h. However in TSB, growth curve was similar indicating that Vi capsule is dispensable for bacterial growth in vitro. It was shown for the first time that lack of Vi antigen slows growth on initial contact with human blood, but gradually they get adjusted.

Intracellular survival of Vi positive and Vi negative *S*. Typhi in macrophage cell lines was studied by Hirose et al. [25]. Growth of Vi negative *S*. Typhi was inhibited in both mouse and human macrophage cell lines. The Vi positive *S*. Typhi were able to survive in resting human macrophage cell line by suppressing the production of tumor necrosis factor-alpha (TNF-alpha), whereas it was stimulated by Vi-negative *S*. Typhi and *S*. Typhimurium.

The loss of Vi antigen does not affect the survival outside the body. Its role is to resist against phagocytosis and serum complement [26]. Even once inside the body, these pathogens do not essentially need Vi capsule for pathogenicity. It is not required for invasion of eukaryotic cells as cell invasion is facilitated by Type IVB pili [27]. The dispensability of Vi capsule is amply demonstrated in *S*. Paratyphi A which causes a disease similar to *S*. Typhi but does not possess Vi antigen [28]. In fact, it has been experimentally shown that removal of Vi capsule enhances the invasion of epithelial cells [7].

So it can be said that the Vi negative isolates of *S*. Typhi have found ways to bypass Vi capsule totally and complete their life cycle successfully. In fact, it has been reported that they are poor formers of biofilm as well [29] which indicates a decreased necessity to produce polysaccharides in general.

S. Typhi requires intact motility and secretion of the invasion-promoting Sip proteins for entry into intestinal cells. These proteins are targets of the type III secretion machinery encoded by the *inv*, *spa* and *prg* loci.

Arricau et al. [30] observed that the production of Sip proteins, flagellin and Vi antigen is differentially modulated by the *RcsB–RcsC* regulatory system and osmolarity at both transcriptional and post-translational levels. Maximal production of Vi polysaccharide prevented the secretion of Sip proteins and flagellin. Transcription of *iagA, invF* and *sipB* was positively influenced by increasing concentration of NaCl but it had negative influence on Vi antigen biosynthesis. It was clearly shown that *RcsB* and osmolarity modulated the invasive capacity of *S*. Typhi.

Structural Analysis of Lipopolysaccharides of Vi Positive and Vi Negative *S*. Typhi

From the discussion above it has become clear that Vi negative *S*. Typhi has separate identity, can occur naturally and have different modes of pathogenesis as compared to Vi positive *S*. Typhi. It necessitates detailed structural studies to gather more information to combat these emerging pathogens.

The cell walls of gram negative bacteria are quite different from those of gram positive bacteria. The lipopolysaccharides in the outer membrane play a major role in pathogenicity and antigenicity of gram negative bacteria. Although

these structures of *S*. Typhi have been studied in detail, comparative studies of these structures between Vi negative and Vi positive *S*. Typhi have not been carried out.

There are three parts of lipopolysaccharides in the outer membrane: lipid A, core (inner and outer), and O-specific polysaccharides (OSPs) (Fig. 2).

Lipid A is endotoxic center and generally conserved. Variations in structure occurs from types of amino sugars, degrees of phosphorylation, presence of phosphate substituents, and nature, chain length, number and location of fatty acyl chains.

Core acts as a link between lipid A and OSP. Inner core (towards lipid A) consists of unusual sugars like Kdo and heptoses. Outer core (towards OSP) consists of common hexoses such as glucose and galactose.

OSP is a surface antigen. It is serologically specific and show enormous structure variability. There are repeating units of 2–8 monosaccharides differing in nature, ring form, sequence, substitution and type of linkage.

We have started a project for fatty acid profiling and structural analysis of Lipid A and structural analyses of O-Specific Polysaccharide (OSP).

We used Gas Chromatography-Mass Spectrometry (GC-MS) for fatty acid analysis of lipid A, compositional or sugar analysis, and methylation or linkage analysis of OSP. Liquid Chromatography-Mass Spectrometry (LC-MS) was used for detailed structural analysis through Tandem MS of lipid A.

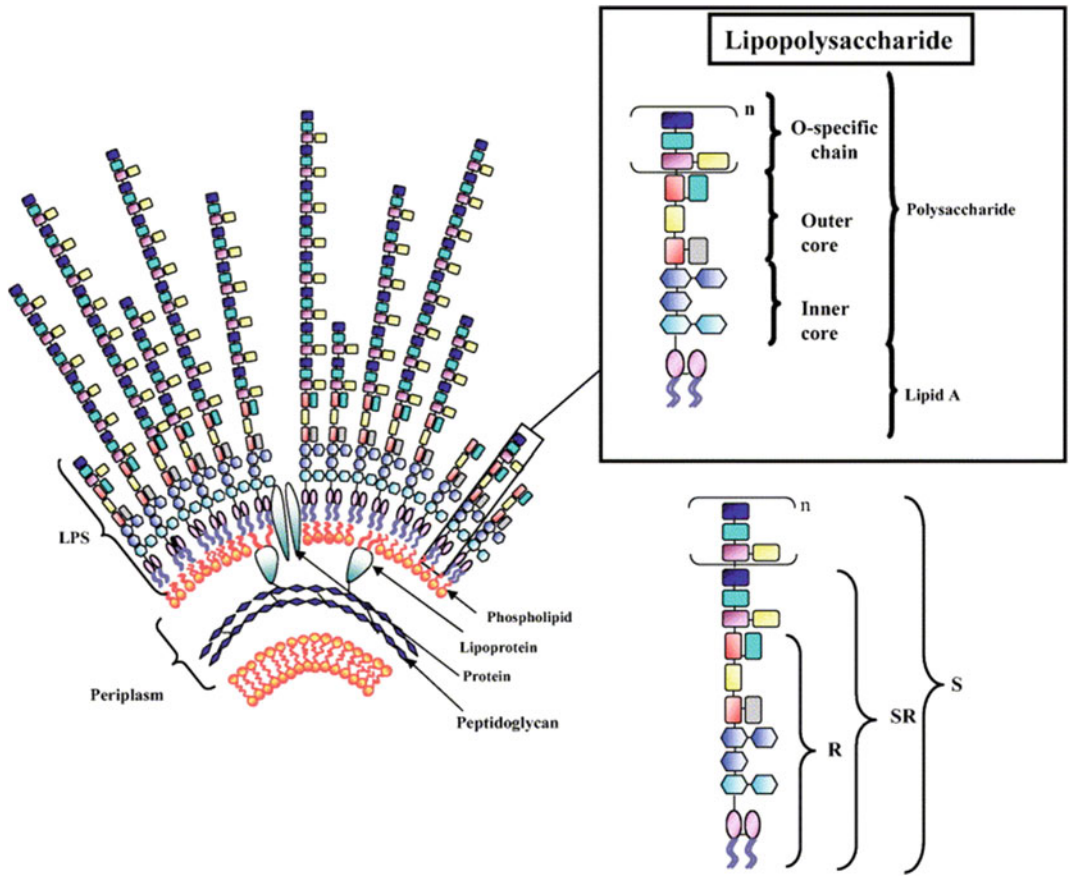

Fig. 2 Structure of bacterial lipopolysaccharides [31]

It was found that Vi positive isolates had more abundance of mono-phosphorylated tetra and pentaacylated lipid A structures whereas Vi negative isolates showed higher intensities of mono and biophosphorylated hexa and hepta acylated lipid A variants (Haque et al. unpublished data). It can be inferred that Vi-negative isolates of *S*. Typhi invest more on lipid A molecule by having higher amount of hexa and hepta acylated lipid A structures to make its membrane more compact and resistant to host defense mechanism. Both types of isolates exhibited heterogeneity and showed significant difference in covalent modifications in lipid A structures which may contribute in endotoxic variation.

We used Nuclear Magnetic Resonance (NMR) to determine number, types of sugars, conformation and linkages of OSP. Chemistry of OSP of both types was found to be significantly different not only in the nature of sugar residues of their repeating units but also in positions and linkages.

Our investigations showed that OSP of Vi negative *S*. Typhi has hydrophobic sugar tyvelose on branched position providing a hydrophobic coating to bacterial surface, which may give additional protection from host defence mechanisms (Haque et al., unpublished data). This difference in chemistry of OSP, indicates that virulence mechanisms of both types may be different.

Preparation of Conjugate Vaccines Effective Against Both Vi Negative and Vi Positive *S*. Typhi

Conjugate vaccines have been a great success story for bacteria having polysaccharide antigens.

Polysaccharide antigens consist of repeated units which enable them to bypass antigen presenting cells (APC) and interact directly with B lymphocytes to induce antibody synthesis. Because of relatively low molecular weight, most of the OSP do not elicit serum antibodies at any age. Therefore, they are considered as haptens [32]. Polysaccharide based vaccines are ineffective in young children less than 2 year old even with booster doses [33].

Conjugation of the polysaccharide antigen with a protein is the basis of conjugate vaccine which acts as a T-cell dependent antigen, with all the associated advantages [34].

After conjugation with a protein, following benefits are gained:

1. Because of protein presence, cellular immune system is evoked leading to higher production of antibodies.
2. Co-presence of carrier protein turns polysaccharide to a T-dependent antigen. These conjugates bind to polysaccharide-specific pre-B cells.
3. IgG1 and IgG3 subclasses dominate antibody responses to protein antigens.
4. Memory cells are formed.
5. Affinity maturation takes place resulting in refinement of B cells and improvement of antibody quality.

Currently licensed polysaccharide-protein conjugate vaccines include *Neisseria meningitidis*, *Hemophilus influenzae* type b, and *Streptococcus pneumonia* [35, 36]. Vi-rEPA conjugate vaccine, prepared by using a nontoxic recombinant *Pseudomonas aeruginosa* exotoxin A (rEPA), has shown better immunogenicity in children aged 5–14 years and adults [37] and 90% efficacy in children age 2–5 years [38]. The emergence of Vi negative *S*. Typhi has necessitated the need of a polysaccharide which is universally present in all *S*. Typhi unlike Vi antigen which is present only in Vi positive *S*. Typhi. O-specific polysaccharides (OSP) are ideally suited for this purpose.

We started work on preparation of immunogenic conjugates of O-specific polysaccharides (OSP) of S. Typhi with diphtheria toxoid (DT). Adipic acid dihydrazide (ADH) was used as a linker to conjugate diphtheria toxoid (DT) with

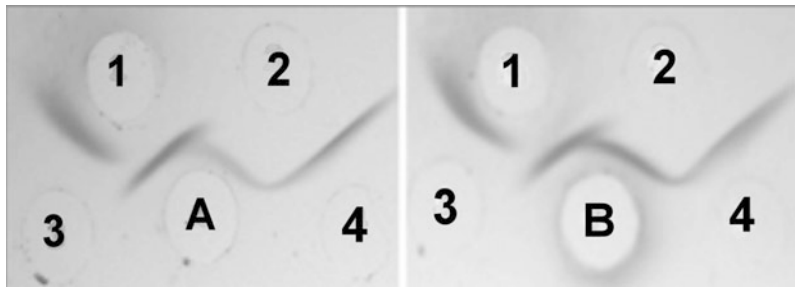

Fig. 3 Double immunodiffusion of conjugates against anti-OSP and anti-DT sera. Wells A and B: *S*. Typhi OSP-AH-DT conjugate-1 and conjugate-2 (100 µg each respectively. Wells 1 and 2: Anti-OSP and anti-DT (15 µl each) respectively. Wells 3 and 4: *S*. Typhi OSP and DT (100 µg each) respectively

OSP of *S*. Typhi. Mice were used as a model to evaluate these conjugates (OSP-AH-DT) for their immunogenicity. As compared with lipopolysaccharides alone, they showed significantly higher levels of IgG ELISA titers (P = 0.0241 and 0.0245). It was found that three injections with 4-weeks interval resulted in better response than regimen of three injections with 2-weeks interval. This showed the success of diphtheria toxoid as a carrier protein for conjugation with Salmonella OSP [39] (Fig. 3).

We extended this study and used OSP of Vi negative *S*. Typhi as antigen. Recombinant exoprotein A of *Pseudomonas aeruginosa* (rEPA) and human serum albumin (HSA) were used as carrier proteins to prepare four different conjugates using either an intermediate linker molecule, adipic acid dihydrazide (ADH) or direct reductive amination. A significantly higher antibody titer was observed in mice injected with conjugate-1 (OSP-HSA) and conjugate 2 (OSP-rEPA) as compared to OSP alone. But antibody production triggered by conjugate 3 (OSP ADH -HSA) and conjugate 4 (OSP ADH - rEPA) were insignificant. We concluded that reductive amination is the superior method to prepare the S. Typhi OSP glycoconjugate. Additionally, rEPA is a better carrier protein than HSA. Therefore, OSP-rEPA conjugate can be very effective typhoid vaccines candidate [Haque et al. unpublished data].

Concluding Remarks

Vi negative *S*. Typhi are emerging as a serious threat. They occur naturally and have different mode of pathogenesis. They have changed the concept of typhoid vaccines. There is a need to know more about these pathogens and how they compare with classical Vi positive *S*. Typhi. It is also important that new vaccines should be based on antigens which are present in both types of *S*. Typhi. Conjugate vaccines are a popular choice because of inherent advantages and notable progress has been made in this direction.

References

1. Crump JA, Luby SP, Mintz ED (2004) The global burden of typhoid fever. Bull W H O 82:346–353
2. Capoor MR, Nair D (2010) Quinolone and cephalosporin resistance in enteric Fever. J Glob Infect Dis 2:258–262
3. WHO 6th International conference on typhoid fever and other salmonellosis (2006) World Health Organization (Reference type: Pamphlet), Geneva
4. Baker S, Dougan G (2007) The Genome of *Salmonella enterica* serovar typhi. Clin Infect Dis 45 (Supplement 1): S29–S33. https://doi.org/10.1086/518143
5. Felix A, Pitt RM (1934) Notes on the Vi antigen of bacillus typhosus. J Path Bact 38:409
6. Wang JC, Noriega FR, Galen JE, Barry E, Levine MM (2000) Constitutive expression of the Vi polysaccharide capsular antigen in attenuated

Salmonella enterica serovar typhi oral vaccine strain CVD 909. Infect Immun 68:4647–4652
7. Bueno SM, Santiviago CA, Murillo AA, Fuentes JA, Trombert AN et al (2004) Precise excision of the large pathogenicity Island, SPI7, in *Salmonella enterica* serovar typhi. J Bacteriol 186:3202–3213
8. Nair S, Alokam S, Kothapalli S, Porwollik S, Proctor E et al (2004) *Salmonella enterica* serovar Typhi strains from which SPI7, a 134-kilobase Island with genes for Vi exopolysaccharide and other functions, has been deleted. J Bacteriol 186:3214–3223
9. Baker S, Sarwar Y, Aziz H, Haque A, Ali A et al (2005) Detection of Vi-Negative *Salmonella enterica* serovar typhi in the peripheral blood of patients with typhoid fever in the Faisalabad region of Pakistan. J Clinc Microbiol 43:4418–4425
10. Santander MJ, Roland KL, Curtiss RIII (2008) Regulation of Vi capsular polysaccharide synthesis in *Salmonella enteric* serotype typhi. J Infect Develop Count 2:412–420
11. Kolyva S, Waxin H, Popoff MY (1992) The Vi antigen of *Salmonella typhi:* molecular analysis of the *viaB*locus. J Gen Microbiol 138:297–304
12. Liston SD, Ovchinnikova OG, Whitfield C (2016) Unique lipid anchor attaches Vi antigen capsule to the surface of *Salmonella enterica* serovar Typhi. PNAS 113:6719–6724
13. Saha MR, Ramamurthy T, Dutta P, Mitra U (2000) Emergence of *Salmonella typhi* Vi antigen-negative strains in an epidemic of multidrug-resistant typhoid fever cases in Calcutta, India. Natl Med J India 13:164
14. Tully JG, Currie JA (1962) Vi-negative strains of salmonella typhosa: attempts to induce w-v reversion and the use of non-vi strains in evaluating typhoid vaccines. J Bacteriol 84:747–753
15. Pickard D, Wain J, Baker S, Line A, Chohan S et al (2003) Composition, acquisition, and distribution of the Vi exopolysaccharide-encoding *Salmonella enterica* pathogenicity island SPI-7. J Bacteriol 185:5055–5065
16. Mehta G, Arya SC (2002) Capsular Vi polysaccharide antigen in *Salmonella enteric* serovar typhi isolates. J Clin Microbio l40:1127–1128
17. Pulickal AS, Callaghan MJ, Kelly DF, Maskey M, Mahat S et al (2013) Prevalence and genetic analysis of phenotypically Vi- negative Salmonella typhi isolates in children from Kathmandu, Nepal. J Trop Pediatr 59:317–320
18. Ali A, Haque A, Haque A, Sarwar Y, Mohsin M et al (2009) Multiplex PCR for differential diagnosis of emerging typhoidal pathogens directly from blood samples. Epidemiol Infect 137:102–107
19. Maurya P, Gulati AK, Nath K (2010) Vi gene stability and SPI-7 in *S*. Typhi status of Vi gene, its expression and Salmonella Pathogenicity Island (SPI-7) in *Salmonella* Typhi in India. Southeast Asian J Trop Med Public Health 41:913–919
20. Wain J, House D, Bhutta Z, Zafar A, Baker S et al (2005) Vi antigen expression in *Salmonella enterica* serovar typhi clinical isolates from Pakistan. J Clin Microbiol 43:1158–1165
21. Sur D, Ochiai RL, Bhattacharya SK (2009) A cluster-randomized effectiveness trial of Vi typhoid vaccine in India. N Engl J Med 361:335–344
22. Feachem GR (1980) Appropriate technology for water supply and sanitation. The World Bank, Directorate of Information and Public Affairs, Washington D.C 20433
23. Hart PJ, O'Shaughnessy CM, Siggins MK, Bobat S, Kingsley RA et al (2016) Differential killing of *Salmonella enterica* serovar typhi by antibodies targeting Vi and lipopolysaccharide O:9 Antigen. PLOS https://doi.org/10.1371/journal.pone.0145945
24. Liaqat S, Sarwar Y, Ali A, Haque A (2015) Comparative growth analysis of capsulated (vi+) and acapsulated (vi-) *Salmonella typhi* isolates in human blood. EXCLI 14:213–219
25. Hirose K, Ezaki T, Miyake M, Li T, Khan AQ et al (1997) Survival of Vi-capsulated and Vi-deleted *Salmonella typhi* strains in cultured macrophage expressing different levels of CD14 antigen. FEMS Microbiol Lett 147(2):259–265
26. Robbins JD, Robbins JB (1984) Reexamination of the protective role of the capsular polysaccharide (Vi antigen) of *Salmonella typhi*. J Infect Dis 150:436–449
27. Lee FK, Morris C, Hackett J (2006) The *Salmonella enteric* serovar Typhi Vi capsule and self-association pili share controls on expression. FEMS Microbiol Lett 261:41–46
28. Helena MB, Seth-Smith (2008) SPI-7: *Salmonella*'s Vi-encoding pathogenicity Island. J Infect Develop Count 2:267–271
29. Haque A (2009) Biofilm is not or poorly produced by Vi negative isolates of *S*. Typhi. The 7th international symposium on invasive salmonelloses, Kilifi, Kenya, 25–28th Jan 2009. Proceedings available on www.ivi.org. Accessed 07 June 2010
30. Arricau N, Ecobichon C, Hermant D, Duffey PS, Waxin H et al (1998) The RcsB–RcsC regulatory system of Salmonella typhi differentially modulates the expression of invasion proteins, flagellin and Vi antigen in response to osmolarity. Mol Microbiol 29:835–850
31. Caroff M, Karibian D (2003) Structure of bacterial lipopolysaccharides. Carbohydr Res 338(23):2431–2447
32. Robbins JB, Schneerson R (1990) Polysaccharide-protein conjugates: a new generation of vaccines. J Infect Dis 161:821–832
33. Jones C (2005) Vaccines based on the cell surface carbohydrates of pathogenic bacteria. An Acad Bras Cienc 77:293–324
34. Goldblatt D (1998) Recent developments in bacterial conjugate vaccines. J Med Microbiol 47:563–567
35. Finn A (2004) Bacterial polysaccharide-protein conjugate vaccines. Br Med Bull 70:1–14

36. Crump JA, Mintz ED (2010) Global trends in typhoid and paratyphoid Fever. Clin Infect Dis 50:241–246
37. Kossaczka Z, Lin FY, Ho VA, Thuy NT, Van Bay P et al (1999) Safety and immunogenicity of Vi conjugate vaccines for typhoid fever in adults, teenagers, and 2- to 4-year-old children in Vietnam. Infect Immun 67:5806–5810
38. Lin FY, Ho VA, Khiem HB, Trach DD, Bay PV et al (2001) The efficacy of a *Salmonella typhi* Vi conjugate vaccine in two-to-five-year-old children. N Engl J Med 344:1263–1269
39. Ali A, Cui C, An SJ, Haque A, Carbis R (2012) Preparation of immunogenic conjugates of *Salmonella enterica* serovar typhi O-specific polysaccharides (OSP) with Diphtheria toxoid (DT). Hum Vaccin Immunother (Formely Human Vaccines) 8 (2):1–5

Changing Trend of Infectious Diseases in Nepal

Shiba Kumar Rai

Abstract

Many infectious/communicable diseases (IDs) are endemic in Nepal. Until a decade and half ago, IDs were the major cause of both morbidity and mortality accounting 70% for both. However, as a result of various preventive measures implemented by both the state and non-state actors, the overall IDs have shown a changing (declining) trend. The most impressive decline has been seen in the intestinal helminth infection. Though the overall burden of IDs is decreasing, several newer infectious diseases (emerging infections) namely, dengue fever, scrub typhus, influenza (H5N1 and H1N1), and others are posing a great public health problem. On the other hand, though sporadic, outbreaks of endemic diseases together with HIV-TB coinfection and infection with drug resistance microbes during recent years have constituted a serious public health as well as medical problem. On the contrary, with the decline of IDs, noninfectious diseases (noncommunicable disease, NCD) namely, diabetes, cancer (and cancer therapy), and others are on the rise particularly in urban areas. Hence, currently Nepal is trapped in "double burden" of diseases. Risk of opportunistic infection has increased in immunocompromised person with NCD. To address the present situation, the multi-sectoral plan and strategies developed must be implemented effectively.

Keywords

Infectious diseases · Communicable diseases Nepal

Introduction

Federal Democratic Republic of Nepal is a brick-shaped small land-linked country situated in South Asia between China in the north and India in the south, east, and west. Nepal is located at 26° 26′ north to 30° 26′ north latitude and 80° 03′ east to 88° 15′ west longitude. The total area is 147,181 km^2 with a length of about 800 km (east to west) and width of 90 to 230 km (north to south). It lies in high seismic zone; just along the "fault line" of two tectonic plates; the Indian plate

S. K. Rai (✉)
Nepal Medical College, Attarkehl, Gokarneswor-8, Kathmandu, Nepal
e-mail: drshibakrai.nepal@gmail.com

S. K. Rai
National Institute of Tropical Medicine and Public Health Research, ShiGan International College of Science and Technology, Narayangopal Chok, Kathmandu, Nepal

R. Adhikari and S. Thapa (eds.), *Infectious Diseases and Nanomedicine III*,
Advances in Experimental Medicine and Biology 1052, https://doi.org/10.1007/978-981-10-7572-8_3

and Eurasian plate and therefore, earthquake occurs frequently. A devastating earthquake of magnitude M7.8 struck in Gorkha District (80 km north-west of Kathmandu—28.250°N latitude and 84.116°E longitude) on April 25, 2015 causing severe impact (both direct and indirect) on human health and economy [1, 2].

Administratively, Nepal is divided into seven provinces, 75 Districts, and 744 local levels (*Sthaniya Taha*) (Metropolitan cities = 4; Sub-metropolitan cities = 13; Municipalities = 246 and Village Councils = 481). Ecologically, it is divided into three broad regions; Mountain (subalpine and alpine region) (>3,000 m to as high as 8,848 m), Hill (subtropical and temperate region) (1,000–3,000 m), and *Terai* (plain and tropical area) (1,000 m). Hence, Nepal has highly diversified ecosystem with various kinds of flora and fauna including microbiota. However, the ecosystem in Nepal is threatened by multiple factors such as loss, degradation, and alteration of natural habitats, overexploitation, alien species invasion, pollution of water bodies, and others including natural disasters, climate change, demographic changes, poverty, and weak law enforcement [3].

According to census 2011, total population is approximately 27 million, out of which about one-fifth live in rural (village) setting. Life expectancy at birth is 69 years [4]. The population growth rate is 1.35% (decreased from 2.62% in 1981 to 1.35% in 2011). Literacy rate is 65.9% (increased from 23.3% in 1981 to 65.9% in 2011) though still there is a gap of 17.7% between males (75.1%) and females (57.4%).

Total fertility rate has been reduced by half during the last two decades (4.6 births per women in 1996 to 2.3 births per women in 2016) [5]. Maternal health care has improved significantly (antenatal care by skilled provider increased from 44% in 1996 to 84% in 2016; delivery at health facility increased from 18% in 1996 to 57% in 2016; and delivery attended by skill provider increased from 19% in 1996 to 58% in 2016). Vaccine (such as BCG, DPT, Polio, Measles) coverage has also increased significantly (43% in 1996 to over 78% in 2016). Nutritional status on children has also improved (stunting 57% 1996 has decreased to 36% in 2016; wasting 15% in 1996 to 10% in 2016; and underweight 42% in 1996 to 27% in 2016). Because of all these, neonatal, infant, and under-five mortality rates have also reduced significantly (neonatal mortality rate: 50 in 1996 to 21 in 2016; infant mortality rate: 78 in 1996 to 32 in 2016; and under-5 mortality rate: 118 in 1996 to 39 in 2016). Because of these achievements, Nepal has been awarded "Child Survival Award" (2009) by GAVI (global alliance for vaccines and immunizations) and "UN MDG-5 Award" (2010) by UN for its achievement in progress child health and maternal health, respectively.

Infectious Diseases in the Past

Planned development of health sector in Nepal began with the first planned development process that began in 1956 (2013 BS). The health system now has been widely expanded in the country. Until two decades ago, infectious diseases (mainly water and airborne diseases including rabies, tetanus, and others) were the common cause of morbidity and mortality in Nepal. About 70% of all health problems and cause of death was associated with infectious diseases [6, 7]. Many children were dying due to easily preventable communicable diseases primarily diarrhea and/or dysentery, typhoid fever, tuberculosis, and other respiratory infections. Until two decades ago, intestinal parasitic infection in some communities was very high (over 70%) and multi-parasitic infection was common [8–11]. Among the soil-transmitted helminth infection, *Ascaris lumbricoides* infection alone was over 75% in some communities with a mean annual prevalence of 35% among patients visiting a teaching hospital in capital city, Kathmandu [10–12]. Over one-third of soil samples tested revealed helminth parasites eggs [13].

High prevalence of soil-transmitted helminth (STH) infection in Nepal was associated with open defecation and in some places, use of feces as fertilizer [10–12]. Until the year 2000, infectious (communicable) diseases were in the top of "top-10 diseases" in Nepal [6, 7, 14]. Many

endemic infectious (communicable) diseases in Nepal, however, have shown a declining trend particularly during the last 10–15 years. Vaccine-preventable diseases such as diphtheria, pertussis (whooping cough), tetanus, polio, measles, and mumps have shown sharp decline. In addition, waterborne and food-borne infectious diseases such as diarrhea, dysentery, typhoid (enteric) fever, hepatitis (A and E), and intestinal parasitic infections particularly the soil-transmitted helminth (STH) infections are also decreasing [10, 15].

High morbidity and mortality rates due to infectious diseases in the past were associated mainly with poor sanitary and hygienic condition of people [6, 7, 11]. Infectious diseases as the cause of death among Nepalese, however, have come down to 49.7% in 2007 from 70% in the year 2000 [6, 7, 16]. However, epidemic-prone diseases, such as cholera and acute gastroenteritis, are endemic in all regions of the country with a constant threat to the public health system [17].

Water and Food-Borne Infection

Diarrheal Diseases

Until a decade ago, diarrheal disease (including cholera and dysentery) was in second position in the list of "top-10 diseases" [18]. However, now the position (rank) has gone down below of the disease list. Nevertheless, diarrhea still constitutes one of the most common causes of morbidity and mortality among children especially among under-five children. Approximately four percent of deaths are associated with diarrheal disease. Enteropathogens have been detected in over two-third of diarrheal feces [19]. Among the travelers, diarrhea is usually caused by *Campylobacter*, enterotoxigenic *Escherichia coli* (ETEC), *Shigella* sp., *Vibrio cholerae*, *Giardia lamblia*, *Entamoeba histolytica*, *Cyclospora cayetanensis*, and *Cryptosporidium parvum* including *Rotavirus* and other viruses [20].

Parasitic diarrhea and dysentery: Different intestinal protozoa causing diarrheal disease include *G. lamblia*, *E. histolytica, C. cayetanensis*, and *C. parvum* are commonly implicated. *E. histolytica* is implicated also in dysentery. Though intestinal helminth parasite has been declined significantly, prevalence of protozoan parasites (*E. histolytica* and *G. lamblia*), remained stable over the time, with higher prevalence of *G. lamblia* in urban areas [15]. Up to 43% of water samples tested in Kathmandu Valley have shown *Giardia* cysts suggesting that most of the infection occurs due to drinking of contaminated water [21]. To address this issue, "ODF (open defecation free) Campaign" has been launched under the "Sanitation and Hygienic Master Plan-2011" of Government of Nepal [22].

Bacterial diarrhea and dysentery: Diarrheal disease-causing bacteria include enterotoxigenic *Esherichia coli* (ETEC), *Shigella* sp., *Campylobacter* sp., *Vibrio cholerae*, and others. This is mainly attributed to bacterial contamination of drinking water, which is very common in Nepal [23].

Cholera has remained endemic since long time to till date with several big epidemics in the past even in Kathmandu Valley and elsewhere in the country. Largest cholera outbreak occurred in Jajarkot District and neighboring Districts in 2009; affecting thirty thousand and causing more than 500 deaths [24]. Up to 26.3% diarrheal cases have been found associated with *V. cholerae*. Most of the *V. cholerae* as well as other bacterial isolates are multidrug resistant. Cholera outbreak due to drug-resistant *V. cholerae* serogroup O1 biotype El Tor serotype Ogawa in Nepal has also occurred (2012). Among the *Vibrio* species, *V. cholerae* has been isolated in 43.5% of sewerage/river system in Kathmandu Valley [25]. All *V. cholerae* isolates we isolated in 2016 rainy summer had O1*rfb* gene and were positive for virulence gene such as *ctxA*, *ctxB*, *tcpA*, *tcpI, hlyA, rtxA, rtxC, rstR, zot,* and *ace*.

Viral diarrhea: It is mainly caused by *Rotavirus*. However, in few cases, *Norovirus* and Adenovirus are also detected [26]. Up to 32.3% of diarrheal cases are found associated with Rotavirus of genotypes: G12P [6] (32.9%) and G1P [8] (19.5%) [27, 28]. Of the *Norovirus*, genotypes: GII.4 Sydney (34.6%) and GII.7 (19.2%) are common.

Typhoid Fever

Typhoid fever caused by *Salmonella enterica* serovars Typhi and Paratyphi A (*S.* Typhi and *S.* Paratyphi A) is endemic in Nepal with peak during pre-monsoon and monsoon season. It is common mainly in communities with poor environmental sanitation leading to the contamination of drinking water and poor hygienic condition [23]. Enteric fever is seen to affect young population. However, year to year numbers of enteric fever cases have been seen slightly decreasing as recorded at one of the tertiary level hospitals in Kathmandu Valley but yet causing a considerable burden (*S. enterica* serovars Typhi: 68.5% and *S. enterica* serovars Paratyphi A 31.5%) [29]. The decrease in the number of enteric fever cases during recent years appears to be attributed to the improvement of sanitary and hygienic condition even in the rural areas primarily because of open defecation free campaign [22]. Outbreaks occur occasionally and some of times due to multidrug-resistant organism spread from a single point source [30] (Fig. 1).

Interestingly, enteric fever due to *S. enterica* serovars Paratyphi A is increasing in Nepal (from 25.0% in years 1993–1997 to 41.0% in years 2008–2011 [31]. Though drug resistance in the organisms was a great problem in the past, meta-analysis has shown to significantly decrease in the odds of multidrug resistance (MDR) over time for both *S. enterica* serovars Typhi and *S. enterica* serovars Paratyphi A ($P < 0.01$); however, prevalence of MDR *S. enterica* serovars Paratyphi A was lower at each time block compared with *S. enterica* serovars Typhi [31].

Viral Hepatitis (A and E)

Waterborne viral hepatitis caused by *Hepatitis A* virus (HAV) and *Hepatitis E virus* (HEV) is common in Nepal with occasional epidemic. Anti-HAV antibody has been reported in 99.1% of study population indicating almost everyone in the community is exposed to HAV [32]. However, the Kathmandu Valley is considered to be hyperendemic of HEV and is responsible for acute hepatitis [33]. Recently, in 2014, big outbreak of hepatitis due to HEV occurred in Biratnagar (second largest city in the country) [34]. This is mainly associated with fecal contamination of drinking water everywhere in the country [23].

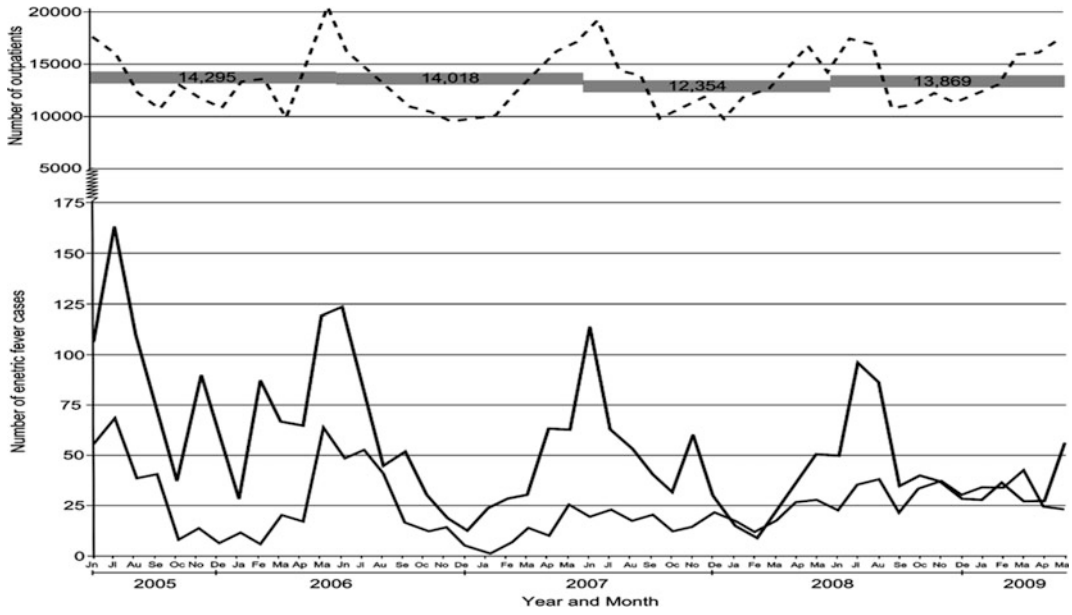

Fig. 1 Enteric fever case burden in patients attending a tertiary level hospital in Kathmandu Valley (2005–2009) [29]

Air Borne Infections

Acute Respiratory Infection

ARI caused by various kinds of pathogens is an important public health problem in Nepal particularly among under-five children. Many people suffer several episodes of ARI, many of them are self-resolved while others develop severe and complicated ARI and some even with fatal outcome. Recently, many "flu outbreaks" caused by various strains. Influenza A viruses have occurred across the country (*details are given in "emerging infection" section*). Both community and hospital-acquired (nosocomial) lower respiratory tract infections caused by MDR pathogens are on the rise. However, ARI has shown a declining trend (both in new cases: 33.37% in 2004/2005 to 31.0% in 2006/2007 and new severe cases: 2.1% in 2004/2005 to 1.2% in 2006/2007) [35]. Currently, ARI cases in under-five children are believed to be about 7.0% [36] with higher case in winter season and are associated mainly with both indoor and outdoor pollution, low socioeconomic status and nutritional condition.

Tuberculosis

Tuberculosis (TB) was one of the most important causes of public health problems in Nepal since a long time. Till one and half decade ago, TB estimated to cause 8,000–11,000 deaths per year. In the year 2000/01, over 31,000 TB patients were registered and treated under the National Tuberculosis Program (NTP), of which 13,000 were new smear positive [37]. The TB control program has achieved its goal in controlling TB significantly primarily due to effective case detection and treatment by DOTS (introduced in 1996) (with success rates of 85% or greater). However, TB remains as one of the major public health problems in Nepal and considered to be disease of poverty (malnutrition). According to Annual Report 2014, a total of 37,025 cases of TB were registered in 2014 out of which 51.0% were pulmonary TB mostly in people aged 15–24 years [38]. According to report, TB-HIV co-infection rate in Nepal is 2.4% (HIV among TB) and 11.6% (TB among HIV) based on the sentinel survey, 2011/12 and the TB program has saved 31,187 lives in 2014 nationally, but still 1049 deaths were reported among general TB cases [38]. However, there is big challenge of multidrug-resistant TB. Currently, 45% of total population is infected with TB, 40,000 people are infected with TB every year; 20,000 new sputum positive cases every year and 5000–7000 people die each year from TB [39].

STH and Other Infections

The decreasing trend of STH infection seen in the past (1986–1992) has been speeded up during the last one and half decade specially after the introduction of deworming program at school, improvement in environmental sanitation and freely available antihelminthic drugs at the healthcare facilities [10]. As a result, according to a systematic review, a sharp decrease in prevalence of STHs among school-aged children in Nepal in last decade with prevalence dropping below 5% for each of STHs with no variation in prevalence in rural and urban areas has been achieved (Fig. 2) [15]. Intestinal parasites particularly STH are known to cause malnutrition and its associated manifestations. Previous studies from Nepal have established that STH cause anemia, vitamin A deficiency, and other micronutrient deficiency among Nepalese [40, 41]. This might have contributed in the decreasing proportion of malnourished children during recent years [5].

Rabies

Though epidemiology and impact of rabies in Nepal are not known well, rabies is endemic in Nepal since long time. As more than 75% of the total anti-rabies vaccine used in Nepal was being used to treat the victims of dog bite cases in Kathmandu Valley, government launched rabies control program with killing of stray dogs in the valley and with the production of rabies vaccine

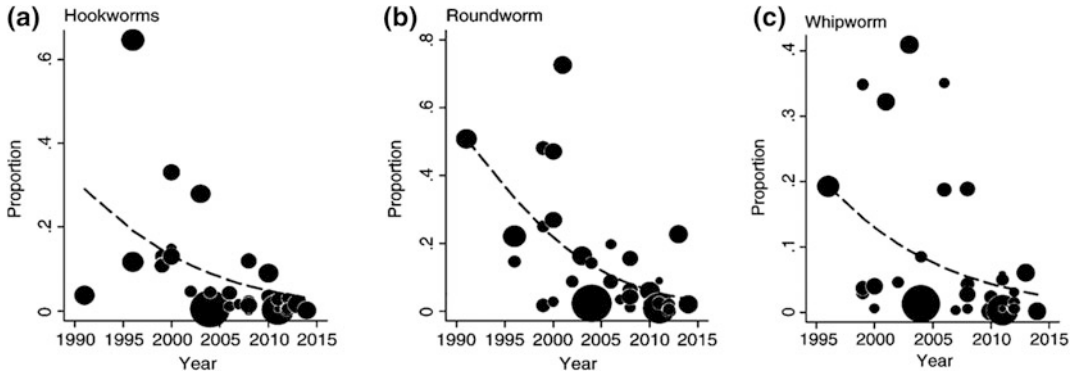

Fig. 2 Sharp decrease in the prevalence of STH in Nepal past decades [15]

within the country. Also, different non-state actors have been conducting rabies control activities over the years [42, 43]. During the period of 1992–1996, a total of 181 human rabid cases were reported (diagnosed clinically; among them one which was diagnosed by mouse inoculation) and were from 37 different Districts with the history of dog bite [44]. Per year, rabies is reported to kill about 100 livestock and 10–100 humans, while about 1,000 livestock and 35,000 humans are reported to receive rabies postexposure prophylaxis, however, these estimates are very likely to be serious underestimations of the true rabies burden [45] (Fig. 3).

Ocular Infections

Ocular infections (conjunctivitis, retinitis, blepharitis and others) caused by bacteria and fungi are common in Nepal. Few cases of ocular cysticercosis, toxoplasmosis, and toxocariasis have also been reported [11]. Recently, Herpes virus associated eye disease is reported to be 10.3% [46]. Epidemic of acute hemorrhagic conjunctivitis occurs on every 2 to 3 years and is found

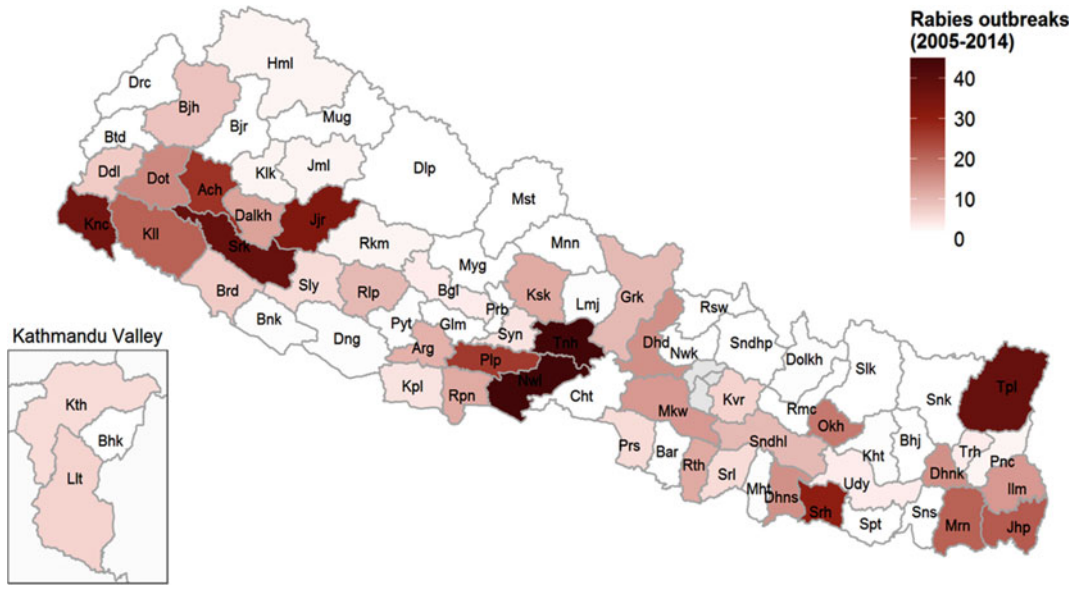

Fig. 3 Map of rabies outbreak in Nepal (2005–2014) [45]

to be associated with viruses such as *Adenovirus* and *Coxsackie virus* [47]. Interestingly, a mysterious ocular manifestation known as SHAPU (seasonal hyperacute panuveitis) predominantly affecting the children is reported only from Nepal [48]. It is presumed to be associated with a white *Tussock* moth however; bacteria (*Streptococcus pneumoniae* and *Acinetobacter* sp.) have also been isolated from SHAPU patients with granulomatous inflammation [48, 49].

Helicobacter Pylori Infection

Helicobacter pylori infection is common in Nepal. The reported prevalence in gastroduodenal diseases (as studied by rapid urease and serological tests, reportedly ranged from 39.0 to 86.6% [50]. In a study, 29.5% endoscopied biopsy materials taken from patients with gastroduodenal complaints were positive *H. pylori* [50]. Histological study has shown prevalence of *H. pylori* in 50.5% [51]. *H. pylori* antibody has been found 16.7% of children (5–16 years) with recurrent abdominal pain indicating that exposure to bacteria begins from small age [52]. Drug resistance in *H. pylori* isolates has been a challenge.

Sexually Transmitted Infections (STI)

STI is common in Nepal but the data are scarce as most of the studies are carried out in high risk groups. Among the patients visiting the tertiary care center for sexually transmitted diseases, majority were of 15–24 years with male to female ratio of 3.19:1 and 52.3% were married [53]. The common STI included genital wart, syphilis, gonorrhea, nongonococcal urethritis, *Herpes simplex virus* infection, HIV/AIDS, and moluscum contagiosum were more common, and according to occupation, students were most common followed by security personnel, housewives, businessmen, unemployed, transport staffs, and others.

HIV infection first reported in 1985 reached its peak in 2005–2009 and then has shown a slow declining trend every year. Currently, over 60,000 people are estimated to be infected and common among sexually active age group particularly among male migrant workers. Overall HIV prevalence in Nepal is estimated at 0.30% in the adult population and it is categorized as a concentrated epidemic [54]. The TB-HIV co-infection rate (the prevalence of HIV infection among TB patients) in Nepal is 2.4% [55].

Two-third of patients had polygamous relationship and married person living singly had more frequent extramarital sexual contact; most common type of partner for sex debut was wife/husband followed by friends and others including commercial sex workers, and patients aged 15–24 years had multiple (2–4) sex partners [53]. Of the patients studied, only 7.7% used condoms consistently [53]. One study showed high STI prevalence among drivers/conductors and migrant workers of sexually active age group [54]. Hence, STI is more common in Districts with highways running through. When, these sexual behaviors and relationships are considered, STI in the community appears to be spreading fast but go unrecorded as many patients get treated confidentially at private clinics. Therefore, the burden of STIs appears to be huge in Nepal [54].

Endemic Vector-Borne Infections

Japanese Encephalitis (JE)

JE in Nepal is endemic in *Terai* (plain) region and constitutes a big public health problem since its entry in 1978 during which similar big outbreak occurred in Indian State of Uttar Pradesh [56]. Cases start to appear in the month of April–May and reach its peak (in thousands) during August–September and declines from October with an average annual mortality rate of 150–300. In 2005, a total of 26,667 cumulative JE cases and total of 5,381 cumulative deaths with average case fatality rate of 20.2% since 1978 was reported [57]. More than 50% of morbidity and 60% of mortality occurred in children (aged below 15 years). JE initially confined in *Terai* with hyperendemicity in western *Terai* Districts has now spread to hilly and even in mountain regions as emerging infectious disease [56, 58–60] (Fig. 4).

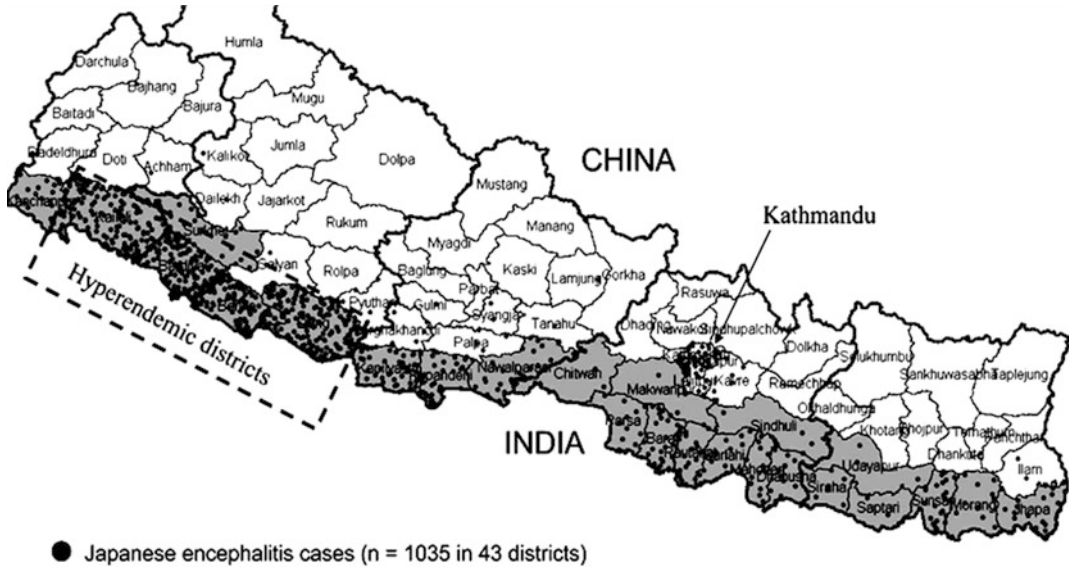

Fig. 4 Distribution of IgM-positive JE cases, May 2004 through April 2006, Nepal. (gray areas in JE endemic areas showing hyperendemicity in western part) [60]

Considering the JE burden and a devastating JE outbreak in 2005 (with 2,000 deaths in poor and rural communities in *Terai* area), mass JE vaccination campaign in JE affected areas was launched in 2006. JE vaccination has shown significant reduction if JE cases in Nepal. A recent impact analysis of immunization showed that vaccination prevented thousands of cases of JE and cut the JE rates in Nepal by at least 78% [61].

Malaria

Despite efforts made to control malaria since 1954, malaria still constitutes one of the major public health problems in Nepal. About 84% of populations were estimated to be at risk of malaria in 2012 with 4% at high risk [62]. About one million people live in areas with a reported incidence of more than one case per thousand populations per year [63]. The recorded confirmed malaria cases from 1963 to 2012 showed highest peak in 1985, after which, as a result of various malaria control efforts made, a significant decline in malaria cases (12,750 in 2002 vs. 2,092 in 2012; decline by 84%) has been observed with some outbreaks in between [62].

Though incidence of malaria has declined sharply during last two decades, malaria is spreading to hilly and even mountainous regions (mainly in river valley/belt and foot hills) as well (Fig. 5 Left) [64]. This appears primarily due to vector adaptation and north–south roads linking endemic *Terai* area and hilly/mountain region and climate change [3]. It is noteworthy that the incidence of indigenous malaria in Nepal is decreasing during last one decade, however, on the contrary, the incidence of imported malaria cases is on the rise (Fig. 5, Right) [64]. All most all imported cases are coming from India and are caused by *Plasmodium falciparum* most of which are drug resistant.

Considering the gravity of malaria burden, Nepal Malaria Strategic Plan 2011–2016 has a vision of malaria-free Nepal by 2026 and is based on the "Long Term National Strategy of Malaria Elimination" [65]. However, there are challenges of increasing entry of malaria cases through open border between Nepal and India, limited access to diagnostic facilities to clinically confirm suspected cases and their treatment, the development of resistance in parasites and vectors, climate change, and shifts of malaria

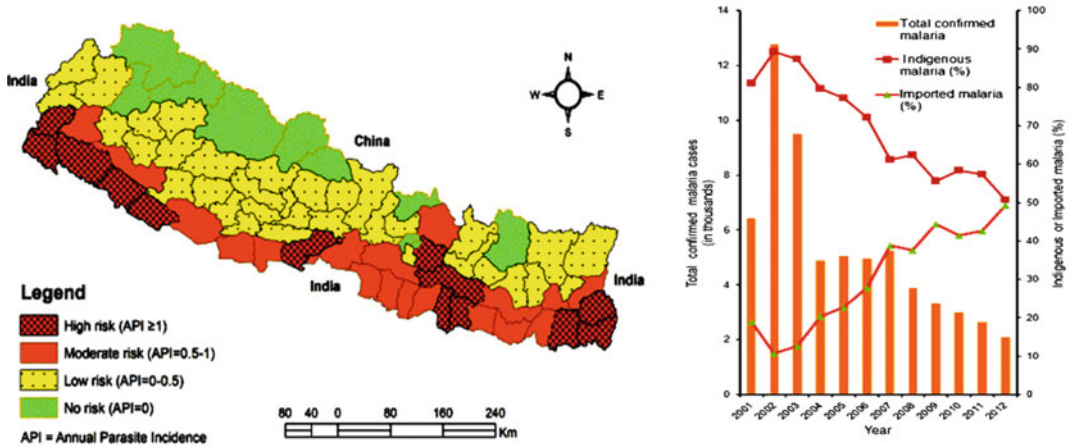

Fig. 5 Classification of malaria risk Districts in Nepal with annual parasite incidence (left) and malaria cases by origin (right) [62]

hotspots to new areas and stable persistence of malaria hotspots in specific areas despite more than 6 years of continuous vector control intervention [3, 62, 64].

Visceral Leishmaniasis (Kala Azar)

Visceral leishmaniasis commonly known as *Kala Azar* (KA) is one of the major public health problems in Nepal and is primarily confined to 12 low altitude tropical climate Districts in eastern *Terai* belt bordering the state of Bihar (India). The annual incidence of KA from 1980 to 2006 is shown in Fig. 6. The average incidence for the years 2004–2006 was about 2.43 per 10,000 populations in the 12 KA endemic Districts of Nepal. It is associated with low socioeconomic status, low literacy rate, and lack of good governance. To address the problems associated with poverty, government has implemented a plan to eliminate the KA from Nepal by 2015 with the reduction of poverty incidence from existing poverty 27% (2010) to at least 16% in KA endemic areas [66, 67]. Because of the implementation of comprehensive KA elimination plan and program, total KA cases and deaths have shown a significant decrease during last 13 years (Fig. 6). However, KA has shown changing epidemiology recently (cases endemic only in eastern *Terai* region have now spread to western *Terai* as well as some hilly Districts) [67].

Lymphatic Filariasis

Lymphatic filariasis (LF) caused by nematode *Wuchereria bancrofti* is endemic in Nepal with great public health impact. Mapping has shown 13% average prevalence in the country (ranging from <1% to as high as 39%) [68]. Keeping in view of the findings, Epidemiology and Disease Control Division is now implementing the National Plan of Action (2003–2020) aimed to eliminate the LF from Nepal. For this, "mass drug administration" (MDA) (Diethylcarbamazine and Albendazole) initiated in Parsa District in 2003, now scaled up to other endemic Districts as well (56 Districts out of 75 have been included). As a result, LF has shown a declining trend during recent years. However, five rounds of MDA were not sufficient to disrupt the transmission cycle in all Districts, probably because high baseline prevalence has posed as a challenge [69].

Opportunistic Infections

Opportunistic infections are increasing in Nepal during recent years. It is associated mainly with the spread of HIV/AIDS and increase of noncommunicable diseases (NCD) like diabetes, malignancies (cancer), chemotherapy/radiotherapy for malignancies, and organ transplantation that augment

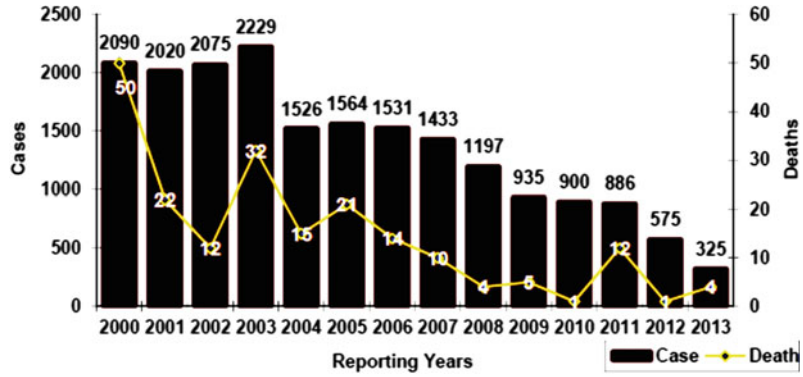

Fig. 6 Trend of *Kala Azar* cases and deaths in Nepal (2000–2013) [67]

immunodeficiency. TB and HIV co-infection is an important example; although TB was common pre-HIV/AIDS era also and was primarily associated with poverty and undernutrition/malnutrition that contribute to immunocompromization and with unavailability of diagnostic and treatment facilities [7, 55].

Opportunistic parasitic infection: Of the various opportunistic parasitosis, cryptosporidiosis is prominent. The prevalence in patients with diarrhea ranges from 0.4 to 17.0% [19, 70–72]. It is more common among young children compared to older people. Among the school going children, it is reported to be 29.4% [73]. Most of *Cryptosporidium* infections are associated with other intestinal protozoan and helminth parasites [72]. Infection is more common during rainy summer season. Nearly half (48.6%) of the young calves of cattle (cow and buffalo) are positive for *Cryptosporidium* oocysts suggesting that calves' feces are the major source of infection in Nepal [74].

Enteric parasites are reported to cause diarrhea (31.13%) of the HIV-seropositive patients. The majority of infections were among patients with CD4 count <200 cells/μl associated with opportunistic parasites (*Cryptosporidium*, *Cyclospora* and *Isospora*) [75]. Seven percent of HIV positive individuals were found infected with opportunistic coccidian protozoa [76]. One study of parasites in HIV/AIDS patients showed *Cryptosporidium* (10.7%), *Giardia* (6.7%), *Entamoeba histolytica* (5.33%), *Cyclospora* (2.67%), *Strongyloides stercoralis* (2.7%), and *Trichuris* (2.67%) [77]. Infection rate was higher in AIDS patients (61.5%) compared with 25.8% HIV-seropositive patients. *Cyclospora* has been detected in nearly 15% of diarrheal fecal samples and in vegetables samples collected in Kathmandu [25, 70, 78].

Toxoplasma gondii (coccidian protozoa) infection rate among apparently healthy population living in different geographical areas ranged from 24 to 76.1% with an average of 45.6% [79, 80]. Overall prevalence is significantly higher in females than in males, similarly higher prevalence is seen among *Tibeto-Burman* compared with *Indo-Aryans* [80]. Region wise higher prevalence is in western region followed by eastern and central regions, respectively. High prevalence is associated with the raw meat eating habits of locals [81]. There is high prevalence in common meat animals (pigs, goats, buffalos and chickens) in Nepal [82]. Prevalence is higher (55.4%) in pregnant women and women with bad obstetric history. Patients with malignancy (cancer) had highest prevalence (68.7%) and must be due to an opportunistic infection [83]. However, till now only one case of congenital toxoplasmosis has been reported [84] (Fig. 7).

Opportunistic fungal infection: According to a recent review, 2% of total populations are estimated to suffer from serious fungal infections (namely, keratitis is (approx. 73 per 100,000), chronic obstructive pulmonary disease allergic bronchopulmonary aspergillosis and severe asthma due to fungal sensitization, chronic pulmonary aspergillosis) in Nepal annually [85]. According to review, of the 22,994 HIV patients with CD4 counts <350, but not on antiretrovirals,

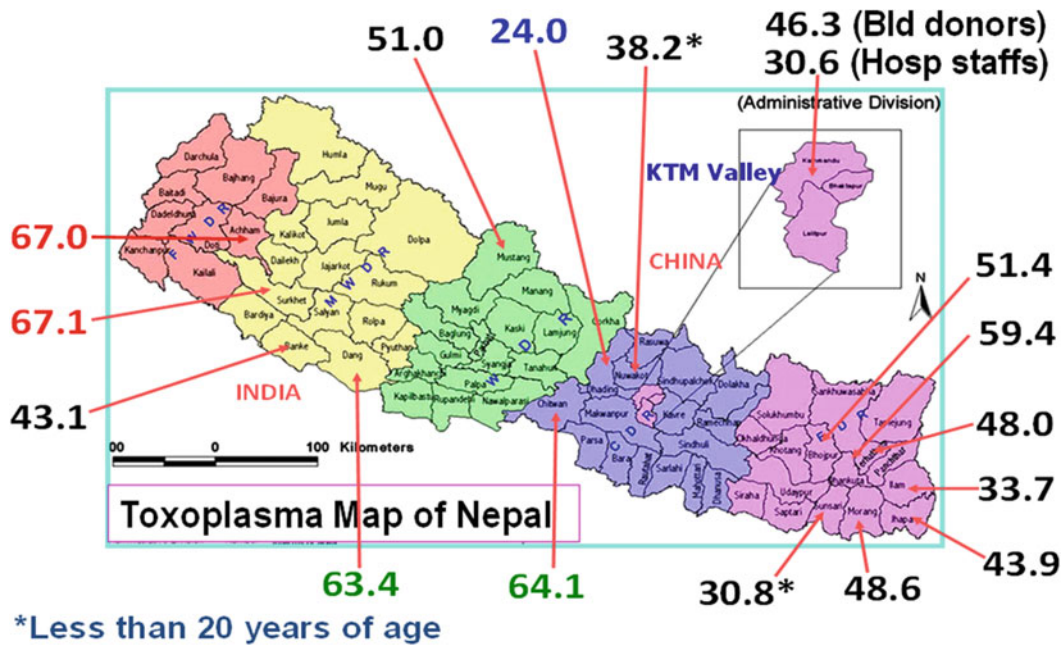

Fig. 7 Scenario of *Toxoplasma* infection in Nepal

Pneumocystis pneumonia infections are estimated at 990 annually. Cases of oral and oesophageal candidiasis in HIV/AIDS patients were estimated at 10,347 and 2950, respectively. Sporadic cases of opportunistic fungal infections have been reported in patients with diabetes, malignancies, and patients undergoing treatment of malignancies. Findings of review of published papers together with mycology expert indicate that there is significant burden of serious fungal infections in Nepal [85, 86].

Hospital Acquired Infection (HAI)

HAI also known as nosocomial infection is a great concern in Nepal though it is said to be improving with time (between 2003 and 2011) at some hospitals [87]. However, infection control committee (ICC) was established in 41.2% (7/17) of the hospitals and of them regular ICC meeting was held in only two hospitals; ICC's operational activities were far from adequate [87]. Accordingly, none of the hospitals studied had an infection control team (ICT). Common HAI causing bacteria in Nepal includes *Staphylococcus aureus*, *Pseudomonas aeruginosa*, *Acinetobacter* sp., *Escherichia coli, Klebsiella* sp., *Enterobacter* sp., *Citrobacter* sp., *Proteus* sp., and others. Most of these HAI bacterial isolates are MDR. These bacteria are mainly associated with urinary tract infection, ventilator-associated pneumonia, surgical site and implant-associated infection, catheter site infection, and soft tissue infections. This is primarily due to high microbial (bacteria and fungi) burden in hospital environment and high pathogen career rate among staffs (hands: 59.2% and nose: 73.7%) mainly *S. aureus* and most of them were highly drug resistant) [88].

Zoonotic Helminthes Infections

Hydatid disease (Echinococcosis) and Cysticercosis: Echinococcosis (hydatid cyst) in different organs has been reported from Nepal but the prevalence in the community is largely unknown [89]. An unusual and interesting case of uncomplicated hydatid cyst in lung (single cyst

of 8 cm) and in liver (two cysts of 7.5 cm each) in a 6-year-old girl has also been reported [90]. As in the case of hydatid cyst, prevalence of cysticercosis is also not known. However, it is suggested that the prevalence ranges from 0.002 to 0.1% in general population in Nepal [91]. Of the total 23,402 biopsied cases recorded at a hospital in Kathmandu Valley, 62 (0.3%) were diagnosed as cases of cysticercosis [89]. The cases of ocular and/or neurocysticercosis are on the rise and thought to be due to the availability of diagnostic facilities (particularly the CT and MRI) during recent years. As reviewed by Rai, there are sporadic reports on other zoonotic parasites [89]. The reported seroprevalence of *Toxocara* antibody is very high (81.0%) though the clinical cases of toxocariasis (visceral and/or ocular larva migraines) are not very common [92]. *Toxocara* eggs rank second (accounting 22.8%) among the helminth eggs contaminating the environment (soil) in Nepal1 [13]. Very rarely, cases of trichinosis, fascioliasis, paragonimiasis, and sparganosis have also been reported [89].

Emerging Infections

Though the overall rate of infectious diseases in South Asia is decreasing, the challenges of existing infectious diseases such as tuberculosis, HIV/AIDS, malaria, and others have been augmented by emerging and growing threats of dengue, chikungunya, healthcare-associated infections, and antimicrobial resistance [93]. Nepal is facing also the challenges of new vector-borne infectious diseases. *Culex* mosquito borne JE first appeared in Nepal in 1978 and limited in western *Terai* area has shown a changing epidemiological pattern (now has spread even in hilly areas) [56–60]. JE still constitute a public health problem despite the immunization against Japanese B encephalitis virus.

Dengue fever (*DF*): First case of *Aedes* mosquito-borne *Dengue virus*, was reported in 2004 from Chitawan District [94]. Since then, *Dengue virus* infection has spread in big way with a series of DF outbreaks in several Districts of Nepal [95–97]. Dengue IgM antibody among feverish patients has been seen in 27.8% to 29.1% with highest prevalence among children (<15 years) [98]. The disease is common during monsoon and post-monsoon season and affects mainly young adults (aged 21–40 years). A shift in *Dengue virus* serotype, serotype 1 in 2010 outbreak to serotype 2 in 2013 outbreak has also been observed [96] (Fig. 8).

The spatiotemporal analysis (2010–2014) has shown that Chitawan District (home for first case of DF) is the hotspot of DF followed by Jhapa and Parsa Districts [99]. Now, *Dengue virus* is spread even in hilly areas including Kathmandu Valley [99]. This has been thought to be associated with change in climate and biodiversity [3, 100–102]. DF and dengue hemorrhagic fever (DHF) might have been underestimated as many cases might have been misdiagnosed and/or undiagnosed. Among the various emerging infections in Nepal, DF has been a great health public problem, however, precise burden of DF and DHF in Nepal remains unknown, since most reports are confined to economically affluent city and/or town areas and do not account for regions of relative social deprivation where disease is more likely to occur [97].

Other emerging viral infections: Very recently, in 2014, first case of chikungunya (transmitted by *Aedes* mosquito) has also been found in Nepal [103, 104]. Serological study among patients presenting with fever has shown seropositive rate of 3.6% [105]. A case of chikungunya has been found even in Kathmandu Valley. West Nile virus infections (usually transmitted by *Culex* mosquito) and *Chandipura virus* (transmitted by *Phlebotomus* sand fly and earlier limited in Chandipura Village of Maharashtra, India) have also been reported from Nepal [106].

Influenza virus: Influenza A virus (H5N1) (avian influenza or bird flu) appeared in Nepal in 2009 with first confirmed outbreak in far-eastern Nepal (called Kakarbhitta) close to Indian border and subsequently, outbreaks occurred in Kathmandu and Bhaktapur Districts in Kathmandu Valley as well as other parts outside of valley causing millions of poultry were died/destroyed

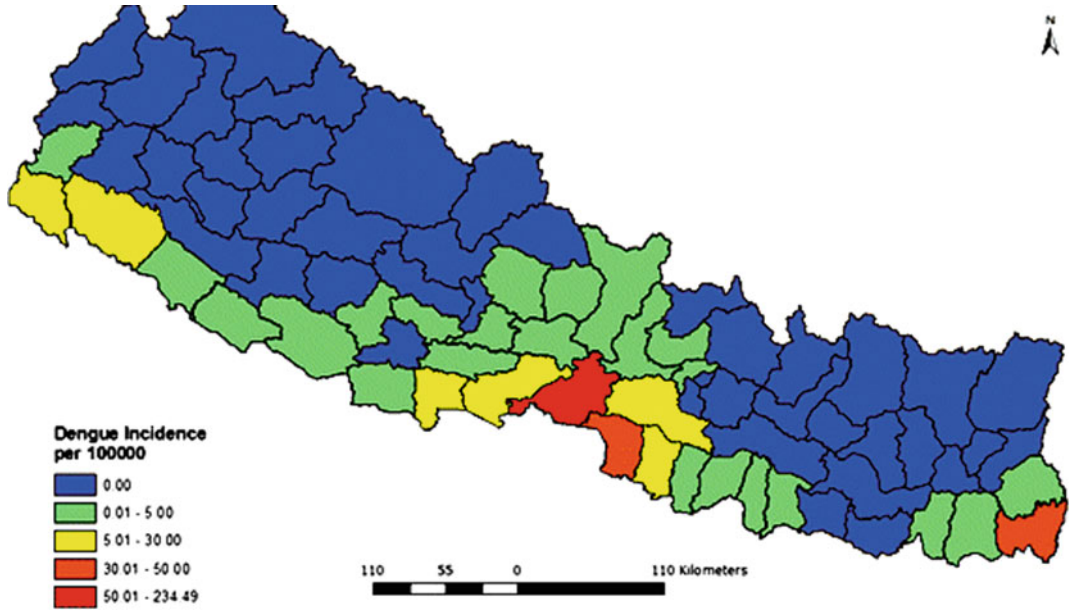

Fig. 8 Annualized average incidence of dengue fever in Nepal (2010–2014) [99]

[107]. Many outbreaks occurred in the year 2013. This resulted into great loss in economy particularly to poultry farmers and farm associated business (egg, meat, and feed business). As a result, government provided compensation to the poultry farmers and businesses concerned for the loss of chicks, eggs, bird feed, and chicken due to the spread of bird flu at six different places. To control H5N1, special plan, program and activities were launched and Nepal has been declared free of H5N1 highly pathogenic avian influenza (HPAI) in May 2014 [108]. However, another variant of avian influenza (H5N8) has been reported this year in eastern Nepal [109].

An outbreak of *Influenza A* (H3N2) was detected at three Bhutanese refugee camps in southeastern Nepal in July 2004 [110]. Outbreak of Pandemic *Influenza A*/H1N1 occurred in Nepal in 2009. Universal *Influenza A virus* was positive in 49.6%, more than half in young people. Among them 28.3% were H1N1 and 21.3% were seasonal influenza A. Case fatality of H1N1 was 1.74% [111]. After 2009 H1N1 is appearing every year with significant number of fatality. This year (Sept. 2017) alone, H1N1 has appeared as epidemic forcing the closure of school in Syanja District in western Nepal and dozens of deaths occurred across the country [112].

Other emerging viruses: Seroprevalence of *Hantavirus* infection is 8.7% with higher prevalence in *Tamang/Sherpa* ethnics (16.0%) who live mainly in hilly/mountain areas [113]. Though no cases of human *Hantavirus* infection have been reported till date (might have gone undiagnosed) it may emerge as a cause of health problem in future. Other viral infections existing in Asia, namely, *Nipah virus* (discovered in Peninsular Malaysia), Middle East respiratory syndrome coronavirus (MERS-CoV), and Crimean-Congo hemorrhagic fever are not evidenced yet. However, there is high possibility of entering of these infections into Nepal anytime in future considering the fact of climate change, vector and agent adaptation, and biodiversity modification during recent years [3].

Scrub typhus: Though, serological evidence of existence of scrub typhus in eastern Nepal was reported long back in 1981 clinical cases reported in 2015 with high numbers from Chitawan District where in 2004, also the first case of

dengue fever was recorded [94, 114, 115]. In the year 2016, over 800 cases were detected from all over the country out of which 14 (1.7%) died. This year (2017), as many as 37 cases have been reported in Chitawan District alone [115]. Scrub typhus, therefore, has constituted one of the newest and important health problems in Nepal, which demands active surveillance and public health awareness about the disease transmission and prevention.

Leptospira infection: First report on leptospirosis in Nepal appeared in 1981 [116]. In 2000, Rai et al. reported *Leptospira* seroprevalence rate of 32.0% among apparently healthy people with equal positive rate among males and females, and *Tibeto-Burman* and *Indo-Aryan* ethnic groups [117]. Seropositive rate among the suspected cases of leptospirosis in central *Terai* and in Kathmandu has been reported at 4.8% and 28.6% [118, 119], respectively. However, in western *Terai*, among the 144 febrile cases, 21% have been reported to be positive for leptospiral antibodies (IgM) indicating the acute leptospirosis [120]. Among the undiagnosed cases of acute encephalitis cases, 51.6% were positive and was higher in the age group of 6–15 years [121]. Most of the positive cases are occurring during rainy summer and autumn season and are associated with rain and flooding, and mostly adults are infected.

Emerging protozoan infection: *Cryptosporidium parvum* is reported in 0.4–17% in loose stool in Kathmandu [19, 70]. Up to 25% of water samples tested in Kathmandu Valley have shown *C. parvum* oocyst. The reported *Cyclospora* infection rate is as high as 30% in loose stool in Kathmandu [122]. Two percent of water samples tested in Kathmandu have shown *Cyclospora* oocysts.

Emerging fungal infection: Documented emerging fungal diseases in Nepal are scanty. Supram et al from Manipal Teaching Hospital; Pokhara in Western Nepal recently reported invasive infections in a group of hospitalized patients caused by *Magnusiomyces capitatus*, an emerging yeast [123]. Considering the increasing number of cases of immunocompromising conditions such as diabetes, malignancies, chemo- and radiotherapy for malignancies and HIV/AIDS, the opportunistic fungal infection must be existed but are not reported.

Issues of Bacterial Drug Resistance

Until 1990s, bacterial drug resistance was not common in Nepal. Drug-resistant *Escherichia coli* was reported in 1978 [124]. For the first time, methicillin-resistant coagulase-negative *Staphylococcus* and methicillin-resistant *S. aureus* (MRSA) reported in 1987 and 1990, respectively [125, 126]. In recent studies, over half of *E. coli*, *Klebsiella pneumoniae* and *Streptococcus pneumoniae* isolates were tested, and over 30% of some *Shigella* sp. and *Vibrio cholerae* isolates were resistant to first-line antibiotics and many other important bacterial pathogens are highly resistant to most first-line and some second-line antibiotics [127]. This resulted primarily due to misuse (overuse, underuse due to lack of awareness and lack of purchasing capacity, inappropriate use/prescribing, excessive use of antibiotic in agriculture/animal husbandry) of antibiotics and other drugs in the society.

Though antibiotic use in agriculture/animal husbandry especially animal food is poorly documented in Nepal, it is believed that antibiotics in animal feeds particularly of meat animals (chickens, pigs and others) are being used massively and are contributing to the overall antibiotic resistance. According to Global Antibiotic Resistance Partnership-Nepal (GARP-Nepal), the volume of veterinary antibiotic sales in Nepal rose over 50% from 2008 to 2012, most through retailers without veterinarian prescription [127]. Due to the indiscriminate and prolonged use of antibiotics in meat animals, high level of antibiotic residues has been found in the marketed meat and consumable broiler chicken liver, in particular, showed very high percentage of antibiotic residue [128]. As a result, some organisms have developed not only multi-drug resistance but pan-resistance and have become an alarming public health concern.

Double-Triple Burden of Disease

Though the prevalence/incidence of infectious (communicable) diseases is decreasing in Nepal, noninfectious (noncommunicable) diseases are on the rise. Hence, Nepal is now facing a double burden of diseases. The decrease in infectious diseases is attributed primarily to the health (curative, preventive and promotive) related activities (immunization, increased access in health service, free primary healthcare services including free essential drugs to poor and marginalized people as stipulated health as "fundamental right" in the constitution-2007, production of different levels of human resources on health including specialized specialist within the country and various efforts made by the state and non-state actors). Moreover, more than 52% of the diarrheal cases are being treated by Female Community Health Volunteers (FCHVs), the interface between healthcare facility and community. This may be the reason that spread and outbreak of various infectious diseases predicted after the earthquake 2015 did not occur. Infectious diseases are common in villages, but town and cities are not completely free of infectious diseases. Interestingly, some of the outbreaks of infectious diseases are occurring only in the town and cities. However, the overall prevalence of infectious diseases has come down. However, unusually heavy rainfall, floods, and landslide are creating good environment for the spread of infectious diseases.

Although infectious (communicable) diseases are decreasing, noncommunicable diseases (NCD) together with emerging/reemerging infectious diseases are on the rise in cities. Hence, there is double-triple burden of disease. The diabetes and associated conditions (nephropathy, retinopathy and others), cardiovascular diseases, cancer, and chronic obstructive pulmonary diseases are the major NCDs which are driven by various forces including aging, rapid but unplanned urbanization and unhealthy lifestyles.

Conclusions

Overall burden of infectious (communicable) diseases is decreasing during recent years. However, there is big challenge of tackling the emerging and reemerging infections. At the same time, there is rapid increase of various noninfectious (noncommunicable) diseases that enhances opportunistic infections. To combat the infections of different kinds, WHO recommended five interventions (innovative and intensified disease management; preventive chemotherapy; studies on vector ecology and management; veterinary public health services; and provision of safe water, sanitation and hygiene) which must be implemented together with the global action plan adopted by World Health Assembly-2915 to address the problem of drug resistance (improve awareness and understanding about antimicrobial resistance; strengthen the knowledge and evidence through surveillance and research; reduce the incidence of infection through effective sanitation, hygiene and infection prevention measures; optimize the use of antimicrobial medicines in human and animal health; develop the economic case for sustainable investment that takes account of the needs of all countries and increase investment in new medicines, diagnostic tools, vaccines, and other interventions) [129].

In this regard, Nepal has developed several plans of action. These includes: "ODF Campaign" that has been launched under the "Sanitation and Hygienic Master Plan-2011", "Nepal water supply, sanitation and hygiene sector development plan: 2016–2030" and "Multisectoral Action Plan for the Prevention and Control of Non-communicable Diseases 2014–2020" (developed in accordance to the Global Action Plan for the Prevention and Control of NCDs 2013–2020 and Infectious Disease Control Guideline [22, 130–133]. Habitat destruction and infectious disease are dual threats to nature and people (as emerging infections), biodiversity and nature conservation [102, 103]. To address this,

"National Biodiversity Strategy and Action Plan 2014–2020" has been developed [3]. To facilitate and coordinate all these and others, "High Level Multi-sectoral Health Services Facilitation and Coordination Committee" has also been formed at National Planning Commission in 2012.

References

1. Ulak N (2015) Nepal's Earthquake-2015: its impact on various sectors. J Tourism Hospitality 7:58–86
2. Shrestha AB, Bajracharya SR, Kargel JS, Khanal NR (2016) The impact of Nepal's 2015 gorkha earthquake—induced geohazards. CIMOD (Int'l Centre for Integrated Mountain Devt) Research Report, Kathmandu, Nepal
3. GoN MoFSC (2014) Nepal biodiversity strategy and action plan 2014–2020. Government of Nepal, Ministry of Forests and Soil Conservation, Kathmandu, Nepal
4. CBS (Central Bureau of Statistics) (2012) Nepal Population and Housing Census 2011. Nat'l Planning Commission, Kathmandu, Nepal
5. NDHS (Nepal Demographic Health Survey) (2016) Ministry of Health & New ERA, Kathmandu, & The DHS Program ICF Rockville, USA
6. Rai SK, Rai G, Hirai K, Abe A, Ohno Y (2001) The health system in Nepal-an introduction. Envt'l Health Prev Med 6:1–8
7. Rai SK, Hirai K, Abe A, Ohno Y (2002) Infectious diseases and malnutrition status in Nepal: an overview. Mal J Nutr 8:191–200
8. Rai SK, Matsumura T, Ono K et al (2001) Intestinal parasitoses in an "unknown disease outbreak" hit rural hilly area in western Nepal. Nepal Med Coll J 2:61–64
9. Rai SK, Bajracharya K, Budhathoki S et al (1995) Status of intestinal parasitoses at TU Teaching Hospital. J Inst Med (Nepal) 17:134–142
10. Rai SK, Kubo T, Nakanishi M et al (1994) Status of soil-transmitted helminthic infection in Nepal. Kansenshogaku Zassi (J Jpn Assoc Infect Dis) 68:625–630
11. Rai SK (2005) Parasitic diseases in Nepal. In: Arizono N, Chai JY, Nawa Y, Takahashi Y (eds) Asian parasitology, Food-borne helminthiasis in Asia; Editor-in-chief: Yano A; vol 1. Federation of Asian Parasitologists, Japan, pp 305–18
12. Rai SK, Rai G (1999) *Ascaris*, ascariasis and its present scenario in Nepal. J Inst Med (Nepal) 21:243–250
13. Rai SK, Uga S, Ono K, Rai G, Matsumura T (2000) Contamination of soil with helminth parasite eggs in Nepal. Southeast Asian J Trop Med Public Health 31:388–393
14. DOHS (Department of Health services) (2000) Annual Report, Goverement of Nepal
15. Kunwar R, Acharya L, Karki S (2016) Trends in prevalence of soil-transmitted helminth and major intestinal protozoan infections among school-aged children in Nepal. Trop Med Int Health 21:703–719
16. Suvedi VK (2007) Of what diseases are Nepalese people dying? Kathmandu Univ Med J 5:121–123
17. WHO. WHO Country Cooperation Strategy Nepal 2013–2017 (2013) WHO Country Office, Kathmandu
18. MoHP (Ministry of Health and Population). Fact-Sheet 2007. Government of Nepal, Kathmandu
19. Ono K, Rai SK, Chikahira M et al (2001) Seasonal distribution of enteropathogens detected from diarrheal stool and water samples collected in Kathmandu. Nepal. Southeast Asian J Trop Med Public Health 32:520–526
20. Pandey P, Bodhidatta L, Lewis M et al (2001) Travelers' diarrhea in Nepal: an update on the pathogens and antibiotic resistance. J Travel Med 18:102–108
21. Kimura K, Rai SK, Rai G et al (2005) Study of *Cyclospora cayetanensis* associated with diarrheal disease in Nepal and Lao DPR. Southeast Asian J Trop Med Public Health 36:1371–1376
22. SCNSA (Steering Committee for National Sanitation and Action) (2011) Sanitation and Hygiene Master Plan, Government of Nepal
23. Rai SK, Ono K, Yanagida J-I, Ishiyama-Imura S, Kurokawa M, Rai CK (2012) A large-scale study of bacterial contamination of drinking water and its public health impact in Nepal. Nepal Med Coll J 14:234–240
24. Pach A, Bhattachan A (2014) Understanding cholera in Nepal (Blog Post, Stop Cholera). https://www.stopcholera.org/blog/understanding-cholera-nepal. Aceessed Oct 2017
25. Rai KR, Rai SK, Bhatt DR et al (2012) Study of medically important *Vibrios* in the sewage of Katmandu Valley, Nepal. Nepal Med Coll J 14:212–214
26. Kurokawa M, Ono K, Nukita M, Itoh M, Thapa U, Rai SK (2004) Detection of viral pathogens from diarrheal fecal samples collected from children in Kathmandu, Nepal. Nepal Med Coll J 6:17–23
27. Ansari S, Sherchand JB, Rijal BP et al (2013) Characterization of rotavirus causing acute diarrhoea in children in Kathmandu, Nepal, showing the dominance of serotype G12. J Med Microbiol 62:114–120
28. Sherchand JB, Cuncliffe NA, Tandukar S et al (2011) Rotavirus disease burden and molecular epidemiology in children with acute diarrhoea age less than 5 years in Nepal. J Nepal Pediatr Soc 31:209–215
29. Karkey A, Arjyal A, Anders K et al (2010) The burden and characteristics of enteric fever at a healthcare facility in a densely populated area of Kathmandu. PLoS ONE 511:e13988

30. Lewis MD, Serichantalergs O, Pitarangsi C et al (2005) Typhoid fever: a massive, single-point source, multidrug-resistant outbreak in Nepal. Clin Infect Dis 40:554–561
31. Karki S, Shakya P, Cheng AC et al (2013) Trends of etiology and drug resistance in enteric fever in the last two decades in Nepal: a systematic review and meta-analysis. Clin Infect Dis 57:e167–e176
32. Sawayama Y, Hayashi J, Ariyama I et al (1999) A ten-year serological survey of hepatitis A, B and C viruses infections in Nepal. J Epidemiol 9:350–354
33. Shrestha SM (2006) Hepatitis E in Nepal. Kathmandu Univ Med J 4:530–544
34. Shrestha A, Lama TK, Karki S et al (2015) Hepatitis E epidemic, Biratnagar, Nepal 2014. Emerg Infet Dis (Lett) 21:711–713
35. Ghimire M, Pradhan YV, Maskey MK (2010) Community-based interventions for diarrhoeal diseases and acute respiratory infections in Nepal. Bull WHO 88:216–222
36. Nepal-Prevalence of acute respiratory infection (ARI) (% of children under 5). https://tradingeconomics.com/nepal/prevalence-of-acute-respiratory-infection-ari-percent-of-children-under-5-q1-lowest-wb-data.html. Accessed 30 Oct 2017
37. Hamlet N, Baral SC (2002) Case study of National Tuberculosis Program implementation in Nepal. World Bank
38. NTP (National Tuberculosis Program) (2014) Annual Report. National Tuberculosis Center, Govt of Nepal, Bhaktapur
39. NTC (National Tuberculosis Center) (2017) Govt of Nepal. http://www.nepalntp.gov.np/. Accessed Oct 2017
40. Rai SK, Nakanishi M, Upadhyay MP (1998) Effect of intestinal helminth infection on some nutritional parameters among rural villagers in Nepal. Kobe J Med Sci (Japan) 44:91–98
41. Rai SK, Nakanishi M, Upadhyay MP et al (2000) Effect of intestinal helminth infection on retinol and ß-carotene status among rural Nepalese. Nutr Res 20:15–23
42. KATC (Kathmandu Animal Treatment Center) (2017) Rabies in Kathmandu and Nepal. http://www.katcentre.org.np/situation/rabies.html. Accessed Oct 2017
43. HART (Himalayan Animal Rescue Trust) (2017) Dog population management, rabies control and eradication, animal welfare improvement. http://www.hartnepal.org/programmes/index.html. Accessed Oct 2017
44. Gongal G (1998) Epidemiology of reported human rabies cases in Nepal, 1992–1996. J Inst Med (Nepal) 20
45. Devleesschauwer B, Aryal A, Sharma BK et al (2016) Epidemiology, impact and control of rabies in Nepal: a systematic review. PLoS Negl Trop Dis 10:1–18
46. Chaudhary M (2016) Clinical and epidemiological profile of herpetic eye disease in a tertiary eye care center. J Inst Med (Nepal) 38:3–9
47. Gurung R, Rai SK, Kurokawa M et al (2003) Acute hemorrhagic conjunctivitis epidemic-2003 in Nepal. Nepal Med Coll J 5:59–60
48. Upadhyay MP, Shrestha BR (2017) SHAPU: forty years on mystery persists. Nepalese J Ophthalmol 9:13–16
49. Manandhar A, Paudel G, Rai CK et al (2008) Seasonal hyper acute pan uveitis—series of cases. Nepal Med Coll J 10:196–198
50. Rai SK, Shah RDP, Bhattachan CL et al (2006) Study on *Helicobacter pylori* associated gastroduodenal problem among Nepalese. Nepal Med Coll J 8:9–13
51. Shrestha S, Paudel P, Pradhan GB et al (2012) Prevalence study of *H. pylori* infection in dyspeptic patients coming to Nepal Medical College Teaching Hospital, Jorpati. Kathmandu Nepal Med Coll J 14:229–233
52. Wagley B, Shrestha M, Shrestha L (2017) Prevalence of *Helicobacter pylori* in children with recurrent abdominal pain. J Inst Med (Nepal) 39:55–59
53. Gyawalee M, Pokharel DB (2014) Pattern of sexually transmitted infections and sexual behavior in patients with genital symptoms. Neaplese J Dermatol Veneriol 12:20–27
54. Karn D, Amatya A, Aryal ER, KC S, Timalsina M (2011) Prevalence of sexually transmitted infections in a tertiary care center. Kathmandu Univ Med J 9:44–8
55. NTC (National Tuberculosis Center) (2017) HIV TB Coninfection. http://www.nepalntp.gov.np/index.php?view=page&id=83. Accessed Oct 2017
56. Kubo T, Rai SK, Rawal S, Pokhrel BM, Shrestha HG, Prasai BR (1996) Changing sero-epidemiological pattern of Japanese encephalitis virus infection in Nepal. J Inst Med (Nepal) 18:1–9
57. Bista MB, Shrestha JM (2005) Epidemiological situation of Japanese encephalitis in Nepal. J Nepal Med Assoc 44:51–56
58. Pant SD (2009) Epidemiology of Japanese encephalitis in Nepal (JE Report). J Nepal Pediatr Soc 29:15–17
59. Pant DK, Tenzin T, Chand R, Sharma BK, Bist PR (2017) Spatio-temporal epidemiology of Japanese encephalitis in Nepal, 2007–2015. PLoS ONE 12: e0180591
60. Wierzba TF, Ghimire P, Malla S et al (2008) Laboratory-based Japanese encephalitis surveillance in Nepal and the implications for a National Immunization Strategy. Am J Trop Med Hyg 78:1002–1006
61. Upreti SR, Lindsey NP, Bohara R et al (2017) Updated estimation of the impact of a Japanese encephalitis immunization program with live, attenuated SA 14-14-2 vaccine in Nepal. PLOS Negl Trop Dis 11:e0005866

62. Dhimal M, Agrens B, Kuch U (2014) Malaria control in Nepal 1963–2012: challenges on the path towards elimination. Malaria J (Open access) 13:241
63. WHO. World Malaria Report 2013. Geneva
64. Dhimal M, O'Hara RB, Karki R et al (2014) Spatio-temporal distribution of malaria and its association with climatic factors and vector-control interventions in two high-risk districts of Nepal. Malaria J (Open acess) 13:457
65. DOHS (2011) Nepal Malaria Strategic Plan 2011–2016 (Revised Version-Dec 2011)
66. Adhikari SR, Supakankunti S, Khan MM (2010) Kala azar in Nepal: estimating the effects of socioeconomic factors on disease incidence. Kathmandu Univ Med J 8:73–79
67. DOHS (Department of Health Services) (2014) National Strategic Guideline on Kala-azar Elimination Program in Nepal, Kathmandu
68. EDCD (Epidemiology and Disease Control Division), Department of Health Services, Nepal. http://www.edcd.gov.np/lymphatic-filariasis-program. Accessed Oct 2017
69. Ojha CR, Joshi B, KC KP et al (2017) Impact of mass drug administration for elimination of lymphatic filariasis in Nepal. PLoS Negl Trop Dis 11: e0005788
70. Takemasa K, Kimura K, May SI et al (2004) Epidemiological survey of intestinal parasitic infections of diarrhoeal patients in Nepal and Lao PDR. Nepal Med Coll J 6:7–12
71. Sherchand JB, Shrestha MP (1996) Prevalence of *Cryptosporidium* infection and diarrhoea in Nepal. J Diarrhoeal Dis Res 14:81–84
72. Dhakal DN, BC RK, Sherchand JB, Mishra PN (2004) *Cryptosporidium parvum*: an observational study in Kanti Children Hospital, Kathmandu, Nepal. J Nepal Health Res Counc 2:1–5
73. Sherchand SP, Joshi DR, Adhikari N et al (2016) Prevalence of cryptosporidiosis among school going children in Kathmandu, Nepal. EC Microbiol 4:641–646
74. Bohara TP (2017) Prevalence of *Cryptosporidium* in livestock reared near Mahakali and Karnali River Basins of Western Nepal Nepal. Technical Report: Feed the Future Innovation Lab for Collaborative Research on Adapting Livestock Systems to Climate Change, *TRB-23-2015*. file:///C:/Users/User/Favorites/Downloads/TRB-23-2015.pdf. Accessed Oct 2015
75. Sherchan JB, Ohara H, Sakurada S et al (2012) Enteric opportunistic parasitic infections among HIV seropositive patients in Kathmandu, Nepal. Kathmandu Univ Med J 38:14–17
76. Amatya R, Shrestha R, Poudyal N, Bhandari S (2011) Opportunistic intestinal parasites and CD4 count in HIV infected people. J Pathol Nepal 1:118–121
77. Sapkota D, Ghimire P, Manandhar S (2004) Enteric parasitosis in patients with Human Immunodeficiency Virus (HIV) infection and acquired immunodeficiency syndrome (AIDS) in Nepal. J Nepal Health Res Counc 2
78. Sherchand JB, Sherchand JB, Cross JH (2007) An epidemiological study of *Cyclospora cayetanensis* in Nepalese people. J Inst Med (Nepal) 29:8–13
79. Rai SK (1999) *Toxoplasma*, toxoplasmosis and its possible implication as possible opportunistic pathogen in (review paper). Nepal Med Coll J 1:81–86
80. Rai SK (2005) *Toxoplasma* Infection in Nepal: an overview. In: Yano A, Nam HW, Anuar AK et al (eds) Asian Parasitology, Toxoplasmosis and Babesiosis in Asia; Edit-in-chief: Yano A, vol 4, Federation of Asian Parasitologists, Japan, pp 82–96
81. Rai SK, Matsumura T, Ono K et al (1999) High Toxoplasma seroprevalence associated with meat eating habit of locals in Nepal. Asia-Pacific J Public Health 11:89–93
82. Rai SK, Kubo T, Yano K et al (1996) Seroprevalence of *Toxoplasma gondii* infection in common meat animals and its public health importance in Nepal. J Inst Med (Nepal) 18:55–60
83. Rai SK, Upadhyay MP, Shrestha HG (2003) Toxoplasma infection in selected patients in Kathmandu. Nepal. Nepal Med Coll J 5:89–91
84. Rai SK, Sharma A, Shrestha RK, Pradhan P (2011) First case of congenital toxoplasmosis from Nepal. Nepal Med Coll J 13:64–66
85. Khwakhali Shrestha U, Denning DW (2015) Burden of serious fungal infections in Nepal. Mycoses 58(Suppl):45–50
86. Nayak N (2016) Burden of fungal infections in Nepal. Nepal J Epidemiol 6:584–585
87. Ohara H, Pokhrel BM, Dahal RK et al (2013) Fact-finding survey of nosocomial infection control in hospitals in Kathmandu, Nepal -a basis for improvement. Trop Med Health 41:113–119
88. Pant J, Rai SK, Singh A et al (2006) Microbial study of hospital environment and career pattern study among staffs of Nepal Medical College Teaching Hospital. Nepal Med Coll J 8:194–199
89. Rai SK (2013) Zoonotic parasitic diseases in Nepal. In Tokoro M. Uga S (eds) Parasitic zoonoses in Asian-Pacific Regions, 1st edn. Sankeisha Co, Nagoya, Japan, pp 10–5
90. Shrestha BM, Sharma GP, Rajbhandari KB (1988) Uncomplicated pulmonary and hepatic hydatid cysts. J Inst Med (Nepal) 10:293–296
91. Bista MB (2006) Epidemiology, prevention and control of human cysticercosis/taeniasis in Nepal. In: Joshi DD, Sharma M, Rana S (eds) Proceedings of present situation challenges in treatment and elimination of Taeniasis/cysticercosis in Nepal. Nati'l Zoonoses & Food Hyg Res Centre, Kathmandu. pp 12–4
92. Rai SK, Uga S, Ono K, Nakanishi M, Shrestha HG, Matsumura T (1996) Serological study of Toxocara infection in Nepal. Southeast Asian J Trop Med Public Health 27:286–290

93. Laxminarayan R, Kakkar M, Horby P, Malavige GN, Basnyat B (2017) Emerging and re-emerging infectious disease threats in South Asia: status, vulnerability, preparedness, and outlook. Brit Med J 357:j1447
94. Pandey BD, Rai SK, Morita K, Kurane I (2004) First case of *Dengue virus* infection in Nepal. Nepal Med Coll j 6:157–159
95. Pun SB (2011) Dengue: an emerging disease in Nepal. J Nepal Med Assoc 51:203–208
96. Gupta BP, Singh S, Kurmi R, Malla R, Sreekumar E, Manandhar KD (2015) Re-emergence of dengue virus serotype 2 strains in the 2013 outbreak in Nepal. Indian J Med Res 142(Suppl):S1–S6
97. Subedi D, Taylor-Robinson AW (2016) Epidemiology of dengue in Nepal: history of incidence, current prevalence and strategies. for future control. J Vector Borne Dis 2016(53):1–7
98. Gupta BP, Mishra SK, Manandhar KD et al (2013) Seroprevalence of *Dengue virus* infection in Nepal. Int'i J Appl Sci Biotechnol 1:224–227
99. Acharya BK, Cao CX, Lakes T, Chen W, Naeem S (2016) Spatiotemporal analysis of dengue fever in Nepal from 2010 to 2014. BMC Public Health 16:849
100. Wu X, Lu Y, Zhou S, Chen L, Xu B (2016) Impact of climate change on human infectious diseases: Empirical evidence and human adaptation. Env Int'l 86:14–23
101. Cunningham AA, Dobson AP, Hudson PJ (2012) Disease invasion: impacts on biodiversity and human health. Phil Trans Roy Soc 367:2804–2806
102. Young HS, Wood CL, Kilpatrick AM, Lafferty KD, Nunn CL, Vincent JR (2017) Conservation, biodiversity and infectious disease: scientific evidence and policy implications. Phil Trans Roy Soc B 372:20160124
103. Pun SB, Bastola A, Shah R (2014) Case report: first report of Chikungunya virus in Nepal. J Infect Dev Countries 8:790–792
104. Pandey BD, Neupane B, Pandey K, Tun NMN, Morita K (2015) Detection of Chikungunya Virus in Nepal. Am J Trop Med Hyg 93:697–700
105. Rutvisuttinunt W, Chinnawirotpisan P, Klungthong C et al (2014) Evidence of West Nile virus infection in Nepal. BMC Infect Dis 14:606
106. Republica National Daily Newspaper. The Chikungunya menace. Kathmandu, Nepal; 20 Sept, 2016
107. Chaudhary S, Pahwa VK (2013) Avian Influenza. J Universal Coll Med Sci 1:1–2
108. The Poultry Site News Desk. http://www.thepoultrysite.com/poultrynews/32348/nepal-declares-freedom-from-h5n1-avian-flu/. Accessed 30 Oct 2017
109. The Himalayan Times. March 14, 2017
110. Daum LT, Shaw MW, Klimov AI (2005) Influenza A (H3N2) Outbreak. Nepal. Emerg Infect Dis 11:1186–1191
111. Adhikari BR, Shakya G, Upadhya BP et al (2009) Outbreak of pandemic influenza A/H1N1 2009 in Nepal. Virol J (Open access) 8:133
112. Kathmandu Post (Daily News Paper). Aug. 3, 2017
113. Rai SK, Shibata H, Nakagawa M et al (1997) Seroepidemiological study of *Hantavirus* infection in Nepal. J Assoc Rapid Methods Automation Microbiol 8:81–86
114. Brown GW, Shirai A, Gan E, Bernthal P (1981) Antibodies to typhus in Eastern Nepal. Trans Roy Soc Trop Med Hyg 75:586–587
115. The Himalayan Times (2017) Scrub typhus cases on the rise in Chitwan District. July 30, 2017. https://thehimalayantimes.com/nepal/scrub-typhus-cases-rise-chitwan/. Accessed 21 Oct 2017
116. Brown GW, Madasamy M, Bernthal P, Groves MG (1981) Leptospirosis in Nepal. Trans R Soc Trop Med Hyg 75:572–573
117. Rai SK, Shibata H, Sumi et al (2000) Serological study of *Leptospira* infection in Nepal by one-point MCA method. J Infect Dis Antimicrob Agents 17:29–32
118. Nepal HP, Acharya A, Gautam R et al (2013) Serological study of Leptospirosis in central Nepal. Int'l J Biomed Adv Res 4:455–459
119. Dahal KP, Sharma S, Sherchand JB, Upadhyay BP, Bhatta DR (2016) Detection of anti-*Leptospira* IgM antibody in serum samples of suspected patients visiting National Public Health Laboratory, Teku, Kathmandu. Int'l J Microbiol 2016:1–4
120. Regmi L, Pandey K, Malla M, Khanal S Pandey BD (2017) Sero-epidemiology study of leptospirosis in febrile patients from *Terai* region of Nepal. BMC Infect Dis 17:628–13
121. KC KP, Shakya G, Malla S et al (2013) Leptospirosis: one of the neglected infectious diseases in Nepal. In: Proceedings of first international conference on infectious diseases and nanomedicine-2012 (ICIDN-2012) 15–18 Dec, 2012, Kathmandu, Nepal
122. Sherchand JB, Cross JH, Jimba M, Sherchand S, Shrestha MP (1999) Study of *Cyclospora caayetanensis* in health care facilities, sewage and green leafy vegetables in Nepal. Southeast J Trop Med Public Health 30:58–63
123. Supram HS, Gokhale S, Chakrabarti A, Shivaprakash MR, Gupta S, Honavar P (2015) Emerging *Magnusiomyces capitatus* infection in Western Nepal. Med Mycol 54:103–110
124. Tanaka T, Tsunoda M, Mitsuhashi S (1978) Drug resistance of *Escherichia coli* isolated in Nepal. Jpn J Med Sci Biol 31:357–359
125. Rai SK, Pokhrel BM, Tuladhar NR, Khadka JB, Upadhyay MP (1987) Methicilin resistant coagulase negative *Staphylococci*. J Inst Med (Nepal) 9:23–28
126. Rai SK, Tuladhar NR, Shrestha HG (1990) Methicillin resistant *Staphylococcus aureus* in a tertiary medical care center. Nepal. Indian J Med Microbiol 8:108–109

127. Basnyat B, Pokharel P, Dixit S, Giri S (2015) Antibiotic use, its resistance in Nepal and recommendations for action: a situation analysis. J Nepal Health Res Counc 13:102–111
128. Raut R, Mandal RK, Kaphle K, Pnat D, Nepali S, Shrestha A Assessment of antibiotic residues in the marketed meat of Kailali and Kavre of Nepal. Int'l J Appl Sci Biotechnol 5:386–9
129. WHO (2015) Global action plan on antimicrobial resistance. Geneva
130. MWSA (Ministry of Water Supply and Sanitation) (2015) Nepal water supply, sanitation and hygiene sector development plan: 2016–2030. Government of Nepal
131. GON (Government of Nepal)-WHO. Multisectoral Action Plan for the Prevention and Control of Non-Communicable Diseases (2014–2020)
132. WHO. Global Action Plan for the Prevention and Control of NCDs 2013–2020. Geneva
133. EDCD (Epidemiology and Disease Control Division) (2016). Infectious Disease Control Guideline, Department of Health Services, Kathmandu

NGSPanPipe: A Pipeline for Pan-genome Identification in Microbial Strains from Experimental Reads

Umay Kulsum, Arti Kapil, Harpreet Singh and Punit Kaur

Abstract

Recent advancements in sequencing technologies have decreased both time span and cost for sequencing the whole bacterial genome. High-throughput Next-Generation Sequencing (NGS) technology has led to the generation of enormous data concerning microbial populations publically available across various repositories. As a consequence, it has become possible to study and compare the genomes of different bacterial strains within a species or genus in terms of evolution, ecology and diversity. Studying the pan-genome provides insights into deciphering microevolution, global composition and diversity in virulence and pathogenesis of a species. It can also assist in identifying drug targets and proposing vaccine candidates. The effective analysis of these large genome datasets necessitates the development of robust tools. Current methods to develop pan-genome do not support direct input of raw reads from the sequencer machine but require preprocessing of reads as an assembled protein/gene sequence file or the binary matrix of orthologous genes/proteins. We have designed an easy-to-use integrated pipeline, NGSPanPipe, which can directly identify the pan-genome from short reads. The output from the pipeline is compatible with other pan-genome analysis tools. We evaluated our pipeline with other methods for developing pan-genome, i.e. reference-based assembly and de novo assembly using simulated reads of *Mycobacterium tuberculosis*. The single script pipeline (pipeline.pl) is applicable for all bacterial strains. It integrates multiple in-house Perl scripts and is freely accessible from https://github.com/Biomedinformatics/NGSPanPipe.

Keywords

Next-generation sequencing · Pan-genome
Core genome · Accessory genome
Bacterial species · Short reads

U. Kulsum · P. Kaur (✉)
Department of Biophysics, All India Institute of Medical Sciences, New Delhi, India
e-mail: kaurpunit@gmail.com

A. Kapil
Department of Microbiology, All India Institute of Medical Sciences, New Delhi, India

H. Singh
Indian Council of Medical Research, New Delhi 110029, India

R. Adhikari and S. Thapa (eds.), *Infectious Diseases and Nanomedicine III*,
Advances in Experimental Medicine and Biology 1052, https://doi.org/10.1007/978-981-10-7572-8_4

Introduction

Bacteria are under constant pressure from changes in niche environment and respond by acquiring new genes or losing existing genes. Hence, the bacterial genome is under constant evolution. The enumeration of the complete gene repertoire of all strains in a particular species can assist in the recognition of the genome architecture of a given bacterial species [1]. Sequencing multiple strains of an organism present the biggest challenge in genome analysis. The recent development of fast, accurate and relatively low-cost Next-Generation Sequencing (NGS) technologies permit rapid and accurate sequencing of multiple genomes simultaneously in a short time period. The accessibility to an exponentially growing number of sequenced bacterial genomes has put forth the possibility to compare simultaneously multiple bacterial genomes as well as a specific bacterial genome with another genome among the same or different bacterial species. A pan-genome is the union set of genes from strains of given species which contain both the variable and invariant region of the genome [2]. The pan-genome comprises the core genome which includes genes present in all the strains of a particular species, the accessory genome which consists of genes present in only some strains of the same species and the unique genes which are present only in a single strain of a species. The accessory genome comprises mobile genetic elements which are involved in both interspecies and intraspecies gene exchange. The pan-genome aims to identify the composition as well as diversity in the gene repertoire in the microbial population. Identification of complete genetic repertoire of a bacterial species [3–7] broadens our understanding of species-specific pathogenesis and enables identification of novel and stable drug targets, vaccine candidates and diagnostic/typing markers. It also aids in understanding the niche/host adaptation and evolution of bacteria under different conditions. The analysis of the bacterial pan-genome has gained popularity in the past decade, wherein a large population of different microbial strains has been studied [3–7].

The large repertoires of genome sequences are rapidly increasing in size as more and more genome sequences are constantly being added. Thus, one of the foremost challenges for data analysis of the generated genome sequences is the availability of tools for generating pan-genome. This makes it imperative to develop tools for fast and accurate analysis of the generated data. Most of the available tools require prior knowledge of bioinformatics tools and computational resources. Different analysis tools and programs available freely online for calculating pan-genome, though versatile, do not read files comprising experimental raw reads directly from the sequencer but require prior preprocessing of short reads. These softwares include PGAP (Pan-genome Analysis Pipeline) [8], PanOCT (Pan-genome Ortholog Clustering Tool) [9] and BPGA (Bacterial Pan-genome Analysis) [10]. PGAP-related analysis depends on the orthologous clusters generated by the protein or gene sequence. It incorporates different tools such as pan-genome profile analysis, cluster analysis, analysis of the genetic variations and analysis based on species evolution. PanOCT is a pan-genome analysis program for closely related species or strains. Both programs require either BLASTP search of the predicted protein or gene in a tabular form or a text file with unique genome identifiers as input for producing orthologous clusters. Orthologous clusters correspond to the set of proteins possessing similar functions in different strains or species. Both PGAP and PanOCT have stringent requirements for further downstream analysis. BPGA is another tool which introduces functional modules like phylogeny-based analysis on core genome or pan-genome, mapping of genes on KEGG and COG databases as well as G + C content analysis. This tool provides a detailed pan-genome analysis but requires the input either in the form of a binary matrix showing the presence or absence of genes in different strains under study or the protein/gene sequence files. Short reads obtained from next-generation sequencer, therefore, initially are required to undergo

preprocessing steps, before they can serve as input for the currently available pan-genome analysis programs. The preprocessing of output reads from sequencer data requires prior knowledge of a number of available public domain programs which have to be run sequentially before the necessary files required for input to these programs are obtained. This preprocessing includes assembly of reads and post-assembly annotation of genes/proteins. Currently, no single one-step pipeline is available in the public domain for connecting NGS reads directly from the sequencer machines to pan-genome identification or other pan-genome analysis programs. To bridge this gap and offer microbiologists unfamiliar with computational tools, a user-friendly pipeline has been developed. The designed 'NGSPanPipe', is a simple and fast pipeline to address the space for pan-genome generation from short reads. The pipeline in addition to incorporating preprocessing of short reads, also generates alignment of reads, gene annotation and indicates the coverage of the reference genome without user intervention. The developed pipeline is user-friendly, reduces data complexity and improves runtime with quick alignment process. It can be easily used by microbiologists without any previous experience on bioinformatics tools.

Approaches for Identification of Pan-genome

The sequence assembly for pan-genome involves two techniques. The reference-based assembly approach requires a prior knowledge of the genome of the species for which the NGS experiment was undertaken [11]. In contrast, the de novo assembly considers that a reference genome is not available for the alignment of sequenced reads [12].

The methodology adopted for comparison of the present pipeline included Velvet1.2.10 for de novo assembly [13] and for reference-based assembly the Columbus extension to Velvet was employed [13]. For de novo assembly, the input for 'velvet' is short experimental read sequences. The program generates an assembly of reads based on hashing and graph building with two executables velveth and velvetg respectively. Initially, dictionary file containing reads of user-defined hash length is created by velveth which then executes a local alignment between the reads. Velvetg then proceeds further by reading the alignments produced by velveth. It builds a graph known as de Bruijn graph [14], simplifies it and resolves the repeats based on user-defined parameters, producing contigs (overlapping reads producing a physical map of the genome). Thus, a reference genome is not necessary for de novo genome assembly. The other protocol for pan-genome construction, reference-based assembly, was performed using Columbus extension of Velvet. This first involves the alignment to an already available reference for the bacterial strain under consideration (generally provided by the user), and then assembling of reads spanning the structural variants obtained after genome alignment to the reference. De novo assembly as well as reference-based assembly involves assembling of reads. An assembly involves mapping of sequence data and its reconstruction by grouping them into contigs. The contigs are further grouped into scaffolds. Contigs are a consensus of continuous overlapping reads. The scaffolds are the arrangement of contigs, their orientation and the gap size between them. The accuracy of contigs and scaffolds is the measure of assembly accuracy. The assembly size is given by calculating the maximum, average and total length of contigs along with its N50 value. Reference-based assembly will thus work well provided the reference genome is related to the genome being analyzed. Hence, to be free from the hassle of assembly and its accuracy, NGSPanPipe uses alignment to reference genome and non-redundant nucleotide ('nt') database while subjecting only smaller set of reads (unannotated reads) for assembly, which saves time and is considerably more accurate in terms of coverage of genome.

Prerequisites for NGSPanPipe

The running of NGSPanPipe requires pre-installation of the free software Perl and BWA (Burrows–Wheeler Aligner) tool [15]. The reference file and Protein Translation Table (ptt) file (*.ptt format as present in NCBI) for the desired organism have to be placed in the script folder created by the user.

The single script pipeline (pipeline.pl) integrating multiple in-house Perl scripts automatically runs the required programs for data preprocessing to generate the required output files. NGSPanPipe is downloadable from https://github.com/Biomedinformatics/NGSPanPipe and executed by running the file pipeline.pl from the terminal through the command 'perl pipeline.pl' to perform pan-genome construction. Details pertaining to the prerequisites for running the script are available at https://github.com/Biomedinformatics/NGSPanPipe/blob/master/README.md.

Input Parameters for NGSPanPipe

NGSPanPipe is a platform-independent (can be run on both Linux and Windows platform) command line tool developed in Perl scripting language for identification of pan-genome. On executing the script, the experimental raw reads obtained from the sequencer machine are automatically read and the pipeline proceeds to generate the pan-genome. The pipeline designed for genome comparisons, performs primary tasks like collapsing of reads, alignment and annotation without any user intervention. NGSPanPipe, before execution, requires input from the command line for details regarding reads in FASTQ format (either zipped or unzipped), reference sequence file (FASTA format), parameter for filtering of reads (number of strains a read should be present into be considered as real read, it has been taken as n = 5 for test data) and reference genome protein translation table (*.ptt) file to which the aligned reads are to be mapped. The pipeline consequently runs a number of publically freely available scripts without human intervention.

Validation of NGSPanPipe with Simulated Reads from the Genome of *Mycobacterium Tuberculosis* Strains

The performance of NGSPanPipe was evaluated and validated on simulated reads of *Mycobacterium tuberculosis* (MTB) (Table 1). The simulated reads were generated using ART simulator [16]. The data source with links to respective MTB strains employed for validation is tabulated in Table 2. The complete workflow (Fig. 1) adopted for the execution of the pipeline for construction of the pan-genome has been described with reference to *MTB*, but is applicable for any microbial or bacterial pan-genome construction.

The occurrence of each read in all 22 strains was checked and an intermittent file with non-redundant reads and a gene set with the presence or absence of the genes in these different strains of MTB was generated. This decreased the overall number of reads

Table 1 Dataset for NGSPanPipe

Species/test set	*Mycobacterium tuberculosis* (23 genomes of which one strain was taken as reference)
Data source	ftp://ftp.ncbi.nlm.nih.gov/genomes/archive/old_refseq/Bacteria/Mycobacterium_tuberculosis
Read length	150 (Paired-end)
Alignment tool	BWA (Burrow–Wheeler Alignment)
Total genes	3906
Genes covered	3511
% coverage	89.88%

Table 2 Data source for testing 'NGSPanPipe'

Data source	Accession number
ftp://ftp.ncbi.nlm.nih.gov/genomes/archive/old_refseq/Bacteria/Mycobacterium_tuberculosis_Beijing_NITR203_uid197218/NC_021054.fna	NC_021054
ftp://ftp.ncbi.nlm.nih.gov/genomes/archive/old_refseq/Bacteria/Mycobacterium_tuberculosis_CAS_NITR204_uid202217/NC_021193.fna	NC_021193
ftp://ftp.ncbi.nlm.nih.gov/genomes/archive/old_refseq/Bacteria/Mycobacterium_tuberculosis_CCDC5079_uid203790/NC_017523.fna	NC_017523
ftp://ftp.ncbi.nlm.nih.gov/genomes/archive/old_refseq/Bacteria/Mycobacterium_tuberculosis_CCDC5079_uid203790/NC_021251.fna	NC_021251
ftp://ftp.ncbi.nlm.nih.gov/genomes/archive/old_refseq/Bacteria/Mycobacterium_tuberculosis_CCDC5180_uid161941/NC_017522.fna	NC_017522
ftp://ftp.ncbi.nlm.nih.gov/genomes/archive/old_refseq/Bacteria/Mycobacterium_tuberculosis_CDC1551_uid57775/NC_002755.fna	NC_002755
ftp://ftp.ncbi.nlm.nih.gov/genomes/archive/old_refseq/Bacteria/Mycobacterium_tuberculosis_CTRI_2_uid161997/NC_017524.fna	NC_017524
ftp://ftp.ncbi.nlm.nih.gov/genomes/archive/old_refseq/Bacteria/Mycobacterium_tuberculosis_EAI5_NITR206_uid202218/NC_021194.fna	NC_021194
ftp://ftp.ncbi.nlm.nih.gov/genomes/archive/old_refseq/Bacteria/Mycobacterium_tuberculosis_EAI5_uid212307/NC_021740.fna	NC_021740
ftp://ftp.ncbi.nlm.nih.gov/genomes/archive/old_refseq/Bacteria/Mycobacterium_tuberculosis_Erdman_ATCC_35801_uid193763/NC_020559.fna	NC_020559
ftp://ftp.ncbi.nlm.nih.gov/genomes/archive/old_refseq/Bacteria/Mycobacterium_tuberculosis_F11_uid58417/NC_009565.fna	NC_009565
ftp://ftp.ncbi.nlm.nih.gov/genomes/archive/old_refseq/Bacteria/Mycobacterium_tuberculosis_H37Ra_uid58853/NC_009525.fna	NC_009525
ftp://ftp.ncbi.nlm.nih.gov/genomes/archive/old_refseq/Bacteria/Mycobacterium_tuberculosis_H37Rv_uid170532/NC_018143.fna	NC_018143
ftp://ftp.ncbi.nlm.nih.gov/genomes/archive/old_refseq/Bacteria/Mycobacterium_tuberculosis_H37Rv_uid57777/NC_000962.fna	NC_000962 (Reference)
ftp://ftp.ncbi.nlm.nih.gov/genomes/archive/old_refseq/Bacteria/Mycobacterium_tuberculosis_Haarlem3_NITR202_uid202216/NC_021192.fna	NC_021192
ftp://ftp.ncbi.nlm.nih.gov/genomes/archive/old_refseq/Bacteria/Mycobacterium_tuberculosis_Haarlem_uid54453/NC_022350.fna	NC_022350
ftp://ftp.ncbi.nlm.nih.gov/genomes/archive/old_refseq/Bacteria/Mycobacterium_tuberculosis_KZN_1435_uid59069/NC_012943.fna	NC_012943
ftp://ftp.ncbi.nlm.nih.gov/genomes/archive/old_refseq/Bacteria/Mycobacterium_tuberculosis_KZN_4207_uid83619/NC_016768.fna	NC_016768
ftp://ftp.ncbi.nlm.nih.gov/genomes/archive/old_refseq/Bacteria/Mycobacterium_tuberculosis_KZN_605_uid54947/NC_018078.fna	NC_018078
ftp://ftp.ncbi.nlm.nih.gov/genomes/archive/old_refseq/Bacteria/Mycobacterium_tuberculosis_RGTB327_uid157907/NC_017026.fna	NC_017026
ftp://ftp.ncbi.nlm.nih.gov/genomes/archive/old_refseq/Bacteria/Mycobacterium_tuberculosis_RGTB423_uid162179/NC_017528.fna	NC_017528
ftp://ftp.ncbi.nlm.nih.gov/genomes/archive/old_refseq/Bacteria/Mycobacterium_tuberculosis_UT205_uid162183/NC_016934.fna	NC_016934
ftp://ftp.ncbi.nlm.nih.gov/genomes/archive/old_refseq/Bacteria/Mycobacterium_tuberculosis_uid185758/NC_020089.fna	NC_020089

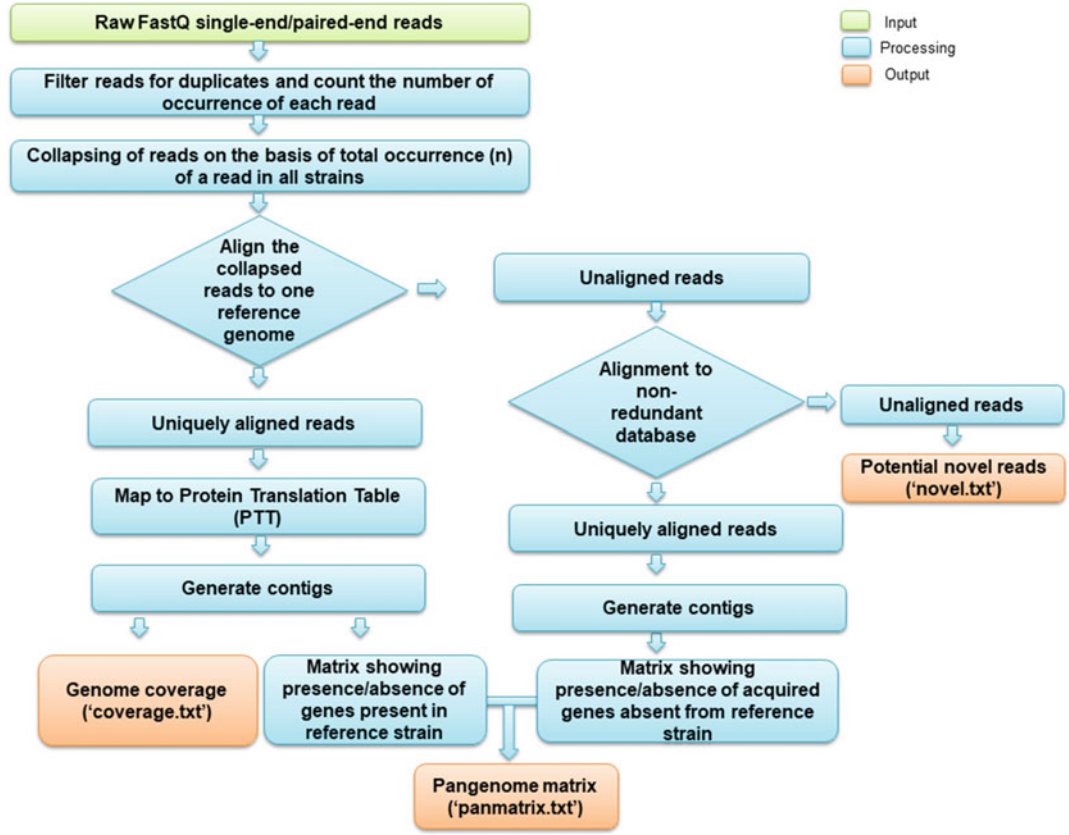

Fig. 1 Workflow of 'NGSPanPipe'. The execution of processing of the pipeline is represented in blue. The input files are indicated in green and the three output files are shown in peach

significantly, thus reducing data complexity and computational cost for aligning the complete set of reads without collapsing.

Further, filtering of reads with at least 'n' copies increased the probability of a read being real and not due to sequencing errors. A read is considered of better quality if it occurs frequently that is present in multiple strains of a species. Subsequent collapsing of reads reduces data complexity and duplicity and cuts computational cost. An in-house developed script (included in the pipeline) collapsed identical reads in different strains under study into one unique read and recorded the identical read count for individual strains. This removes duplicate reads thus reducing data size and complexity.

The simulated reads occurring in two or more strains were extracted for alignment to a randomly chosen reference genome (MTB, H37Rv, complete genome, NC_000962.fna) using BWA tool. Subsequently, reads uniquely aligned (X0 = 1) were extracted and mapped onto protein translation table (PTT) of the reference test strain (NC_000962.ptt), downloaded from NCBI ftp site (ftp://ftp.ncbi.nlm.nih.gov/genomes/archive/old_refseq/Bacteria/Mycobacterium_tuberculosis_H37Rv_uid57777/NC_000962.ptt). The file, .ptt, available from NCBI is used to define the boundaries of the open reading frames. The coverage was calculated taking into account reads which fall within the range of each gene in. ptt.

Reads that did not align to the reference genome were aligned against non-redundant nucleotide ('nt') database using BLAST [17] to

scrutinize reads of the bacterial genome, acquired by the test genome. Since the size of 'nt' is very large (~100 GB), creating an index for alignment with BWA tool requires a large amount of memory. Hence, in the pipeline, the data was split into smaller files to reduce computational cost. BWA tool was used to generate an index for all the files separately. These indexed files were then used as reference for alignment. Uniquely mapped reads were further extracted from this alignment and a matrix created to evaluate the presence/absence of acquired genes in MTB strains. This observed presence or absence of genes reflects the variations in the bacterial genome within the same species and is associated with microbial genome diversity. Reads which failed to align to the reference genome and 'nt' database were identified as unannotated novel reads.

Output Files Generated from NGSPanPipe

This pipeline employing a novel approach uses experimental reads as input, collapses them and generates three output files:

(i) coverage.txt, which contains the positions of the genome covered by the reads produced by the sequencer. This file shows the maximum coverage of whole genome by the reads, ensuring accuracy for further analysis.
(ii) panmatrix.txt; a binary matrix file in the 0/1 format which shows the presence/absence of genes in different strains. 0 denotes the absence of genes while 1 represents the presence of genes in that particular strain. The output binary file can serve as a direct input for other pan-genome analysis programs like PanOCT, BPGA and PGAP which use binary matrix for further downstream analysis.
(iii) novel.txt: This file stores the unannotated reads, which are neither present in the reference genome of studied strains nor observed in any other bacterial genome under study.

Significance of NGSPanPipe

The initial alignment and subsequent mapping of simulated collapsed reads from 22 MTB strains against reference strain NC_000962 identified 3511 genes (coverage.txt) from available 3906 in Protein Translation Table (.ptt). Hence the genome coverage given by NGSPanPipe after alignment to reference test genome and annotation was 89.88% (3511 genes) (Table 1). The genome coverage obtained on the same set of MTB strains for reference-based assembly was 74.34% (2904 genes) and for de novo assembly was 57.42% (2243 genes) (Fig. 2).

The unidentified genes obtained from NGSPanPipe were subjected to BLAST against Database of Essential Genes (DEG) [18] with e-value cutoff of 0.00001 to confirm that no essential gene is missed out by NGSPanPipe algorithm. The essential genes are genes which are crucial for the survival of bacteria. DEG contains all currently available reported genes considered vital for the foundation of bacterial life. The homologs found in DEG indicated that majority of the unidentified genes from this pipeline were not essential for the survival of the species. The undetected genes were also compared with those genes unidentified by both reference-based assembly and de novo assembly. Our pipeline not only identified all the genes detected by these tools but also successfully recognized additional genes unidentified by these protocols. Hence, NGSPanPipe reported the least number of unidentified genes amongst them. NGSPanPipe, thus, is better than reference-based assembly for pan-genome identification as demonstrated and validated using simulated MTB NGS reads. The identified and unidentified genes by NGSPanPipe, reference-based assembly and de novo assembly is listed in comparison.xls file present in GitHub (https://github.com/Biomedinformatics/NGSPanPipe/raw/master/comparison.xls).

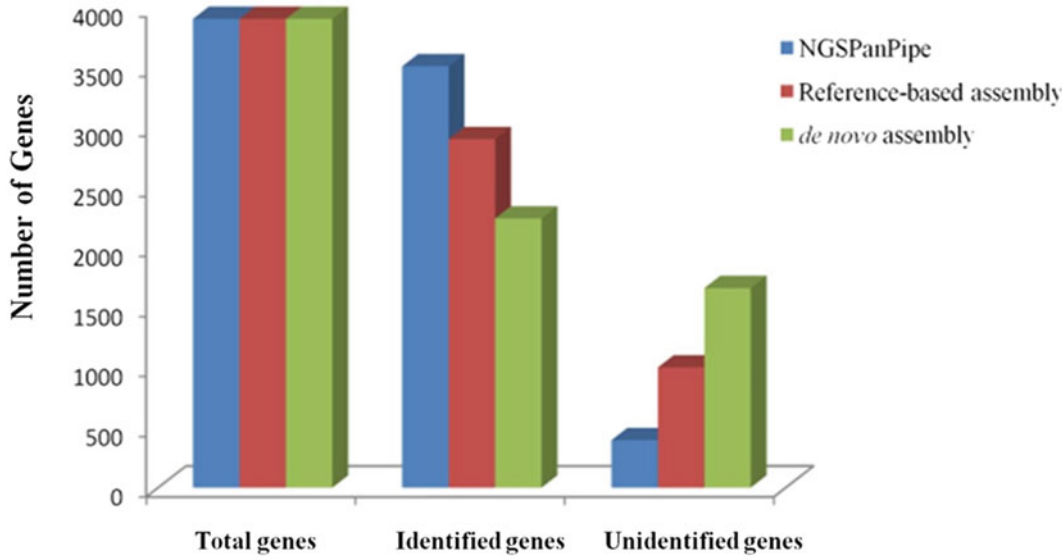

Fig. 2 Comparison of 'NGSPanPipe', Reference-based and *de novo* assembly

The unmapped reads subjected to alignment to 'nt' database creates a matrix of acquired genes in different strains of test genome. The acquired genes are those genes that are not observed in the reference genome but might have been obtained from other bacterial genomes under stress in order to adapt to new environments/host. Hence, these variations observed in the related bacterial genes are associated with microbial diversification wherein the microbes adapt to the environment through genome rearrangements. This occurs due to horizontal gene transfer or through mutations as Single Nucleotide Polymorphisms (SNPs) as a consequence of exposure of the bacterial population to different environments [19]. Genomic comparison of the strain in question and reference strain can also pinpoint virulence factors which are associated with gene acquisition or/and gene reduction. Further comparative analysis of the patterns pertaining to the variations in the occurrence of genes in a species can assist in deciphering the gene and genome evolution as well as the pathogenesis of the microbial organism [20]. The matrix file of identified genes from reference genome and acquired genes collectively represent the pan-genome (panmatrix.txt). A whole genome or pan-genome sequence analysis of clinical isolates from infectious diseases can identify outbreak regions and establish patient transmission data [21]. Similarly, a comparison of susceptible and resistant strains can aid analysis of the resistome. It can also provide leads to determinants of antibiotic resistance as well as reveal newer drug targets. The unannotated reads (stored in 'novel.txt') may represent novel drug resistance strains and pave the way for the development of better antimicrobials.

Profile Statistics

The developed procedure outputs genome coverage as reads, which are based on aligned and unaligned reads to the reference genome. Hence it becomes imperative to discern the accuracy of alignment in terms of True Positives (TP), True Negatives (TN), False Positives (FP) and False Negatives (FN). The reads aligned to reference genome were evaluated by alignment to 'nt' database and based on their alignment to *Mycobacterium tuberculosis* genes. The percentage calculated for true positives, true

negatives, false positives and false negatives was 66.66%, 26.96% 0.05% and 25.84%, respectively. Sensitivity, specificity and accuracy were calculated by the formulae [22, 23]:

Sensitivity = TP/TP + FN
Specificity = TN/TN + FP
Accuracy = TP + TN/TP + TN + FP + FN

This reflected a specificity and sensitivity of 99.81% and 99.86%, respectively, while the accuracy of NGSPanPipe was calculated to be 78.32%.

Concluding Remarks

Advanced sequencing technologies have brought microbial genomics to the forefront. The availability of both pathogenic and non-pathogenic bacterial genomes has revolutionized the study of infectious diseases. Concomitantly, it has necessitated the development of tools for a detailed evaluation of the microbial community in terms of the increasingly available bacterial genome sequences. Therefore, NGS pipelines are an integral necessity in a research setup especially related to clinical microbiological applications. NGSPanPipe is an efficient single executable Perl script for collapsing of reads, alignment and contig generation by incorporating NGS experimental raw reads. The single script integrating multiple Perl scripts is entirely automated requiring minimal user intervention to provide pan-genome matrix. The output files produced by the script include the genome coverage file which gives the count of base pairs covering a particular location on the genome and the binary matrix file of pan-genome indicating the presence/absence of genes depicting core, accessory and strain-specific genes. The gene variations marked exclusively in all genomes will ease out analysis related to virulence or host adaptations of different microbes. This binary matrix file can be directly inputted to other pan-genome programs for further comprehensive analysis. The proteins which are conserved in all the strains of a bacterial species comprise the core genome while those present in some but not all strains constitute the accessory genome. The unique protein families in a particular strain are strain specific. Strain-specific gene differences can be exploited to understand the evolution of respective microbial genomes and their relationship with the host. The pan-genome can be analyzed further for identification of drug targets against the bacteria. The core, accessory and strain-specific genome can be studied for the similarities and variations among strains. The third output file with reads which failed to align to the reference genome and non-redundant databases can be further computationally explored and can lead to the identification of novel pathways and enable researchers to identify novel and stable drug targets, vaccine candidates and diagnostic/typing markers. Mapping of NGS data to reference sequences of bacterial genomes has also become an important tool in pathogen discovery [24].

With the increase in the number of reads, the runtime and memory usage also increase. The time taken for mapping of reads, which is the main process in many applications, controls the complete run. Thus, the pipeline incorporates the collapsing of reads to enable quick processing and reduce redundancy of genes in the dataset as well as mapping to the reference genome with high accuracy. Currently, the publically available analysis tools and applications require processed bacterial genome sequences. The developed pipeline is advantageous as unlike other tools, it accesses raw experimental reads of sequenced strains directly from the sequencer machine without any preprocessing for identifying pan-genome. The output-processed genome sequences produced from the pipeline can then serve as direct input to various genome analysis tools. NGSPanPipe is presently the only freely available pipeline that bridges the gap between NGS raw reads to pan-genome analysis programs. Moreover, it is platform independent, user-friendly and can be used by microbiologists with little or no acquaintance to computational tools.

Availability

The pipeline is freely available at https://github.com/Biomedinformatics/NGSPanPipe.
The README.md file contains detailed information concerning execution of NGSPanPipe.

Acknowledgments PK and AK acknowledge the financial support from Indian Council of Medical Research. UK thanks the UGC for grant of the fellowship. The authors thank Dr. Amit Katiyar for discussions. PK is grateful for the invitation to present her work at the 'Second International Conference on Infectious Diseases and Nanomedicine—2015' held during 15–18 December 2015 in Kathmandu, Nepal.

References

1. Didelot X, Bowden R, Wilson DJ, Peto TEA, Crook DW (2012) Transforming clinical microbiology with bacterial genome sequencing. Nat Rev Genet 13:601–612
2. Tettelin H, Masignani V, Cieslewicz MJ, Donati C, Medini D, Ward NL, Angiuoli SV, Crabtree J, Jones AL, Durkin AS et al (2005) Genome analysis of multiple pathogenic isolates of Streptococcus agalactiae: implications for the microbial "pan-genome". Proc Natl Acad Sci USA 102:13950–13955
3. Hogg JS, Hu FZ, Janto B, Boissy R, Hayes J, Keefe R, Post JC, Ehrlich GD (2007) Characterization and modeling of the Haemophilus influenzae core and supragenomes based on the complete genomic sequences of Rd and 12 clinical nontypeable strains. Genome Biol 8:R103
4. Holt KE, Parkhill J, Mazzoni CJ, Roumagnac P, Weill FX, Goodhead I, Rance R, Baker S, Maskell DJ, Wain J et al (2008) High-throughput sequencing provides insights into genome variation and evolution in Salmonella Typhi. Nat Genet 40:987–993
5. D'Auria G, Jimenez-Hernandez N, Peris-Bondia F, Moya A, Latorre A (2010) Legionella pneumophila pangenome reveals strain-specific virulence factors. BMC Genom 11:181
6. Rasko DA, Rosovitz MJ, Myers GS, Mongodin EF, Fricke WF, Gajer P, Crabtree J, Sebaihia M, Thomson NR, Chaudhuri R et al (2008) The pangenome structure of Escherichia coli: comparative genomic analysis of E. coli commensal and pathogenic isolates. J Bacteriol 190:6881–6893
7. Serruto D, Serino L, Masignani V, Pizza M (2009) Genome-based approaches to develop vaccines against bacterial pathogens. Vaccine 27:3245–3250
8. Zhao Y, Wu J, Yang J, Sun S, Xiao J, Yu J (2012) PGAP: pan-genomes analysis pipeline. Bioinformatics (Oxford, England) 28:416–418
9. Fouts DE, Brinkac L, Beck E, Inman J, Sutton G (2012) PanOCT: automated clustering of orthologs using conserved gene neighborhood for pan-genomic analysis of bacterial strains and closely related species. Nucleic Acids Res 40:e172
10. Chaudhari NM, Gupta VK, Dutta C (2016) BPGA-an ultra-fast pan-genome analysis pipeline. Sci Rep 6:24373
11. Schneeberger K, Ossowski S, Ott F, Klein JD, Wang X, Lanz C, Smith LM, Cao J, Fitz J, Warthmann N et al (2011) Reference-guided assembly of four diverse Arabidopsis thaliana genomes. Proc Natl Acad Sci USA 108:10249–10254
12. Baker M (2012) De novo genome assembly: what every biologist should know. Nat Methods 9:333–337
13. Zerbino DR, Birney E (2008) Velvet: algorithms for de novo short read assembly using de Bruijn graphs. Genome Res 18:821–829
14. Limasset A, Cazaux B, Rivals E, Peterlongo P (2016) Read mapping on de Bruijn graphs. BMC Bioinformatics 17:237
15. Li H, Durbin R (2009) Fast and accurate short read alignment with Burrows-Wheeler transform. Bioinformatics (Oxford, England) 25:1754–1760
16. Huang W, Li L, Myers JR, Marth GT (2012) ART: a next-generation sequencing read simulator. Bioinformatics (Oxford, England) 28:593–594
17. Altschul SF, Gish W, Miller W, Myers EW, Lipman DJ (1990) Basic local alignment search tool. J Mol Biol 215:403–410
18. Luo H, Lin Y, Gao F, Zhang CT, Zhang R (2014) DEG 10, an update of the database of essential genes that includes both protein-coding genes and noncoding genomic elements. Nucleic Acids Res 42:D574–D580
19. Bryant J, Chewapreecha C, Bentley SD (2012) Developing insights into the mechanisms of evolution of bacterial pathogens from whole-genome sequences. Future Microbiol 7:1283–1296
20. Bentley SD, Parkhill J (2015) Genomic perspectives on the evolution and spread of bacterial pathogens. In: Proceedings of the Royal Society B: Biological Sciences, p 282
21. McGann P, Bunin JL, Snesrud E, Singh S, Maybank R, Ong AC, Kwak YI, Seronello S, Clifford RJ, Hinkle M et al (2016) Real time application of whole genome sequencing for outbreak investigation—What is an achievable turnaround time? Diagn Microbiol Infect Dis 85:277–282

22. Fawcett T (2006) An introduction to ROC analysis. Pattern Recogn Lett 27:861–874
23. Powers DMW (2011) Evaluation: From Precision, Recall and F-Measure to ROC, Informedness, Markedness & Correlation. J Mach Learn Technol 2:37–63
24. Lecuit M, Eloit M (2014) The diagnosis of infectious diseases by whole genome next generation sequencing: a new era is opening. Front Cell Infect Microbiol 4:25

Potential Treatment Options in a Post-antibiotic Era

R R Bragg, C M Meyburgh, J-Y Lee and M Coetzee

Abstract

Following the Golden Age of antibiotic discovery in the previous century, the rate of antibiotic discovery has plummeted during the past 50 years while the incidence of antimicrobial resistance is ever-increasing. Presently, humankind is forced to address a major public health threat in the form of multiple drug resistance and urgent action is required to halt the advent of a post-antibiotic era. This chapter aims to draw the attention to the escalating global crisis of antimicrobial resistance fueled by the irresponsible use of antibiotics in healthcare and animal production sectors. The merits of alternative prevention and treatment options, including vaccines, herbal products, bacteriophages, and improved biosecurity measures are also discussed.

Keywords

Antibiotics · Vaccines · Essential oils
Bacteriophages · Antimicrobial resistance

R. R. Bragg (✉) · C. M. Meyburgh · J-Y Lee · M. Coetzee
Department of Microbial, Biochemical and Food Microbiology, Faculty of Natural and Agricultural Sciences, University of the Free State, Bloemfontein 9300, Republic of South Africa
e-mail: braggrr@ufs.ac.za

Introduction

The rapid development of antibiotic resistance has forced mankind to reconsider the administration of antimicrobial therapies. Upon initial discovery, antibiotics were understandably regarded as a miracle drug and the advent of World War II ushered in the development of antibiotics into industrial scale in order to treat countless casualties.

Continual and sustained misuse has stretched the therapeutic capabilities of antibiotics close to their limits, and mankind is now faced with the very tangible potential of a post-antibiotic era. The major contributor to this deteriorating situation is excessive and imprudent use of antibiotics in healthcare settings and animal production sector. Lack of development of novel antimicrobial drugs due to the indifference of the pharmaceutical sector to the threat of resistance has also contributed to the current state of affairs [1, 2].

There is increasing pressure on the animal production sector to limit or totally cease the use of antibiotics. Pressure on producers to raise antibiotic-free food animals does not come from the authorities, but from the consumers and investors. Consequently, various popular fast-food chain restaurants have issued statements indicating that they will be eliminating all antibiotics of importance to human medicine from chicken supply [3]. Such decisions require

R. Adhikari and S. Thapa (eds.), *Infectious Diseases and Nanomedicine III*,
Advances in Experimental Medicine and Biology 1052, https://doi.org/10.1007/978-981-10-7572-8_5

alternatives to antibiotics for the production of animals.

Possible Treatment Options

There are a number of possible treatment options, which include the search for novel antimicrobial compounds and alternatives such as various herbal products, improved and novel vaccine development, the use of bacteriophages and phage-associated enzymes, and the improvement in biosecurity. These alternatives and their potential for use in a post-antibiotic era will be the focus of this review.

Novel Antimicrobials and Alternatives

Modern medicine must address the inescapable fact that the supply of available, effective antibiotics is being rapidly depleted [1]. Despite these stark realities, recent reports warn of a considerable discrepancy between the burden of multidrug-resistant infections and progress in the development of novel antibiotics [4]. The approval of new antimicrobial agents by the United States Food and Drug Administration (FDA) has decreased by 56% over a period of 20 years (1983–2002) [5]. During the Golden Age of antibiotics, between 1930 and 1960, 20 novel classes of antibiotics were produced while the possibility of the emergence of antimicrobial resistance fueled by antibiotic overuse was recognized but not considered serious by microbial geneticists of that time [2].

Although the development of new antimicrobials within preexisting classes has many advantages, development of new classes of antimicrobials utilizing novel antimicrobial mechanisms is the only solution to counteract emerging multiple drug resistance [5]. However, there are very few novel classes of antibiotics in the pipeline. In the past 50 years, only a handful of novel classes of antibiotics have been discovered, which include oxazolidinones [6], lipopeptides, [7] and oxadiazoles [8]. The slow rate of discovery of novel antimicrobials coupled with lengthy clinical trials of up to 8 years [5] creates a grim outlook for the future of anti-infective medicine. Research has been forced to consider alternative sources to either replace or complement antibiotic treatment.

Herbal Products

Essential Oils (EOs) are a group of phytochemicals of importance mainly to the fragrance and flavor industry, although the antimicrobial properties of these compounds have been recognized since antiquity [9]. Interest in "natural" antimicrobials and preservatives has resurfaced due to the global antibiotic resistance crisis. Presently, the antimicrobial activity of EOs are applied in commercial products as diverse as pesticides, insecticides [10], food preservatives [11], disinfectants [12], cosmetics [13], dental root canal sealers [14], and feed supplements for swine, poultry, and ruminants [15].

A ban on antibiotic growth promoters in animal diets in the European Union by the Food and Drug Administration in 2006 launched a search for a blend of synergistic EO compounds that aid growth promotion and exhibit antimicrobial properties. A commercial EO product, containing 18% thymol and cinnamaldehyde, was shown to improve weight gain and reduced the occurrence of diarrhea in weaned pigs, possibly as a result of improved nutrient digestibility [16]. The blend of thymol and cinnamaldehyde has proven antimicrobial properties, targeting pathogenic bacteria such as *Salmonella* and *Eschericha coli,* while positively affecting the gut microbiota of the host [17].

In the poultry industry, an increase in the use of herbal products beyond their intended use is observed. The herbal product Mentofin was first marketed as an aid to reduce vaccination reactions in poultry when vaccinated with live virus vaccines by the spray vaccination route. Subsequently, experimentation on the antimicrobial activities of this product, not only against bacterial but also viruses such as Newcastle disease virus [18] and various *Eimeria* species [19], was undertaken. Work on the effects of essential oils on parasites, which cause coccidiosis in poultry, is of particular relevance as many authorities are also including the anti-coccidial drugs in the ban

on antibiotic growth promoters. This leaves the poultry producer in a very difficult position, as the control of the various *Eimeria* species outside of the chicken is very difficult to do because of the highly resistant oocyst stage of the parasite.

Improved Vaccine Development

In addition to antibiotics, another valuable treatment option in the fight against infection is vaccines. The use of vaccines reduces the occurrence of antimicrobial resistance by various mechanisms [20]. Antimicrobial resistance acquisition is accelerated by overexposure of bacteria to antibiotics. Vaccination can contribute to the less frequent administration of antibiotics by targeting bacterial pathogens directly and indirectly *via* the effects of herd immunity [20]. Establishment of herd immunity diminishes the frequency of infection within a population and also plays an important role in preventing infections in communities where the need for effective antibiotics is crucial, such as immunocompromised or immunodeficient patients [20–22].

The ideal vaccine should meet several safety, efficacy, and production criteria. The absence of capacity for reversion to virulence and lack of residual pathogenicity coupled with minimal side effects are typically desired features regarding safety. Killed- and live-attenuated vaccines based on empirical design have saved countless lives in the past century, although this approach to vaccine design presents several limitations. Advancements in the study of microbial pathogenesis and the host immune response were elemental to the development of safer, second-generation vaccines based on purified antigenic components, genetically altered toxins and polysaccharide–protein conjugates [23]. Despite the remarkable progress made in the past century in the field of vaccinology, the traditional approach to vaccine development cannot be applied successfully to all pathogens. Intracellular pathogens, microbes that cannot be cultured in vitro and microbes that display antigenic variability present particular challenges to first- and second-generation vaccines [24].

It is very difficult to routinely obtain 100% protection with many of the bacterial vaccines based on the whole bacterial cell. With viral vaccines, 100% protection is achievable. This is based on the functioning of the immune response in an individual. When vaccinated with a viral vaccine, the humoral immune response will produce virus-specific antibodies. When the individual is later exposed to the virus, these circulating antibodies will bind to the virus and prevent the virus from binding to its target cell. The virus is immediately neutralized. In the case of bacterial vaccines, the humoral immune response will also produce antibodies, which will bind to invading bacteria. However, the binding of antibodies to a bacterium does not neutralize the bacterium and the pathogen can still replicate and produce exotoxins. The bound antibodies attract complement which in turn attracts neutrophils which destroy the bacterium. The bound antibodies also attach macrophages, which bind to the crystallizable fragment (F_c) region of an antibody and these macrophages destroy the bacterium. This process is not as rapid as the defense mechanism against viruses, thus making bacterial vaccines less effective.

Novel Approaches to Vaccine Development for Bacteria

The emergence of recombinant DNA and genome sequencing technology heralded a new era in the field of vaccinology [25]. The widespread availability of genomic data that accompanied these technologies enabled the development of a groundbreaking new approach to vaccine design with the ability to overcome the limitations of empirical design. This novel approach, termed reverse vaccinology, utilizes full genome sequence data and bioinformatics to identify potential antigens that hold promise as vaccine targets.

Reverse vaccinology was first successfully applied to *Neisseria meningitidis* serogroup B (MenB), the causative agent of meningococcal meningitis that has been the focus of much vaccine research for the past 40 years. Utilization of the capsular polysaccharides of *N. meningitidis* as a vaccine target was successfully applied

in 4 of the 5 pathogenic serogroups, but failed in MenB [26]. The MenB capsular polysaccharide is identical to polysialic acid [α(2 → 8)*N*-acetyl neuraminic acid], a carbohydrate expressed on the cell surface of vertebrate neural cells. Therefore, polysialic acid is a poor immunogen in humans and may elicit autoantibodies [27]. Alternative vaccine candidates for MenB had to be identified using reverse vaccinology. In this approach, the full genome sequence of the virulent MenB strain MC58 was determined [28] and bioinformatics tools were employed to identify open reading frames that encoded putative cell surface and exported proteins [26]. Candidate genes were cloned in *Escherichia coli* to be expressed, and successfully expressed proteins were tested for the ability to elicit bactericidal antibodies in mice. Over 90 previously unknown surface proteins were discovered by this technology, and 29 of these were capable of eliciting bactericidal antibodies. Furthermore, the genomic approach addressed possible antigenic variability in MenB strains by comparing candidate gene sequences from a diversity of strains in order to identify a single index sequence as reference [26]. The genome-based vaccinology approach has also been used to discover vaccine candidates against antibiotic-resistant pathogens *Staphylococcus aureus* and *Streptococcus pneumoniae* [29].

Bacteriophages have been utilized not only as vaccine delivery vehicles, but the concept of phage display has also been used in the discovery of antigens. The basis of phage display technology was created in 1985 when it was illustrated that a foreign gene sequence could be fused to the coat protein of filamentous phage M13, resulting in the display of the foreign protein on virions produced in *Escherichia coli* [30]. The first reported application of an engineered phage as an antigen delivery vehicle involved the expression of the circumsporozoite protein of the malaria parasite *Plasmodium falciparum* fused to the minor coat protein (pIII) of filamentous phage f1 [31]. These recombinant phages can be easily amplified and thus serve as a useful source of antigen and were shown to be immunogenic in rabbits [31]. In addition, filamentous phages have been shown to be potent adjuvants capable of boosting the immune response against a displayed antigen [32]. Phage virions are also useful as delivery vehicles for nucleic acid vaccines. In contrast to naked DNA vaccines, phage coat proteins protect the antigen-encoding sequence from degradation, therefore phage DNA vaccines display increased stability. Phage DNA vaccines are produced by cloning an antigen-encoding gene sequence into a eukaryotic cassette, which includes a promoter, 5′-UTR (5′- untranslated region), open reading frame, 3′-UTR (3′-untranslated region), and poly (A) tail, within the phage genome [33]. The application of random peptide libraries in antigen discovery and vaccine development was illustrated by screening a dodecamer random peptide library against polyclonal serum against *Avibacterium paragallinarum* strain 0083 (serovar A), identifying peptides that specifically interacted with polyclonal antibodies [34]. A selected peptide sequence was recombinantly expressed in *E. coli* GI826, resulting in the display of the epitope on the bacterial surface. In vivo antigenicity was demonstrated by injecting chickens intramuscularly with the bacteria expressing the epitope, resulting in protection against challenge with *A. paragallinarum.*

Bacteriophage Therapy

Bacteriophages are viruses that prey on bacterial cells [35]. The application of bacteriophages to fight bacterial infection predates the use of antibiotics, although interest in bacteriophage therapy diminished as more effort was invested in antibiotic development after World War II [36]. Recent surges in the occurrence of antibiotic resistance have signaled renewed interest in bacteriophage therapy.

Bacteriophage therapy displays various advantages in comparison to antibiotic treatment. One of the most frequently cited advantages of using bacteriophages to fight infections is their high level of host specificity, which translates to a very low probability of a population of bacteria developing resistance. This highly specific mode

of action directly contrasts with antibiotics, which typically display broad-spectrum antimicrobial activity. The ability of bacteriophages to exclusively target pathogenic bacteria ensures that the microbiota of the host is not affected, thereby reducing the risk of secondary or opportunistic infections occurring. Bacteriophage therapy is nontoxic and administration thereof rarely results in allergic reactions [37], whereas antibiotic administration can cause fatal allergies in certain cases [38].

One of the greatest appeals of phage therapy is arguably the ability to bypass the emergence of resistance associated with chemotherapeutic administration [36]. In order to broaden the host range of a phage treatment and to address issues relating to specificity and resistance, a tailored cocktail of phages may be utilized [36, 39] However, bacteria have evolved several defense mechanisms against phage predation, comparable to either adaptive or innate immunity in higher organisms [40]. The major bacterial resistance mechanisms are listed in Table 1, including the most well-known bacterial defense against viral infection, the restriction/modification system, which prevents phage replication in the host by cutting phage nucleic acid at unique sequences [40, 41]. Contrasting other defense mechanisms listed here, the clustered regularly interspaced short palindromic repeats (CRISPRs) and the CRISPR-associated (Cas) (CRISPR/Cas) system can be likened to adaptive immunity in vertebrates. The CRISPR–Cas defense system operates by inserting spacers, derived from DNA or RNA of invaders, into CRISPR loci of the host genome [42]. These nucleotide sequences act as recognition elements to recognize and destroy matching viral nucleic acids, thus endowing the prokaryotic host with "immunological memory" [43].

The survival of phages despite the presence of bacterial immune mechanisms points to the fact that infectious phages are continuously present. Phages are capable of evolving to infect completely resistant host populations [44] and have risen to the challenge of adaptive immunity. Anti—CRISPR/Cas genes, capable of evading the bacterial adaptive immune response, have been discovered recently in genomes of phages infecting *Pseudomonas aeruginosa* [45] and an adaptive immune evasion system encoded by the *Vibrio cholerae* phage ICP1 has been shown to use the CRISPR/Cas system to target a phage-inhibitory chromosomal island of the host for destruction [46]. These remarkable discoveries offer insight into the survival of phages, despite widespread and effective adaptive immune mechanisms in bacteria, and is indicative of a progressive arms race between co-evolving phages and their hosts [45, 46].

Phage enzymes

When mature bacteriophage particles are assembled within the host cell, ready to infect a new cell, a number of factors are responsible for their release. Primarily, enzymatic cleavage of the cell wall from within the cell is achieved by lysozymes, endopeptidases, or amidases, which are collectively termed endolysins, produced by dsDNA bacteriophages [47]. To allow endolysins to reach the cell wall, proteins such as holins are often incorporated in this system. Holins are usually small proteins that have transmembrane spanning properties that allow them to create holes in the cell membrane through which the endolysins can access the cell wall [48].

A myriad of endolysins from different bacteriophages exist, showing diverse modes of action. Heterologous expression of enzymes enhances the use of endolysins, because of the options that it brings to phage-related treatment. Advantages of endolysins over antibiotics are specificity for the target organism, ability to diffuse through biofilms, and lower probability of bacterial resistance [47], while the drawbacks or challenges of endolysins are their specificity (where cause of infection is unknown) and the natural barriers that protect cells, such as cell membranes and cell walls [49].

Some studies have focused on the use of native or mutated forms of endolysins [50] such as murein hydrolase from streptococcal bacteriophage C1 applied in vivo showed activity against oral streptococci in mice [51]. A pneumococcal phage amidase, Pal, from phage Dp-1 was tested on 15 strains of *Streptococcus pneumonia* and resulted in 4.0 cfu/ml $\log_{10}$ decreases in 30 s when treated

Table 1 Bacterial mechanisms of resistance to phage infection

Resistance mechanism	Description
Adsorption resistance	Absence of receptor molecules on bacterial surfaces prevents binding of phage to host cell
Immunity to superinfection	Inhibition of phage replication by recognition of a phage-associated motif
Abortive infection	Inhibition of phage replication by the suicide of infected bacteria
Restriction/modification enzymes	Restriction enzymes cleave incoming foreign DNA at specific sequences
CRISPRs–Cas proteins	Phage DNA is integrated into CRISPR loci and transcribed into short, noncoding RNAs. These RNAs and Cas proteins recognize and silence foreign genetic elements

with 100 *U* of expressed and purified Pal [52]. The enzyme from *Stenotrophomonas maltophilia* that has high similarity to bacteriophage lambda endolysin has shown activity against both Gram positive and negative bacteria without EDTA treatment of outer membrane in the latter [53]. Others have developed chimeric forms of endolysins taking advantage of different aspects of the enzymes. The cell wall binding domain of staphylococcal endolysin Lys87, found to have a broad host range, was fused to the catalytic domains of two *Enterococcus faecalis* endolysins, Lys168 and Lys170, which resulted in highly soluble lytic enzymes that also had activity against Methicillin-Resistant *Staphylococcus aureus* (MRSA) strains [54]. Thus, the interest of bacteriophage endolysins as treatment options are increasing and obstacles such as permeability and specificity are being surmounted. There are different uses for the endolysins and expressed phage enzymes, which delve into food and medical fields. In the latter, they are a welcome addition, whether as prevention, treatment, or a supplement to antibiotics.

Furthermore, polysaccharide-degrading phage-encoded enzymes can be applied in the destruction of microbial biofilms. A large proportion of pathogenic microbes produce biofilms, defined as a three-dimensional matrix of Extracellular Polysaccharides (EPSs) surrounding a community of microbial cells at inhibit the penetration of antibiotics to basal layers. A clear illustration of the application of phage depolymerases as a therapeutic option is a lytic T7 phage engineered to express DspB, an enzyme that degrades β-1, 6-N-acetyl-D-glucosamine, a crucial component of *E. coli* biofilms [55]. Upon infection of the outer biofilm layer, DspB is produced intracellularly and released in the biofilm when the host cell is lysed. The engineered phage was shown to reduce biofilm cell counts by close to 99.997%, a significantly higher level of reduction in comparison to the wild-type T7 phage [55].

Improvements in Biosecurity

In animal production, and particularly poultry production, biosecurity should play a critical role in disease prevention. However, there are many misconceptions around biosecurity in animal production, which results in poor or inadequate protection. In human medicine, biosecurity is also still an area of concern in most healthcare facilities and this poor biosecurity is the cause of most, if not all, of nosocomial infections. In a post-antibiotic era, biosecurity in both animal production and in human medicine needs to be seriously reconsidered. In both the fields, the selection of the product to use for the biosecurity needs is based often on cost alone with very little attention being given to the efficacy of the product. This needs to change in a post-antibiotic era, where improved biosecurity might be the only viable option to control bacterial diseases in a post-antibiotic era.

Full Continual Disinfection Program

Development of a novel formulation of a Didecyl Dimethyl Ammonium Chloride (DDAC)-based disinfectant (Virukill) allowed for the development

of a continual disinfection program for poultry. This program did not only make use of this modified DDAC based product in the effective pre-placement disinfection of poultry houses, but was also used for the continual treatment of the drinking water and the regular disinfection of the air around the birds [56]. Extensive experimentation on the safety of the use of this product in such a continual disinfection program was carried out (data not shown) to ensure both the safety and efficacy of this continual disinfection approach to disease control in poultry production. In an experiment where this approach was evaluated, it was demonstrated that the use of such continual disinfection could not only dramatically reduce the bacterial counts in the poultry house, but could also reduce the mortality rates in the flock [57]. Furthermore, in this experiment, the two set of control pens required treatment with antibiotics to control colisepticaemia in the flocks. In the continual disinfection pens, no colisepticaemia was observed and thus no antibiotics were used to treat these birds. This is a clear indication that the implementation of good biosecurity practices can substantially reduce the need for antibiotics.

Resistance to disinfectants

In a post antibiotic era, improved biosecurity practices and the proper use of disinfectants represent the most feasible strategies for the control of bacterial disease. Similar to antibiotics, the usage of disinfectants is also accompanied by the development and spread of resistance. Two main mechanisms of resistance to disinfectants are described [58]. Intrinsic resistance, typically demonstrated by Gram-negative bacteria [59], is described as reduced susceptibility to a disinfectant as a result of natural properties displayed by the cell, whereas acquired resistance refers to resistance or tolerance arising from mutations in chromosomally encoded genes or acquisition of plasmids or transposons [60, 61].

Microbial cells respond disparately to biocides due to variation in the composition of extracellular structures and physiology [61]. In order to be effective, a disinfectant must cross the outer layers of the cell. The composition of the outer layers of the cell, and thus the Gram stain property, therefore influences the organism's susceptibility to disinfectants [61]. Gram-negative bacteria, especially *Pseudomonas aeruginosa* [62], display severe intrinsic resistance to disinfectants due to the presence of a lipopolysaccharide layer that restricts access to the outer membrane [62–65]. The formation of biofilms by microorganisms represents another form of intrinsic resistance, whereby decreased sensitivity to disinfectants may result from the production of degradative enzymes and neutralising compounds or interaction between the biofilm and the disinfectant [61, 66, 67]. Resistance is primarily acquired *via* acquisition of antimicrobial resistance genes located on plasmids, transposons or integrons [59, 61]. Acquired resistance occurs when resistant clones emerge within a microbial community as a result of exposure to disinfectants at sub-inhibitory concentrations or long-term exposure to quaternary ammonium compounds (QACs) [59, 68, 69].

Quaternary Ammonium Compound Resistance Genes

Quaternary ammonium compounds are widely used as disinfectants in various settings [70, 71]. However, the acquisition of multidrug-resistance genes equips bacteria with the ability to counteract the effects of QACs and adapt to unfavourable conditions [59, 63, 72].

Plasmid-borne QAC resistance genes are readily found in *Staphylococcus aureus* isolated from various sources [60, 71–77]. The *qac* genes encode membrane embedded efflux proteins responsible for the expulsion of hydrophobic compounds such as QACs, cationic biocides and intercalating dyes [70, 71, 78]. The QAC resistance genes described in staphylococci include *qacA, B, G, H, J* and *smr*. Products of the resistance genes *qacA* and *qacB* are members of the Major Facilitator Superfamily (MFS) [76] and these genes are found on plasmids larger than 3 kilobases (kb) [71, 79–81]. The genes *smr, qacG, qacH*, and *qacJ* typically found in gene cassettes on smaller plasmids and encode proteins that belong to the small multidrug resistance (SMR) family [71, 79–81].

Link Between Antibiotic and Disinfectant Resistance

Quaternary ammonium compound resistance genes are commonly located on the same genetic units as antibiotic resistance genes, which may lead to the development of co-resistance and cross-resistance between QACs and antibiotics of relevance in the clinical setting [59]. Both QAC and antibiotic resistance genes are found on class 1 integrons in clinical and environmental isolates [82, 83]. The integrons, functioning as collectors of resistance gene cassettes, readily pick up new resistance genes located on plasmids [59, 83, 84]. Thus, antibiotic resistance gene cassettes and qac resistance genes are often associated on genetic vectors travelling between various species [82, 85, 84]. Widespread use of QACs in cosmetic products is thought to have been responsible for initial selective pressure, leading to the spread of the class 1 integron and consequently the interspecies dissemination of antibiotic and QAC resistance [59, 83]. Furthermore, efflux pumps encoded by QAC resistance genes confer cross-resistance to both QACs and antimicrobial compounds [59].

Conclusions

Adaptation and resistance are naturally occurring phenomena inherent to biological systems, although the giant menace of antibiotic resistance we are facing is purely man-made. Like our predecessors, we have again turned to nature for deliverance in the form of botanical compounds and bacteriophages. Facing an impending post-antibiotic era, mankind can learn vitally important lessons from the ability of microbes to rapidly adapt and survive in challenging environments. The same skill and acumen that brought forth the discovery of antibiotics are again required to generate alternative treatments and improved stewardship strategies to preserve our current arsenal of antibiotics and ensure the sustainability of anti-infective treatment. Lastly, the role of prophylactic strategies, such as vaccination and disinfection, in the prevention of infectious disease and consequently the reduction of antibiotic usage should not be neglected.

References

1. Coates A, Halls G, Hu Y (2011) Novel classes of antibiotics or more of the same? Br J Pharmacol 163:184–194
2. Davies J (2006) Where have all the antibiotics gone? Can J Infect Dis Med Microbiol 17:287–290
3. Natural Resources Defense Council (2016) New antibiotics scorecard: number of top restaurant chains restricting use in chicken doubled in 2016 [Internet]. https://www.nrdc.org/media/2016/160920. Accessed 27 July 2017
4. European Centre for Disease Control and Prevention (2009) The bacterial challenge: time to react [Internet]. Reproduction. 2009. http://ecdc.europa.eu/en/publications/Publications/0909_TER_The_Bacterial_Challenge_Time_to_React.pdf
5. Spellberg B, Powers JH, Brass EP, Miller LG, Edwards JE (2004) Trends in antimicrobial drug development: implications for the future. Clin Infect Dis 38:1279–1286
6. Barbachyn MR, Ford CW (2003) Oxazolidinone structure-activity relationships leading to linezolid. Angew Chemie Int Ed 42:2010–2023
7. Kern WV (2006) Daptomycin: first in a new class of antibiotics for complicated skin and soft-tissue infections. Int J Clin Pract 60:370–378
8. O'Daniel PI, Peng Z, Pi H, Testero SA, Ding D, Spink E et al (2014) Discovery of a new class of non-B-lactam inhibitors of penicillin-binding proteins with gram-positive antibacterial activity. J Am Chem Soc 136:3664–3672
9. Boyle W (1955) Spices and essential oils as preservatives. Am Perfum Essent Oil Rev 66:25–28
10. Isman MB, Miresmailli S, Machial C (2011) Commercial opportunities for pesticides based on plant essential oils in agriculture, industry and consumer products. Phytochem Rev 10:197–204
11. Mith H, Duré R, Delcenserie V, Zhiri A, Daube G, Clinquart A (2014) Antimicrobial activities of commercial essential oils and their components against food-borne pathogens and food spoilage bacteria. Food Sci Nutr 2:403–416
12. Bouaziz M, Yangui T, Sayadi S, Dhouib A (2009) Disinfectant properties of essential oils from *Salvia officinalis* L. cultivated in Tunisia. Food Chem Toxicol 47:2755–2760
13. Ziosi P, Manfredini S, Vertuani S, Ruscetta V, Radice M, Sacchetti G et al (2010) Evaluating essential oils in cosmetics: antioxidant capacity and functionality. Cosmet Toilet 6:32–40

14. Manabe A, Nakayama S, Sakamoto K (1987) Effects of essential oils on erythrocytes and hepatocytes from rats and dipalmitoyl phosphatidylcholine-liposomes. Jpn J Pharmacol 44:77–84
15. Jouany J-P, Morgavi DP (2007) Use of "natural" products as alternatives to antibiotic feed additives in ruminant production. Anim Int J Anim Biosci 1:1443–1466
16. Li P, Piao X, Ru Y, Han X, Xue L, Zhang H (2012) Effects of adding essential oil to the diet of weaned pigs on performance, nutrient utilization, immune response and intestinal health. Asian-Australasian J Anim Sci 25:1617–1626
17. Bento MHL, Ouwehand AC, Tiihonen K, Lahtinen S, Nurminen P, Saarinen MT et al (2013) Essential oils and their use in animal feeds for monogastric animals-effects on feed quality, gut microbiota, growth performance and food safety: a review. Vet Med (Praha) 58:449–58
18. Barbour EK, Shaib H, Azhar E, Kumosani T, Iyer A, Harakeh S et al (2013) Modulation by essential oil of vaccine response and production improvement in chicken challenged with velogenic newcastle disease virus. J Appl Microbiol 115:1278–1286
19. Barbour EK, Bragg RR, Karrouf G, Iyer A, Azhar E, Harakeh S et al (2015) Control of eight predominant *Eimeria* spp. involved in economic coccidiosis of broiler chicken by a chemically characterized essential oil. J Appl Microbiol 118:583–591
20. Mishra RPN, Oviedo-Orta E, Prachi P, Rappuoli R, Bagnoli F (2012) Vaccines and antibiotic resistance. Curr Opin Microbiol 15:596–602
21. Azzari C, Resti M (2008) Reduction of carriage and transmission of *Streptococcus pneumoniae*: The beneficial "side effect" of pneumococcal conjugate vaccine. Clin Infect Dis 47:997–999
22. Gonçalves G (2008) Herd immunity: recent uses in vaccine assessment. Expert Rev Vaccines 7:1493–1506
23. Serruto D, Serino L, Masignani V, Pizza M (2009) Genome-based approaches to develop vaccines against bacterial pathogens. Vaccine 27:3245–3250
24. Finco O, Rappuoli R (2014) Designing vaccines for the twenty-first century society. Front Immunol 5:1–6
25. Rappuoli R (2001) Reverse vaccinology, a genome-based approach to vaccine development. Vaccine 19:2688–2691
26. Pizza M, Scarlato V, Masignani V, Giuliani MM, Arico B, Comanducci M et al (2000) Identification of vaccine candidates against serogroup B meningococcus by whole-genome sequencing. Science 287:1816–1820
27. Romero JD, Outschoorn IM (1994) Current status of meningococcal Group B vaccine candidates: capsular or noncapsular? Clin Microbiol Rev 7:559–575
28. Tettelin H, Saunders NJ, Heidelberg J, Jeffries AC, Nelson KE, Eisen JA et al (2000) Complete genome sequence of *Neisseria meningitidis* serogroup B strain MC58. Science 247:1809–1815
29. Sette A, Rappuoli R (2012) Reverse vaccinology: developing vaccines in the era of genomics. Immunity 33:530–541
30. Smith GP (1985) Filamentous fusion phage: novel expression vectors that display cloned antigens on the virion surface. Science 228:1315–1317
31. De La Cruz VF, Lal AA, McCutchan TF (1988) Immunogenicity and epitope mapping of foreign sequences via genetically engineered filamentous phage. J Biol Chem 263:4318–4322
32. Van Houten NE, Zwick MB, Menendez A, Scott JK (2006) Filamentous phage as an immunogenic carrier to elicit focused antibody responses against a synthetic peptide. Vaccine 24:4188–4200
33. Aghebati-Maleki L, Bakhshinejad B, Baradaran B, Motallebnezhad M, Aghebati-Maleki A, Nickho H et al (2016) Phage display as a promising approach for vaccine development. J Biomed Sci 23:1–18
34. Wang H, Gao Y, Gong Y, Chen X, Liu C, Zhou X et al (2007) Identification and immunogenicity of an immunodominant mimotope of *Avibacterium paragallinarum* from a phage display peptide library. Vet Microbiol 119:231–239
35. Elbreki M, Ross RP, Hill C, O'Mahony J, McAuliffe O, Coffey A (2014) Bacteriophages and their derivatives as biotherapeutic agents in disease prevention and treatment. J Viruses 2014:1–20
36. Bragg R, Boucher C, van der Westhuizen W, Lee J-Y, Coetsee E, Theron C et al (2016) Bacteriophage therapy as a treatment option in a post-antibiotic era. In: Kon KV, Rai M (ed) Antibiotics resistant: mechanisms and new antimicrobial approaches, 1st ed. Elsevier, Amsterdam, pp 309–28
37. Slopek S, Weber-Dabrowska B, Dabrowski M, Kucharewicz-Krukowska A (1987) Results of bacteriophage treatment of suppurative bacterial infections in the years 1981–1986. Arch Immunol Ther Exp (Warsz) 35:569–83
38. Bhattacharya S (2010) The facts about penicillin allergy: a review. J Adv Pharm Technol Res 1:11–17
39. Örmälä A, Jalasvuori M (2013) Should bacterial resistance to phages be a concern, even in the long run? Bacteriophage:3
40. Abedon ST (2012) Bacterial "immunity" against bacteriophages. Bacteriophage 2:50–54
41. Labrie SJ, Samson JE, Moineau S (2010) Bacteriophage resistance mechanisms. Nat Rev Microbiol 8:317–327
42. Barrangou R, Fremaux C, Devaux H, Richards M, Boyaval P, Moineau S et al (2007) CRISPR provides acquired resistance against viruses in prokaryotes. Science 315:1709–1712
43. Rath D, Amlinger L, Rath A, Lundgren M (2015) The CRISPR-Cas immune system: biology, mechanisms and applications. Biochimie 117:119–128
44. Buckling A, Rainey PB (2002) Antagonistic coevolution between a bacterium and a bacteriophage. Proc R Soc London B:931–6

45. Bondy-Denomy J, Pawluk A, Maxwell KL, Davidson AR (2016) Bacteriophage genes that inactivate the CRISPR/Cas bacterial immune system. Nature 493:429–432
46. Seed KD, Lazinski DW, Calderwood SB, Camilli A (2013) A bacteriophage encodes its own CRISPR/Cas adaptive response to evade host innate immunity. Nature 494:489–491
47. Fischetti VA (2005) Bacteriophage lytic enzymes: novel anti-infectives. Trends Microbiol 13:491–496
48. Wang I-N, Smith DL, Young R (2000) Holins: The protein clocks of bacteriophage infections. Annu Rev Microbiol 54:799–825
49. Catalão MJ, Gil F, Moniz-Pereira J, São-José C, Pimentel M (2013) Diversity in bacterial lysis systems: bacteriophages how the way. FEMS Microbiol Rev 37:554–571
50. Tišáková L, Vidová B, Farkašovská J, Godány A (2014) Bacteriophage endolysin Lyt μ1/6: characterization of the C-terminal binding domain. FEMS Microbiol Lett 350:199–208
51. Nelson D, Loomis L, Fischetti VA (2001) Prevention and elimination of upper respiratory colonization of mice by group A streptococci by using a bacteriophage lytic enzyme. Proc Natl Acad Sci 98:4107–4112
52. Loeffler JM, Nelson D, Fischetti VA (2001) Rapid killing of *Streptococcus pneumoniae* with a bacteriophage cell wall hydrolase. Science 294:2170–2172
53. Dong H, Zhu C, Chen J, Ye X, Huang YP (2015) Antibacterial activity of *Stenotrophomonas maltophilia* endolysin P28 against both gram-positive and gram-negative bacteria. Front Microbiol 6:1–8
54. Fernandes S, Proença D, Cantante C, Silva FA, Leandro C, Lourenço S et al (2012) Novel chimerical endolysins with broad antimicrobial activity against methicillin-resistant *Staphylococcus aureus*. Microb Drug Resist 18:333–343
55. Lu TK, Collins JJ (2007) Dispersing biofilms with engineered enzymatic bacteriophage. Proc Natl Acad Sci 104(27):11197–202
56. Bragg RR (2004) Limitation of the spread and impact of infectious coryza through the use of a continuous disinfection programme. Onderstepoort J Vet Res 71:1–8
57. Bragg RR, Plumstead P (2003) Continuous disinfection as a means to control infectious diseases in poultry: evaluation of a continuous disinfection programme for broilers. Onderstepoort J Vet Res 70:219–229
58. Russell AD (1998) Bacterial resistance to disinfectants: present knowledge and future problems. J Hosp Infect 43 (Supple):S57–68
59. Hegstad K, Langsrud S, Lunestad BT, Scheie AA, Sunde M, Yazdankhah SP (2010) Does the wide use of quaternary ammonium compounds enhance the selection and spread of antimicrobial resistance and thus threaten our health? Microb Drug Resist 16:91–104
60. Russell AD (1997) Plasmids and bacterial resistance to biocides. J Appl Microbiol 83(2):155–65
61. McDonnell G, Russell AD (1999) Antiseptics and disinfectants: activity, action, and resistance. Clin Microbiol Rev 12:147–179
62. Méchin L, Dubois-Brissonnet F, Heyd B, Leveau JY (1999) Adaptation of *Pseudomonas aeruginosa* ATCC 15442 to didecyldimethylammonium bromide induces changes in membrane fatty acid composition and in resistance of cells. J Appl Microbiol 86 (5):859–66
63. White DG, McDermott PF (2001) Emergence and transfer of antibacterial resistance. J Dairy Sci 84: E151–E155
64. Paulsen IT, Park JH, Choi PS, Saier MH Jr (1997) A family of Gram-negative bacterial outer membrane factors that function in the export of protiens, carbohydrates, drugs and heavy metals from Gram-negative bacteria. FEMS Microbiol Lett 156:1–8
65. Adair FW, Geftic S, Gelzer J (1971) Resistance of *Pseudomonas* to quaternary ammonium compounds. Appl Microbiol 21:1058–1063
66. Gilbert P, Collier PJ, Brown MR (1990) Influence of growth rate on susceptibility to antimicrobial agents: biofilms, cell cycle, dormancy, and stringent response. Antimicrob Agents Chemother 34:1865–1868
67. Campanac C, Pineau L, Payard A, Baziard-Mouysset G, Roques C (2002) Interactions between biocide cationic agents and bacterial biofilms. Antimicrob Agents Chemother 46:1469–1474
68. Buffet-Bataillon S, Tattevin P, Bonnaure-Mallet M, Jolivet-Gougeon A (2012) Emergence of resistance to antibacterial agents: the role of quaternary ammonium compounds—a critical review. Int J Antimicrob Agents 39:381–389
69. McBain AJ, Ledder RG, Moore LE, Carl E, Gilbert P, Catrenich CE (2004) Effects of quaternary-ammonium-based formulations on bacterial community dynamics and antimicrobial susceptibility. Appl Environ Microbiol 70:3449–3456
70. Bjorland J, Sunde M, Waage S (2001) Plasmid-borne *smr* gene causes resistance to quaternary ammonium compounds in bovine *Staphylococcus aureus*. J Clin Microbiol 39:3999–4004
71. Bjorland J, Steinum T, Kvitle B, Waage S, Sunde M, Heir E (2005) Widespread distribution of disinfectant resistance genes among staphylococci of bovine and caprine origin in Norway. J Clin Microbiol 43:4363–4368
72. Ioannou CJ, Hanlon GW, Denyer SP (2007) Action of disinfectant quaternary ammonium compounds against *Staphylococcus aureus*. Antimicrob Agents Chemother 51:296–306
73. Bjorland J, Steinum T, Sunde M, Waage S, Heir E (2003) Novel plasmid-borne gene *qacJ* mediates resistance to quaternary ammonium compounds in equine *Staphylococcus aureus*, *Staphylococcus simulans*, and *Staphylococcus intermedius*. Antimicrob Agents Chemother. 47(10):3046–52
74. Heir E, Sundheim G, Holck AL (1999) Identification and characterization of quaternary ammonium compound resistant staphylococci from the food industry. Int J Food Microbiol 48:211–219

75. Heir E, Sundheim G, Holck AL (1999) The *qacG* gene on plasmid pST94 confers resistance to quaternary ammonium compounds in staphylococci isolated from the food industry. J Appl Microbiol 86:378–388
76. Heir E, Sundheim G, Holck AL (1998) The Staphylococcus *qacH* gene product: a new member of the SMR family encoding multidrug resistance. FEMS Microbiol Lett 163:49–56
77. Anthonisen I, Sunde M, Steinum TM, Sidhu MS, Sørum H (2002) Organization of the antiseptic resistance gene *qacA* and Tn 552 -related β -lactamase genes in multidrug-resistant *Staphylococcus haemolyticus* strains of animal and human origins. Antimicrob Agents Chemother 46:3606–3612
78. Langsrud S, Sundheim G, Borgmann-Strahsen R (2003) Intrinsic and acquired resistance to quaternary ammonium compounds in food-related *Pseudomonas* spp. J Appl Microbiol 95(4):874–82
79. Alam MM, Ishino M, Kobayashi N (2003) Analysis of genomic diversity and evolution of the low-level antiseptic resistance gene *smr* in *Staphylococcus aureus*. Microb Drug Resist 9:S-1–S-7
80. Littlejohn TG, DiBerardino D, Messerotti LJ, Spiers SJ, Skurray RA (1991) Structure and evolution of a family of genes encoding antiseptic and disinfectant resistance in *Staphylococcus aureus*. Gene 101:59–66
81. Paulsen IT, Brown MH, Dunstan SJ, Skurray RA (1995) Molecular characterization of the Staphylococcal multidrug resistance export protein QacC. J Bacteriol 177:2827–2833
82. Gillings MR, Holley MP, Stokes HW (2009) Evidence for dynamic exchange of qac gene cassettes between class 1 integrons and other integrons in freshwater biofilms. FEMS Microbiol Lett 296:282–288
83. Gillings MR, Xuejun D, Hardwick SA, Holley MP, Stokes HW (2009) Gene cassettes encoding resistance to quaternary ammonium compounds: a role in the origin of clinical class 1 integrons? Int Soc Microb Ecol J 3:209–215
84. Recchia GD, Hall RM (1995) Gene cassettes: a new class of mobile element. Microbiology 141:3015–3027
85. Partridge SR, Recchia GD, Stokes HW, Hall M (2001) Family of Class 1 integrons related to In4 from Tn 1696. Society 45:3014–3020

Encapsulation of Theophylline in Gelatin A–Pectin Complex Coacervates

Nirmala Devi, Chayanika Deka, Prajnya Nath and Dilip Kumar Kakati

Abstract

The present study aims at synthesizing gelatin A–pectin complex coacervates and encapsulation of theophylline in the polymer system. Variation and optimization of different reaction parameters such as pH, ratio between the polymers and cross-linker concentration was carried out to attain higher product yield. Relative viscosity, turbidity and UV-visible measurements were done for optimization. The optimum ratio between gelatin A–pectin was fixed at weight ratio 42:8 and pH=3.5. It was further observed that adhesion between the microcapsules decreased by the use of sodium carboxymethyl cellulose (SCMC) to the coacervate. The synthesized microcapsules were characterized by using spectroscopic techniques to assess their formation, drug loading and chemical interaction between theophylline and coacervate. Scanning electron microscopy (SEM) revealed the formation of microcapsules. Study relating to the encapsulation efficiency and swelling of the complex coacervates were also carried out.

Keywords

Gelatin-A · Coacervation · Pectin
Microencapsulation · Theophylline

Introduction

In the recent years, complex coacervation is gaining significant attention in the field of agriculture as slow and controlled release fertilizer and pesticides, food and flavoring systems [1], insect repellent formulations and in drug delivery systems, due to its simple method of preparation and cheaper ingredients. It involves the electrostatic interaction between the oppositely charged polyelectrolytes to form polymer rich and poor regions called as coacervates and supernatant [2] respectively. The coacervate phase is usually more viscous and concentrated and thus can be easily distinguishable from the original polymer solution [3].

Gelatin A is a mixture of peptides and proteins which is produced by the partial hydrolysis of collagen and has been reported as an excellent material for industrial, pharmaceutical, photographic and medical applications due to its biocompatible, biodegradable and non-toxic nature. When heated it melts to liquid and solidifies on cooling and with water it forms a semi-solid

N. Devi (✉)
Department of Science & Humanities, National Institute of Technology Nagaland, Chumukedima, Dimapur 797103, Nagaland, India
e-mail: nirmaladevi2040@gmail.com

C. Deka · P. Nath · D. K. Kakati
Department of Chemistry, Gauhati University, Guwahati 781014, Assam, India

R. Adhikari and S. Thapa (eds.), *Infectious Diseases and Nanomedicine III*,
Advances in Experimental Medicine and Biology 1052, https://doi.org/10.1007/978-981-10-7572-8_6

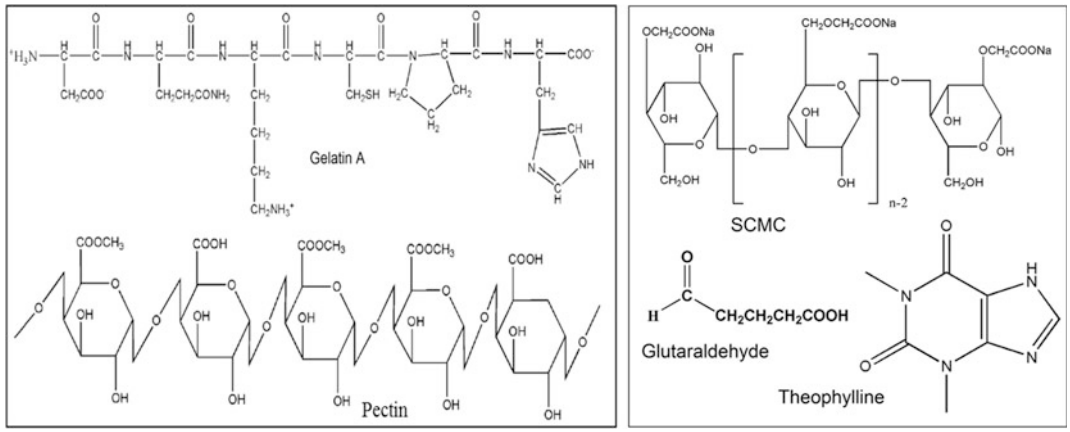

Fig. 1 Chemical structure of gelatin A and pectin, SCMC, glutaraldehyde, and theophylline

colloid gel. Pectin is a galacturonic acid rich polysaccharide which is commonly used in food as gelling and thickening agent. Henri Braconnot, a French chemist and pharmacist, was the first who isolated and described pectin in 1825. It is mainly found in apples, guavas, oranges, plums and other citrus fruits. It has been known to act against constipation, nausea, diarrhea and wound remedial formulations. It has also been used in drug release and carrier formulations targeted to the gastrointestinal tract as various forms such as microcapsules, matrices, tablets, beads and film etc due to its biocompatible and biodegradable nature. Amphoteric protein gelatin A attains a positive charge at acidic pH and so, it is expected that it can easily undergo coacervation at lower pH with pectin, is negatively charged [4]. The chemical structure of both gelatin A and pectin is shown in Fig. 1.

Glutaraldehyde (chemical structure is shown in Fig. 1) was used as cross-linking agent as it exhibits the ability to react and cross-link proteins, creating a structure that is more stable than that attained by the physical aggregation of polymer molecules and hence leads to the formation of a broad range of conjugates in generating thermally and chemically stable cross-links [5].

During complex coacervation, due to high electrostatic attractive interaction between the oppositely charged polymers, particle aggregation takes place that creates a problem. Particles adhere with each other and to the container surface. For decreasing the coacervate particle aggregation, various coalescence reducing substances were reported to be used in complex coacervation systems [6]. Such physiochemical properties could however be controlled by fine controlling of the extent of cross-linking, addition of anti-adhesive agents [6, 7] etc. Sodium carboxymethyl cellulose (SCMC, Fig. 1) was reported to be more effective anti-adhesive agent than others in the literature [8]. Furthermore, an excellent hydrophilic polymer SCMC has several advantages over other inorganic anti-adhesive agents because of its eco-friendliness and superior film-forming ability [9]. Glutaraldehyde has been used as the cross-linking agent due to its high reactivity and commercial availability.

One of the most frequently used drug for the treatment of chronic asthmatic symptoms is theophylline (1,3-dimethyl-7H-purine-2,6-dione or 1,3-dimethylxanthine), the chemical structure of which is shown in Fig. 1. The drug that was reported to be extracted initially from tea leaves and scientist Albrecht Kossel carried out the first

successful chemical identification of it [10]. It is also found naturally in foods such as chocolate and coffee. Theophylline has a narrow therapeutic index and so it should be taken in a very small dose as prescribed by physician, to avoid toxicity. Toxicity leads to side effects such as trembling, nausea, headache, dizziness, heartburn, stomach pain, loss of appetite etc. [11]. Theophylline was used as model drug for encapsulation due to its short half-life and good oral bio-availability. The drug was encapsulated in a non-porous polymeric coacervate complex so that the system delivers the drug at a pre-determined rate for a long time (at least 12 h).

The present study aims at synthesizing stable gelatin A–pectin coacervate complex microcapsules and optimizes the variables like polymer ratio and pH of the medium for maximum yield. For optimization relative viscosity, turbidity and UV spectroscopic measurements were conducted. Microencapsulation of theophylline at different reactant compositions was also carried out. Swelling index and encapsulation efficiency were also determined. The prepared microcapsules were characterized by FTIR spectroscopy to assess their formation, drug loading, chemical interaction if any between theophylline and coacervate complex. SEM was used to study the confirmation of formation of microcapsules.

Experimental Design

Materials

Pectin and theophylline was purchased from Himedia Laboratories, Mumbai (India); glutaraldehyde 25%, HCl and acetic acid from E. Merck (India); NaOH, sodium acetate, potassium hydrogen phosphate (KH_2PO_4) from Qualigens (India); sodium carboxy methyl cellulose (SCMC) from Rankem (India), and Gelatin A from Sigma-Aldrich Inc. (USA) were purchased used for the experiments. Double-distilled ionized (DDI) water was used throughout the whole experiment and all other chemicals used were of analytical grade.

Methods

Optimization of Gelatin a to Pectin Ratio

For the formation of microcapsules at first optimization was done to determine the best suitable ratio for the formation of maximum microcapsules. 0.5% (w/v) solution of both gelatin A and pectin were prepared separately at 60 °C in distilled water. Then the two polymeric solutions were mixed in varying proportion under mechanical stirring at same temperature. The product formation was followed by measuring the relative viscosity, turbidity and absorbance in UV spectrophotometer of decanting filtrate. Product formed at the end of the reaction was separated, dried in vacuum oven and yield was recorded. From the yield, a particular range of ratios were ascertained at which the two polymeric solutions gave the maximum yield. Then ratios between pre-determined ranges of ratios were selected and the above process was repeated with 0.1% polymer solutions. Again, relative viscosity, turbidity and absorbance in UV-visible spectrometer of the mixtures were recorded to fix the ratio that gave maximum yield. Turbidity measurements were carried out in a NepheloTubidity Meter 131 (Systronics). For this a mixture of hexamethylenetetramine and hydrazine sulfide was taken as reference solution.

Polyelectrolyte complexation is highly dependent on pH. Therefore, the solutions of the polymer are prepared in buffer solutions. 0.1% (w/v) gelatin A and pectin solutions were prepared in the sodium acetate buffer of pH = 3.6 buffer solution and the synthetic process were repeated. Product formed was dried after decantation of unreacted liquid and then weighed. Relative viscosity and absorbance in UV–visible spectroscopy of decanted liquid was taken. On the basis of above observations, a ratio was fixed at which maximum amount of coacervate complex can be obtained [12–14].

Optimization of PH

10% (v/v) solution of acetic acid, 2.5% (v/v) solution of sodium hydroxide and 0.5% (w/v) solution of each polymer were prepared separately in distilled water. The polymer solutions were

mixed at the predetermined ratio at which maximum yield was obtained. Then different mixtures were subjected to varying pH (2–5), in order to determine the suitable pH for maximum yield. Variation of pH was done by careful dropwise addition of either NaOH or acetic acid solution to mixtures, made in water. The pH variation was measured using the Digital pH meter 335 (Systronics). The instrument was standardized using buffer capsule of pH 4 and pH 7. Viscosity measurements of decanted liquid were also done in order to confirm the pH. Viscosity measurements were carried out using Ostwald's Viscometer.

Preparation of Neat Cross-Linked Coacervate Complex

0.5% (w/v) solutions of both gelatin A and pectin were prepared separately in distilled water by stirring the solutions at about 60 °C. After that gelatin A was taken in a beaker and pectin was added dropwise with constant stirring until a turbid mixture was formed. The mixture was allowed to settle down. The upper clear liquid was decanted and product was recovered.

Swelling Study

Equal amount of dry neat coacervate complex and glutaraldehyde cross-linked coacervate were weighed first. The each coacervate complex was immersed into solutions of pH 1.2, 6.6, 7.0 and 7.4 and allowed to swell, until a swollen equilibrium was reached. Weights of the complexes were measured at definite intervals of time. Complex was then taken out from the solution and weighed after the liquid was wiped out with tissue paper. Mean value of the experiments carried out in triplicate were represented. The equilibrium swelling index (Eq. 1) was calculated from the following formula [15]:

$$\text{Swelling Index} = \left[\left(W_g - W_o\right)/W_o\right] \times 100\%, \quad (1)$$

where, W_g = weight of the pieces in the swelling medium

W_o = initial weight of the pieces.

Microencapsulation of Theophylline

Two percent (w/v) aqueous solution of gelatin A and pectin were prepared individually in DDI by magnetic stirring at 60 °C. Theophylline was dissolved in the solution of gelatin A by magnetic stirring for 15 min to get a clear solution. The pectin was then added dropwise to the above solution at the optimum polymer ratio determined earlier, with constant mechanical stirring. After complete mixing, pH was decreased to 3.5–4 using acetic acid. The system temperature was decreased to 5 °C along with continuous mechanical stirring. SCMC was added dropwise to the above solution, followed by glutaraldehyde addition. Then temperature was increased slowly to about 45 °C. Continuous stirring for 3 h under a controlled heating in a water bath at 40–45 °C was carried out. After this, stirring was stopped and mixture was allowed to cool and settle down. Drug loaded coacervate complex thus formed was filtered, washed several times with water to remove any unreacted substances and then freeze dried.

Calibration Curve of Theophylline

To determine the encapsulation efficiency of theophylline in the microcapsules, a standard calibration curve was made. Theophylline is soluble in water. A known concentration of theophylline was dissolved in distilled water and was scanned in the range of 200–800 nm by using a UV visible spectrophotometer. Dilute solutions of theophylline were prepared in de-ionized water at different pH (pH = 7, 7.4 and 1.2) and absorbance of all solutions were recorded in UV-spectrometer [UV-1800 (SHIMADZU) instrument]. The absorption maxima were found at wavelengths 272 and 277 nm respectively. Recording and plotting of the absorbance values obtained in the study with different concentrations gave linear calibration curve. From the calibration curve, the unknown concentration of theophylline was determined by recording the absorbance value of the solution.

Encapsulation Efficiency

One gram of theophylline encapsulated coacervate complex was treated with 100 mL water and

stirred with magnetic stirrer for about 10 h without heating. After filtering the solution, absorption for the filtrate at 272 nm in UV-visible spectrophotometer was recorded. These values were then compared with that of pure theophylline and the encapsulation efficiency (EE) % (Eq. 2) was calculated using the following equation [16]:

$$\mathrm{EE}(\%) = (\mathrm{W}_1/\mathrm{W}_2) \times 100\%, \qquad (2)$$

where, W_1 = Actual drug loaded in a weighed amount of microcapsules
= drug content per gram of microcapsule x yield of microcapsules
W_2 = Theoretical drug loading
= amount of drug (g) taken during the formulation.

Characterization and Testing

The FT-IR spectra of all the samples and the loaded microcapsules were recorded in Perkin Elmer RXI FT-IR spectrometer in the range 4000–450 cm^{-1} using KBr method. The microcapsule formation was studied via SEM observation in a JSM-6360 (JEOL) Scanning Electron Microscope. Surface morphology of the theophylline encapsulated microcapsules and neat coacervate complex of gelatin A and pectin were studied at an accelerating voltage of 15kV after placing the dry samples on brass holder and sputtering with gold.

Results and Discussion

Study of Variation of Gelatin A and Pectin Ratio on Yield of Coacervate Complex

The preparation of coacervate complex was followed by drying and weighing the product and measuring turbidity and viscosity of the supernatant liquid after removal of the product. The absorbance of the supernatant liquid at specific wavelengths (272 and 277 nm in UV-visible region) was also measured. A comparison was made between different % of gelatin present in the polymer mixture to % yield, absorbance, relative viscosity, and turbidity of supernatant liquid. From that optimum polymer ratio was derived.

Again from the Beer–Lambert's law, we know that absorbance increases with the increase in concentration. The minimum absorbance corresponds to the minimum amount of gelatin in the solution, i.e., the maximum yield of gelatin A–pectin coacervate complex. As suggested by Shinde et al. [4], the maximum yield of coacervate product of gelatin A and pectin was obtained when the gelatin % ranges from 80 to 90%.

From Fig. 2a, it is observed that the percent yield increases with increase in gelatin concentration up to 80%. After that, the percent yield decreases. So, a maximum yield is obtained when the gelatin percent was between 80–90%. From Fig. 2b, it can be seen that the relative viscosity increases with increase in gelatin % up to a limit and then it starts decreasing. Similar variation of turbidity as that of relative viscosity is observed with increase in gelatin percent (Fig. 2c).

Absorbance at both wavelengths is found to be increased with increase in the gelatin concentration and reaches a maximum, after which absorbance decreases as can be seen in Fig. 2d. The explanation could be put forward in this way—at the initial stage very minute amount of products are formed and absorbance for unreacted substances increases. It is known that both viscosity and turbidity depend on the concentration of the solution. So, the lowest viscosity and lowest turbidity indicate the lowest concentration of unreacted species in the liquid and hence indicates maximum product formation. Again, from Beer–Lambert's law it is known that absorbance increases with increase in concentration. The minimum absorbance corresponds to the minimum amount of unreacted substances in the solution, i.e., the maximum yield of gelatin A–pectin coacervate complex. After determining the optimum ratio range, the particular ratio that gives maximum yield was determined. It is clear from the graphs that absorbance and relative viscosity at 84% was lower. So, it is confirmed that gelatin A

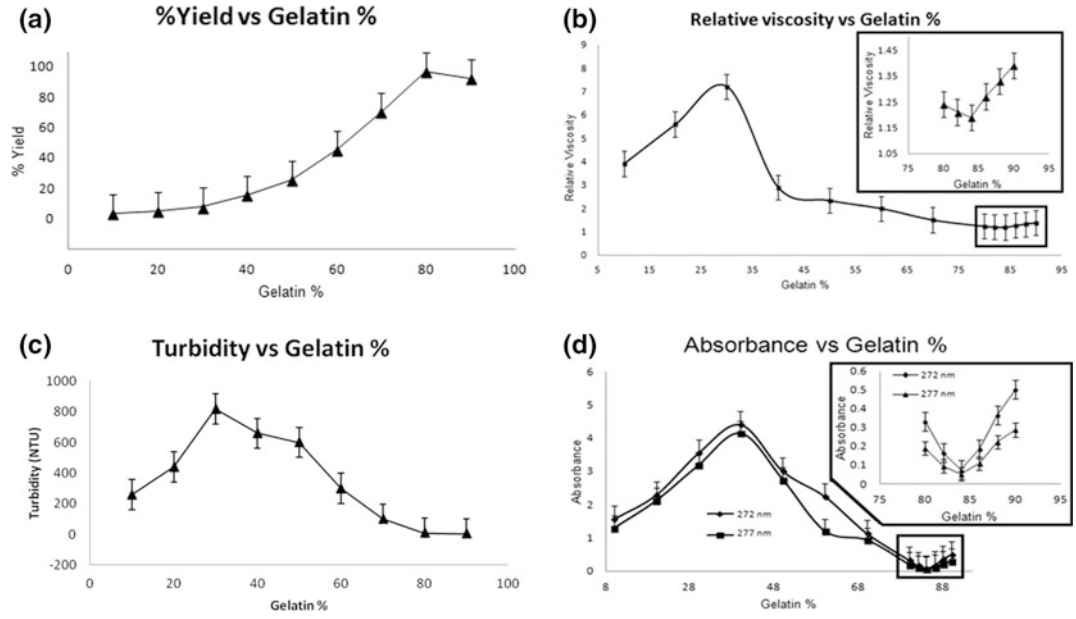

Fig. 2 Optimization profile for gelatin–pectin beads in terms of **a** % yield, **b** viscosity, **c** turbidity, and **d** absorbance

and pectin when mixed in 5.25:1 ratio (84% gelatin A) maximum amount of gelatin–pectin coacervate product is formed. Thus, the optimum ratio of gelatin A to pectin was fixed at 5.25:1.

Variation of pH on the Yield of Complex Coacervate

For the optimization of pH, the optimized ratio between polymer solutions was maintained. The reactions were studied at pH 2.5–5. The percent yield, relative viscosity was measured. From Fig. 3a and b, it was found that maximum yield of the coacervate and lesser supernatant viscosity was obtained at pH 3.5, i.e. optimum pH is 3.5. Saravanan et al. [14] also reported that complex coacervation of gelatin A–pectin takes place at pH around 3.5–4.

Study of Swelling Index with Variation of pH

The swelling study was carried out at different pH 1.2, 6.6, 7.0, and 7.4 for the neat (Fig. 4a) as well as for two cross-linked coacervate products (Fig. 4b and c). For all three sets, it was observed that coacervate complexes have higher percentage swelling value at higher pH which decreases with decrease in pH. The poor swelling ability of coacervate complexes under an acidic medium can be explained in this way that at lower pH free amino groups of gelatin A get protonated, which results in an increase in electrostatic interaction between carboxy group of pectin with amino groups of gelatin A. This strong interaction results in a dense structure, which has lower swelling tendency.

It is observed from Fig. 4a–c that cross-linked products show lower percentage swelling values. Means et al. [9] observed that cross-linker, glutaraldehyde links rapidly to the active amino groups of protein, forming covalent bond and thus gives compact structure. So, with the increased use of cross-linker, stability of coacervate complex increases and swelling decreases. Swelling results also indicate that for the same amount of cross-linker, swelling increases at higher pH. Nimni et al. [17] observed that in alkaline medium, the cross-linking efficiency decreases. The reason he explained is that in alkaline medium, amino groups are neutralized and carboxy groups

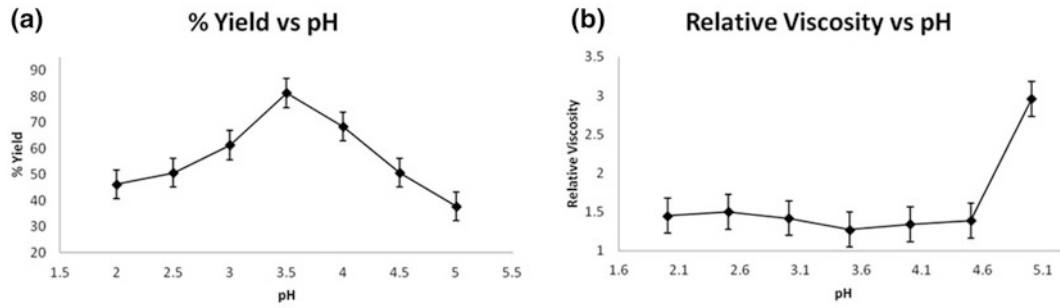

Fig. 3 Optimization profile for pH in terms of **a** % yield, and **b** relative viscosity

remained negatively charged. So, electrostatic attractive interaction between the charged functional groups vanished and domination of repulsive force between carboxy group results in swelling.

FTIR Spectroscopic Study

Natural polymer pectin contains free carboxyl groups and provides negative charge to the pectin molecules whereas presence of amino groups in gelatin A, which is a protein, imparts positive charge at lower pH range. Polyelectrolyte complex coacervation between the two oppositely charged poly-ions gives out amide linkages [14]. To verify the creation of amide linkage and hence to confirm complexation between gelatin A and pectin, FTIR spectroscopic characterization technique was utilized. The FTIR spectra of gelatin A, pectin, complex coacervate of both the polymers, theophylline and thephylline loaded microcapsule were shown in Fig. 5. IR absorption peak at 3448 cm^{-1} for the amino groups in the protein was seen in Fig. 5a, spectrum of gelatin A [14]. Moreover, the spectrum of gelatin A showed several characteristic absorption bands which could be assigned as peak at 2927 cm^{-1} is due to C–H stretching frequency of alkenes; 2854 cm^{-1} is due to C–H stretching of alkanes; 1654 cm^{-1} is due to C=O stretching of amide; 1257 cm^{-1} is due to the C–O stretching of carboxylic group and 1083 cm^{-1} is due to C–N stretching of amines are observed. FTIR spectrum of pectin illustrated the stretching frequency for C=O of carboxylic acid group at 2931 cm^{-1} and methyl ester group at 1747 cm^{-1} [18]; characteristic peaks at 3398 cm^{-1} and 1076 cm^{-1} were assigned to the alcoholic O–H stretching and C–O stretching of ether respectively.

The appearance of new peak at 1597 cm^{-1} in the sample of complex coacervate of gelatin A and pectin could be attributed to the amide group formation and confirming thereby the polyelectrolyte complexation between the two natural polymers. Moreover, another new band at 1111 cm^{-1} appeared because of the existence of acetate groups that was produced by the reaction of the O-H groups provided by the gelatin A chains and glutaraldehyde [19]. Characteristic absorption peak observed at 1712 cm^{-1} is due to the presence imide stretching of heterocyclic moiety of theophylline [19]. The IR spectrum of anhydrous theophylline also showed the following characteristic peaks—3359 cm^{-1} due to the N–H stretching; 3120, 3043, 2989, 2924, 2808 cm^{-1} are due to the C–H stretching; 1670 cm^{-1} is due to the C=O stretching for tertiary amide; 1566 cm^{-1} is due to the N–H bending; 1446 cm^{-1} is due to the C–H stretching; 1242 cm^{-1} is due to the C–N stretching. The IR spectrum of the theophylline-loaded microcapsules showed characteristic peaks for theophylline at 3166, 1712, 1666, 1562, 1446 and 1238 cm^{-1}, from which we can interpret that no chemical interaction between theophylline and other components of microcapsule occurred [20].

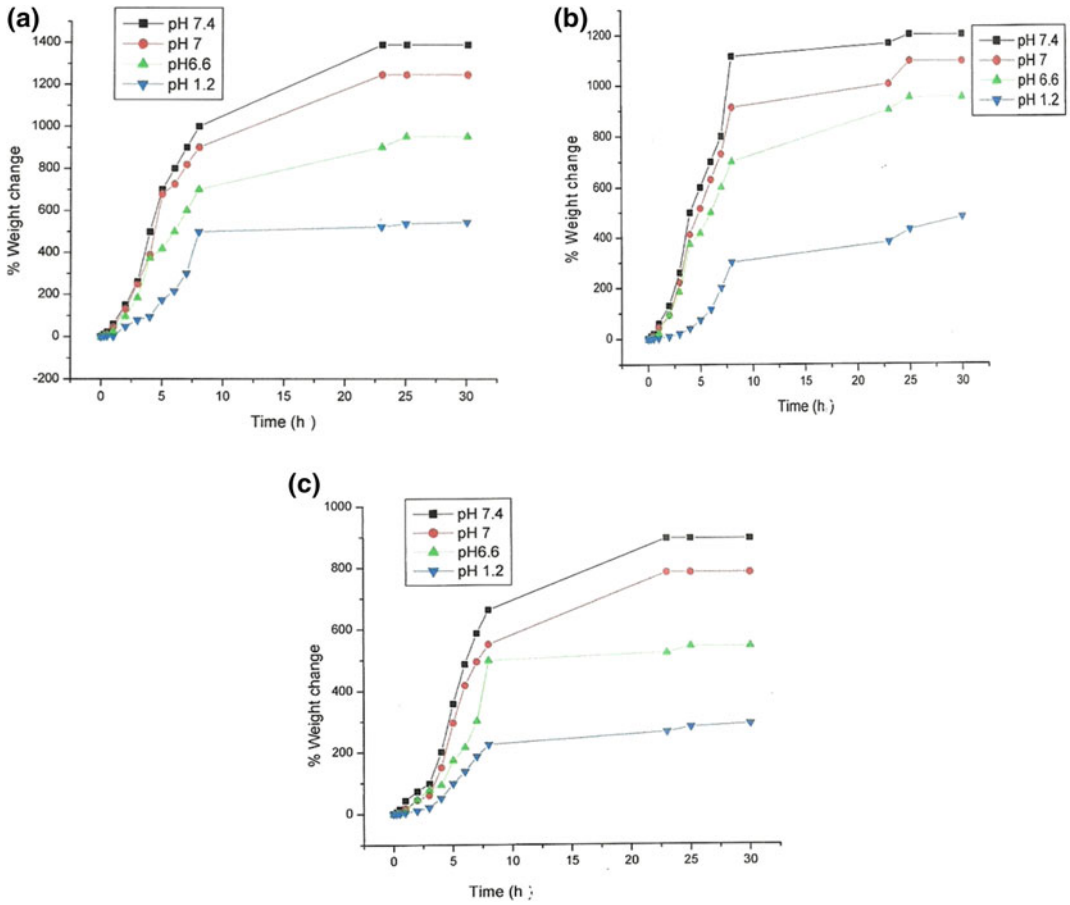

Fig. 4 Swelling profile for **a** neat coacervate complex, and cross-linked coacervate product with **b** 2 mmol and **c** 7 mmol glutaraldehyde

Morphology Study

To know the physicochemical nature and surface morphology of the gelatin A and pectin polyelectrolyte complex coacervate microcapsules, particles dried under vacuum oven were characterized by Scanning Electron Microscopy. It provided a direct proof of the shape of drug loaded, neat and cross-linked coacervate complex. Figure 6a shows the SEM photomicrograph of dried neat gelatin A–pectin coacervate complex. The image revealed the formation non-porous, non-uniform film with aggregation. Figure 6b shows the SEM micrographs of gelatin A–pectin coacervate complex after the addition of the cross-linker, glutaraldehyde. As can be seen from the micrographs, the aggregation between the particles decreased forming some dense structures (aggregation through covalent interaction) or more precisely can be so called "particles" with non-uniform shape and size. The adhesion between the particles is supposed to be decreased after the addition of SCMC. So, the scanning electron micrographs of the particles, after the addition of SCMC, were recorded. The process was described earlier. It can be seen from the scanning electron micrographs (Fig. 6c) that adhesion between the particles decreased. The scanning electron micrographs of theophylline loaded dried microcapsules are shown in Fig. 6

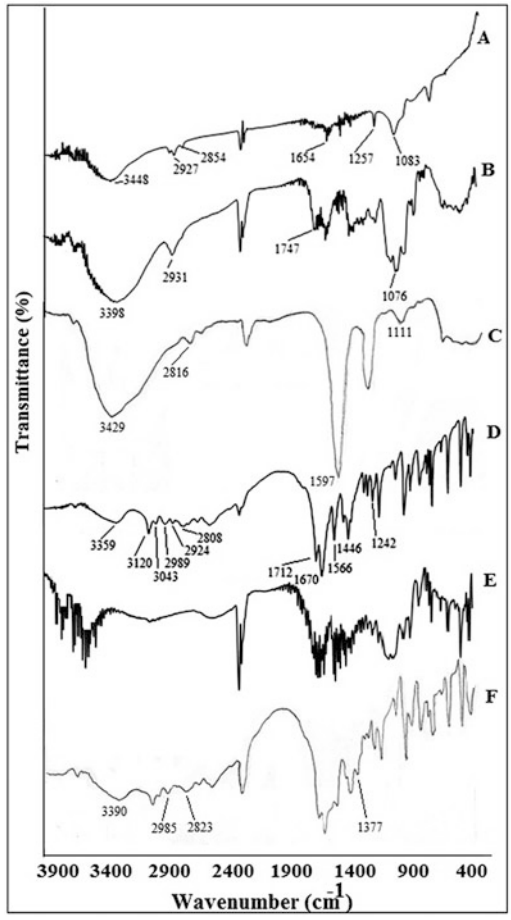

Fig. 5 FTIR Spectra of **a** gelatin A, **b** pectin, **c** neat gelatin A–pectin coacervate, **d** theophylline, **e** physical mixture of gelatin A, pectin and theophylline, and **f** theophylline-loaded microcapsules

d–f. As seen from the above micrographs, the microcapsules are found to be spherical in shape.

Encapsulation Efficiency

Encapsulation efficiency is an important parameter to determine the stability of the coacervate microcapsule for encapsulation of active material. Theophylline encapsulation in gelatin A–pectin coacervate complex was carried out under different reaction conditions varying the content of polymers, theophylline, cross-linker, and SCMC. Thirteen different reactions were performed varying proportions of different reactants. The gelatin A: pectin ratio and pH were maintained at 42: 8 and 3.5 respectively for all the reactions performed.

As depicted at Table 1, it was observed that on increasing the loading of theophylline (from 0.1 to 1.5 g) the encapsulation efficiency (% EE) increased from 17.96 to 74.71%, when the amounts of all other ingredients except theophylline were kept constant. On increasing the concentration of SCMC (0.5% w/v) from 5–20 mL (0.025–0.1 g) keeping the amount of polymer, amount of loaded drug, theophylline and cross-linker constant no observable change occurred for %EE. Again, when polymer concentrations were increased, keeping the concentration of glutaraldehyde, quantity of the drug loaded and amount of SCMC to be constant it was observed that %EE increased from 58.16 to 75.23%. These data show that encapsulation efficiency is highest with lowest amount of cross-linker, and a higher percentage of polymer solutions. However, this aspect needs further investigation. Again keeping other parameters constant, increasing the amount of cross-linker from 2 to 7 mmol, encapsulation efficiency was found to increase from 67.41 to 73.38%, for the reason that of crosslinking improved rigidity of the system, which in turn lessens the leaching of theophylline out of the microspheres [19]. Yan-Fei et al. [21] reported that cross-linking of gelatin A with glutaraldehyde gives three dimensional networks and increases the internal surface area for absorption of drug. Furthermore, it can be concluded that the microencapsulation process variables influences the active agent encapsulation efficiency significantly in microspheres and accordingly encapsulation efficiency in microsphere formulations can be tuned by changing the reaction parameters and variables, which are studied and reported in previous literature as well [21].

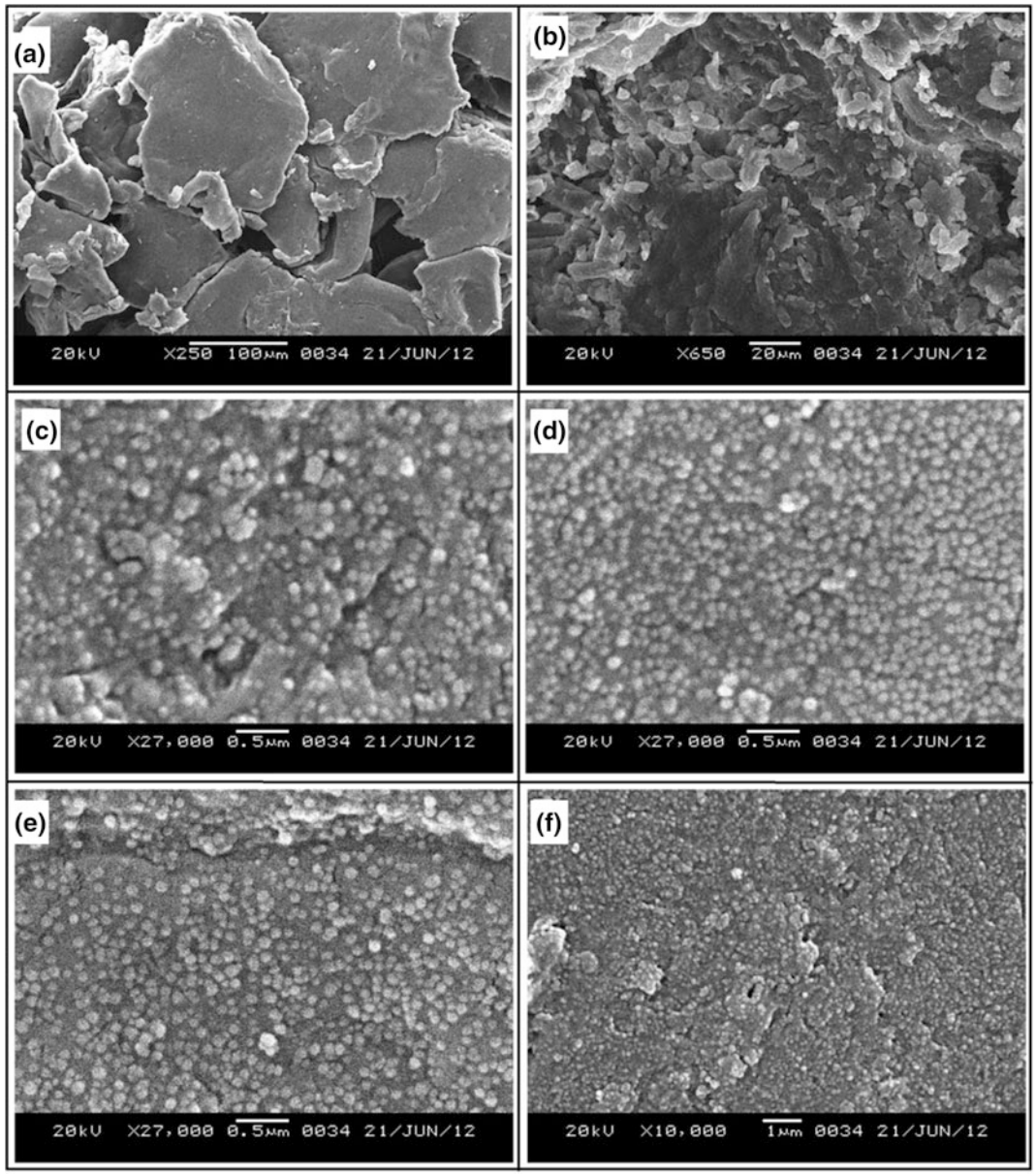

Fig. 6 SEM of (**a**) neat coacervate complex, coacervate complex on addition of **b** 2 mmol glutaraldehyde, **c** 0.025 g SCMC and 2 mmol glutaraldehyde (unloaded), **d** 0.025 g SCMC and 2 mmol glutaraldehyde (1 g theophylline loaded), and cross-linked coacervate complex on addition of (**e**) 0.05 g SCMC and 2 mmol glutaraldehyde (1 g theophylline loaded **f** 0.1 g SCMC and 7 mmol glutaraldehyde (1 g theophylline loaded)

Table 1 Encapsulation behavior of the theophylline-loaded microcapsules under varying reaction conditions [Concentration of gelatin = 2% (w/v), concentration of pectin = 2% (w/v), concentration of SCMC = 0.5% (w/v)]

Gelatin (g)	Pectin (g)	Theophylline (g)	Glutaraldehyde (mmol)	SCMC (g)	Encapsulation efficiency (%)
1.68	0.32	0.1	2	–	17.96
1.68	0.32	0.5	2	–	53.23
1.68	0.32	1	2	–	67.58
1.68	0.32	1.5	2	–	74.71
1.68	0.32	1	2	0.025	66.29
1.68	0.32	1	2	0.05	67.35
1.68	0.32	1	2	0.1	67.41
1.68	0.32	1	4	0.1	69.19
1.68	0.32	1	7	0.1	73.38
1.68	0.32	1	–	0.1	48.24
0.84	0.16	1	2	0.1	58.16
2.52	0.48	1	2	0.1	75.23

Conclusions

Gelatin A–pectin coacervate synthesis is dependent on variables like polymer ratio, concentration Gelatin A–pectin complex coacervate synthesis is dependent on variables like polymer ratio, concentration of two polymers, pH and reaction medium. Optimum gelatin A: pectin ratio and pH were found to be 42:8 and 3.5, respectively to get the maximum yield of coacervate. The formation of the complex by reaction between the two oppositively charged polymers was confirmed by FTIR spectroscopic data. The formation and physicochemical nature of the microcapsules were also investigated. The complex coacervation was influenced by the amount of polymer, cross-linker and drug. The active agent encapsulation was proved from the FTIR study. The results indicate the possibility of using gelatin A–pectin coacervate complex for encapsulating theophylline and use in pharmaceutical industries.

Acknowledgements The research work has been sponsored partially by the University Grants Commission UGC BSR Scheme (RFMS) (C. D.). The authors are thankful to the UGC for financial assistance. The authors are also thankful to SAIF, North Eastern Hill University, Shillong for the SEM images.

References

1. Polk A, Amsden B, De Yao K, Peng T, Goosen MF (1994) Controlled release of albumin from chitosan-alginate microcapsules. J Pharm Sci 83:178–185
2. Tsuchida E, Abe K (1982) Interactions between macromolecules in solution and intermacromolecular complexes. In: Tsuchida E, Abe K (eds) *Interactions between macromolecules in solution and intermacromolecular complexes: advances in polymer science*, vol 45. Springer, Berlin, Heidelberg, pp 1–119
3. Bungenberg de Jong HG (1949) Complex colloidal system. In: Kruyt HR (ed) Colloid science: chapters VIII and X, vol 2. Elsevier, New York
4. Shinde UA, Nagarsenker MS (2009) Characterization of gelatin-sodium alginate complex coacervation system. Indian J Pharm Sci 71:313–317
5. Madene A, Jacquot M, Scher J, Desobry S (2006) Flavor encapsulation and controlled release—a review. Int J Food Sci Technol 41:1–21
6. McMullen JN, Newton DW, Becker CH (1984) Pectin–gelatin complex coacervates II: effect of microencapsulated sulfamerazine on size, morphology, recovery, and extraction of water-dispersible microglobules. J Pharm Sci 73:1799–1803
7. Saravanan M, Kishore GS, Ramachandran S, Rao GS, Sridhar SK (2002) Preparation and characterization of nimesulide microcapsules by gelatin-pectin complex coacervation. Indian Drugs 39:368–372
8. Tiebackx FWZ (1911) Gleichzeitige Ausflockung zweier Kolloide. Chem Ind Kolloide 8:198–201
9. Means GA, Feeney RE (1971) Chemical modification of proteins. Holden Day, Inc., San Francisco, Cambridge, London, Amsterdam

10. Kossel A (1889) Über das Theophyllin, einen neuen Bestandtheil des Thees. Hoppe-Seyler's Z Physiol Chem 13:298–308
11. Löfgren C, Walkenström P, Hermansson A-M (2002) Microstructure and rheological behavior of pure and mixed pectin gels. Biomacromol 3:1144–1153
12. Devi N, Sarmah M, Khatun B, Maji TK (2017) Encapsulation of active ingredients in polysaccharide-protein complex coacervates. Adv Coll Interface Sci 239:136–146
13. Devi N, Maji TK (2009) Preparation and evaluation of gelatin/sodium carboxymethyl cellulose polyelectrolyte complex microparticles for controlled delivery of isoniazid. AAPS PharmSciTech 10:1412
14. Saravanan M, Rao KP (2010) Pectin–gelatin and alginate–gelatin complex coacervation for controlled drug delivery: influence of anionic polysaccharides and drugs being encapsulated on physicochemical properties of microcapsules. Carbohyd Polym 80:808–816
15. Rathna GVN, Chatterji PR (2003) Controlled drug release from gelatin-sodium carboxymethylcellulose interpenetrating polymer networks. J Macromol Sci Part A 40:629–639
16. Prasertmanakit S, Praphairaksit N, Chiangthong W, Muangsin N (2009) Ethyl cellulose microcapsules for protecting and controlled release of folic acid. AAPS PharmSciTech 10:1104–1112
17. Nimni ME, Cheung D, Strates B, Kodama M, Sheikh K (1987) Chemically modified collagen: a natural biomaterial for tissue replacement. J Biomed Mater Res 21:741–771
18. Ouajai S, Shanks R (2005) Composition, structure and thermal degradation of hemp cellulose after chemical treatments. Polym Degrad Stab 89:327–335
19. Sullad AG, Manjeshwar LS, Aminabhavi TM (2010) Polymeric blend microspheres for controlled release of theophylline. J Appl Polym Sci 117:1361–1370
20. Shivakumar HN, Sarasija S, Desai BG (2007) Design and evaluation of ph sensitive minitablets for chronotherapeutic delivery of theophylline. Ind J Pharmaceutical Sci 69:73–79
21. Yan-Fei L, Ke-Long H, Dong-Ming P, Ding P, Gui-Yin L (2007) Preparation and characterization of glutaraldehyde cross-linked ocarboxymethylchitosan microspheres for controlled delivery of pazufloxacin mesilate. Int J Biol Macromol 41:87–93

Characterization and Antimicrobial Property of Some Heavy Metals Containing Ayurvedic Drugs

Prasamsha Panta, Tika Ram Bhandari, Bidit Lamsal and Rameshwar Adhikari

Abstract

Ayurvedic medicines are often used in different formulations, the heavy metals, which are generally referred to as being toxic. In this work, we report on the physicochemical characterization and biological activity of some typical Ayurvedic drugs available in the market that contain arsenic, mercury and lead with the emphasis on their antibacterial performance. Among the formulations studied, some of the drugs with 'amorphous' texture (and higher solubility) were found quite active against some bacterial strains whereas the formulations possessing crystalline texture (and low solubility) were found practically ineffective. The moderate activity of some drugs against Gram-negative bacteria fairly suggested the presence of the small-sized polar molecules which was also supported by the FTIR spectroscopic data.

Keywords

Ayurvedic drug · Heavy metal
Antimicrobial agent · FTIR · Microscopy

P. Panta · T. R. Bhandari · B. Lamsal · R. Adhikari (✉)
Research Centre for Applied Science and Technology (RECAST), Tribhuvan University, Kathmandu, Kirtipur, Nepal
e-mail: nepalpolymer@yahoo.com

Introduction

Ayurveda is the traditional medicinal practice of South Asia. It is a practice which describes in detail not only curative medicine system but also other aspects of health such as lifestyle, food and hygiene [1, 2]. Its use is documented in many standard texts dating from around 500 CE, although its origin is believed to be more than 4000 years old. The ingredients widely used in Ayurvedic formulations are basically derived from various plants, animals, metals and their compounds as well as minerals.

One of the branches of the *Ayurvedic* practice dealing with formulation containing the ingredients from using mineral sources is called *Rasasastra*. A significant part of this branch comprises the formulations based on metals such as iron, gold, silver, mercury, arsenic, lead and many other substances. *Ayurveda* describes the elaborate procedure for the fabrication of these medicines which are believed to be potent in very less quantity [1, 3].

Thus, also heavy metals find extensive applications are Ayurvedic formulations which are generally considered as toxic [4] for human health according to modern medical practices. *Bhasmas* are excellent examples of Ayurvedic formulations using metals (including iron, copper, zinc mercury, cadmium, lead and arsenic) and their compounds as well as minerals. However, use of heavy metal in medicine has been a

R. Adhikari and S. Thapa (eds.), *Infectious Diseases and Nanomedicine III*,
Advances in Experimental Medicine and Biology 1052, https://doi.org/10.1007/978-981-10-7572-8_7

controversial topic since the negative effects of these metals have been discovered [5, 6]. These metals are believed to increase the risk of health condition including lung infection, kidney damage and heart disease and learning difficulty in children. Mercury, arsenic and lead are further the major metals whose use in consumer products is being greatly discouraged [4].

Toxicity due to heavy metal ions follows various mechanisms. Replacement of other metals from enzymes, binding with protein, catalysis of free radical generation is few of the pathways for metal toxicity. The lethal dose and physiological effect of metals depend on several factors such as oxidation state, nature of ligands attached, physical state and chemical composition of the formulation. It has been proved that even seemingly toxic metals in some oxidation state can be non-poisonous to human. Therefore, branding a product unsafe solely on its total metal concentration might not be justified [4, 7].

The *Ayurvedic* drugs are readily available in local Nepali market. The preparation, prescription and selling of the drugs is being carried out by pharmaceutical companies as well as *Vaidyas* (the local medics who have learned the art from their ancestors). In order to standardize and document the process of the Ayurvedic formulations as well as determine their toxicity, a thorough study of the physicochemical properties and biological effects of these drugs is needed. This study aims at analysing the effect of selected heavy metal containing Ayurvedic drugs on Gram-positive and Gram-negative bacteria and understanding the underlying structural component responsible for such action.

Materials and Methods

The commercially available drugs were kindly provided by Singhadurbar Vaidyakhana Vikash Samiti (Singha Durbar Ayurvedic Drug Development Board), a government body responsible for fabrication, standardization and distribution of the Ayurvedic drugs. Total seven samples were collected which contained three different kinds of heavy metals.

Antibacterial action of each drug was determined using disc diffusion method. One Gram-positive (*Streptococcus tonsillitis*) and one Gram-negative (*Escherichia coli)* bacteria were used as test organism. Muller Hilton Agar (MHA) was used as growth medium. 30 mg of Tetracycline was used as standard. 30 and 45 mg test samples along with control disc were administered on MHA containing culture plate. The plates were incubated at 30 °C for 24 h and the zone of inhibition was measured.

Bright-field optical microscopy (OM) was performed with 10 and 40 times magnifications whereby manually ground sample both in dry state and as water suspension was observed. Fourier transfer infrared (FTIR) spectroscopy of the samples in ATR mode was performed in powder state. Absorption spectra on mid-infrared region (650–4000 cm^{-1}) were recorded with a resolution of 1 cm^{-1}

Results and Discussion

Physical States and Solubility

The samples were analysed for their physical form stability and solubility. All the samples possessed solid texture, showed form stability under given humidity and room temperature upon exposure to the laboratory environment for 2 weeks. Two of the samples (namely, *Rasamanikya* and *Sasasindur*; see Table 1) showed visibly reddish or red crystalline texture. The solubility of samples numbered 1 and 3 in lemon juice, albeit temporary, may be attributed to the unstable complex formation.

The drug suspensions can have different toxicity profile than that of free metal ions, thereby making these drugs safe for consumption. The selective activity of drugs in Gram-negative bacteria might indicate the presence of various small molecules as the latter ones larger than 0.1 nm cannot penetrate through the outer layer of Gram-negative bacteria. Moreover, the porin channel requires polar structure, which might be possible due to the presence of metals as well as hydroxyl groups in the compound [8–11].

Table 1 List of the sample drugs used in this work with their physical state and constituent metals present (as per manufacturer information)

S. No.	Drug's name	Constituent	Physical state
1	Rasamanikya	Arsenic	Reddish crystalline solid
2	Mahayogaraja Guggulu	Lead	Black solid
3	Rasasindur	Mercury	Red crystalline solid
4	Sutasekhar Rasa	Mercury	Black solid
5	Siddhapraneshvara Rasa	Mercury	Black solid
6	Navarasa	Mercury	Black solid
7	Swashkuthar Rasa	Arsenic + Mercury	Black solid

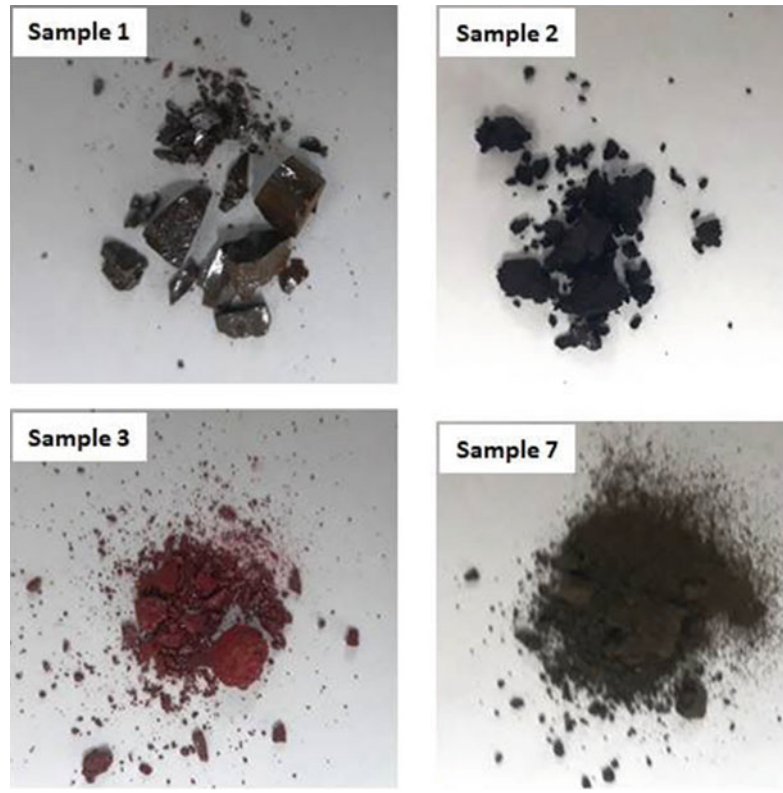

Fig. 1 Photographs of some of the samples studied as listed in Table 1

Crystalline structure of samples might be the reason for insolubility of the drugs.

The samples were found to have a wide range of solubility. Although most samples dispersed in water easily, samples 1 and 3 (which had seemingly crystalline texture) did not dissolve in water or any common solvents such as ethanol, chloroform, toluene and cyclohexane. These samples readily dissolved in lemon juice, however, and precipitation was observed after keeping the sample still overnight. Lemon juice was used in this case as these drugs are recommended by the Ayurvedic doctors to be consumed with lemon juice.

The photographs of some of the samples are presented in Fig. 1. Based on the external textures, it can be easily identified that the samples numbered as 1 and 3 have depicted reddish and

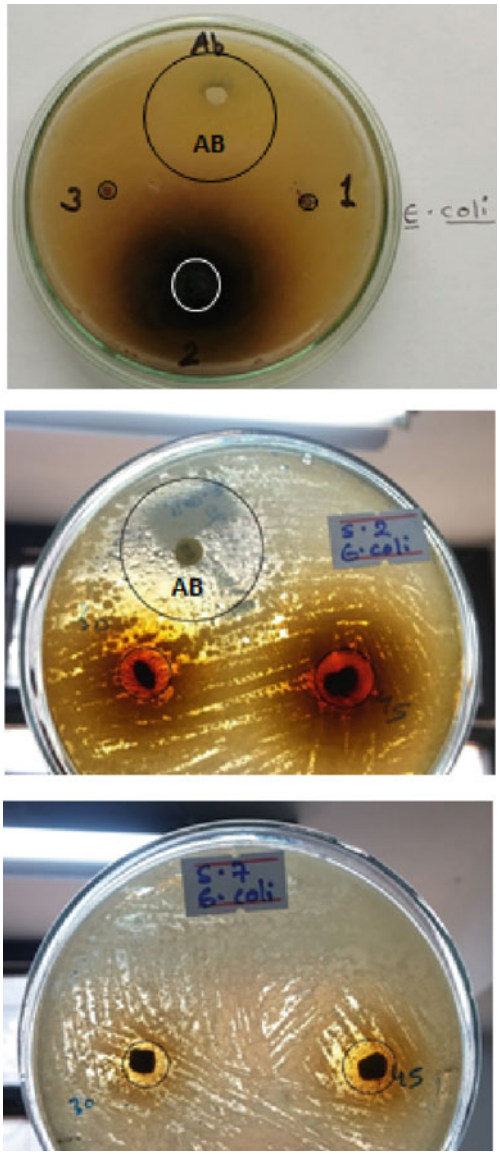

Fig. 2 Photographs showing the zone of inhibitions produced by different samples as indicated against the bacterium *Escherichia coli*

red crystalline textures with lustrous appearance. The 'crystalline' samples were not readily dispersed in water as expected. The rest of the samples showed quite amorphous nature and were also easily dispersible in water.

All the samples were subjected to the antibacterial susceptibility tests on two different bacterial strains, viz. *E. coli* and *Streptococcus* using an antibiotic (AB) streptomycin, as a control. The results obtained for some specimens are presented in Fig. 2.

Antimicrobial susceptibility test shows that some samples could inhibit the growth of *E. coli*. Although the zone of inhibition shown by the test samples was less than that of standard antibiotic, samples 2 and 7 showed inhibition with identical concentration as that of standard but with different extent (see Fig. 2). Increase in the size of inhibition zone was observed on increasing the concentration. Samples 1 and 3 were not diffused in the media. Furthermore, no drug was found to inhibit *Streptococcus*.

To further characterize the materials structurally, optical microscopy was used using cross polarizers which could provide clues on crystalline texture of the materials. The results are presented in Fig. 3 for some drugs samples. Sample 1, which exhibited sharp-edged crystalline texture in the photographs (in Fig. 1), shows the lump of needle-like crystals with a particular orientation. Similar texture was observed for sample 3 (results not shown here).

On the other hand, sample 2 which was quite amorphous powder and depicted no crystalline texture in the photograph rather showed some needle-like texture in the optical micrographs. The large part of the drug was, however, made of amorphous areas (shown by dark lumps in Fig. 3). Consequently, this sample was readily dispersed in water. Completely amorphous structure was observed for sample 7, as expected.

FTIR spectra of selected samples are given in Fig. 4. The plots show the presence of organic group in samples 4, 5 and 7. Each of them was dispersible in water and showed no crystalline texture. All samples show peaks at 1010, 1390, 1610, 2850 and 2920 cm^{-1}. The peaks are in agreement with previous works [5]. Peaks at 2920, 2850 and 1390 cm^{-1} correspond to C H vibration of CH_3 and CH_2 group while that at 1010 cm^{-1} corresponds to CO vibration. The broad peak from 3000 to 3500 cm^{-1} indicates the presence of bound as well as free OH probably from water and/or alcohol/phenol group. Peak at 1610 cm^{-1} indicates unsaturation as alkene or aromatic ring [6, 7, 9].

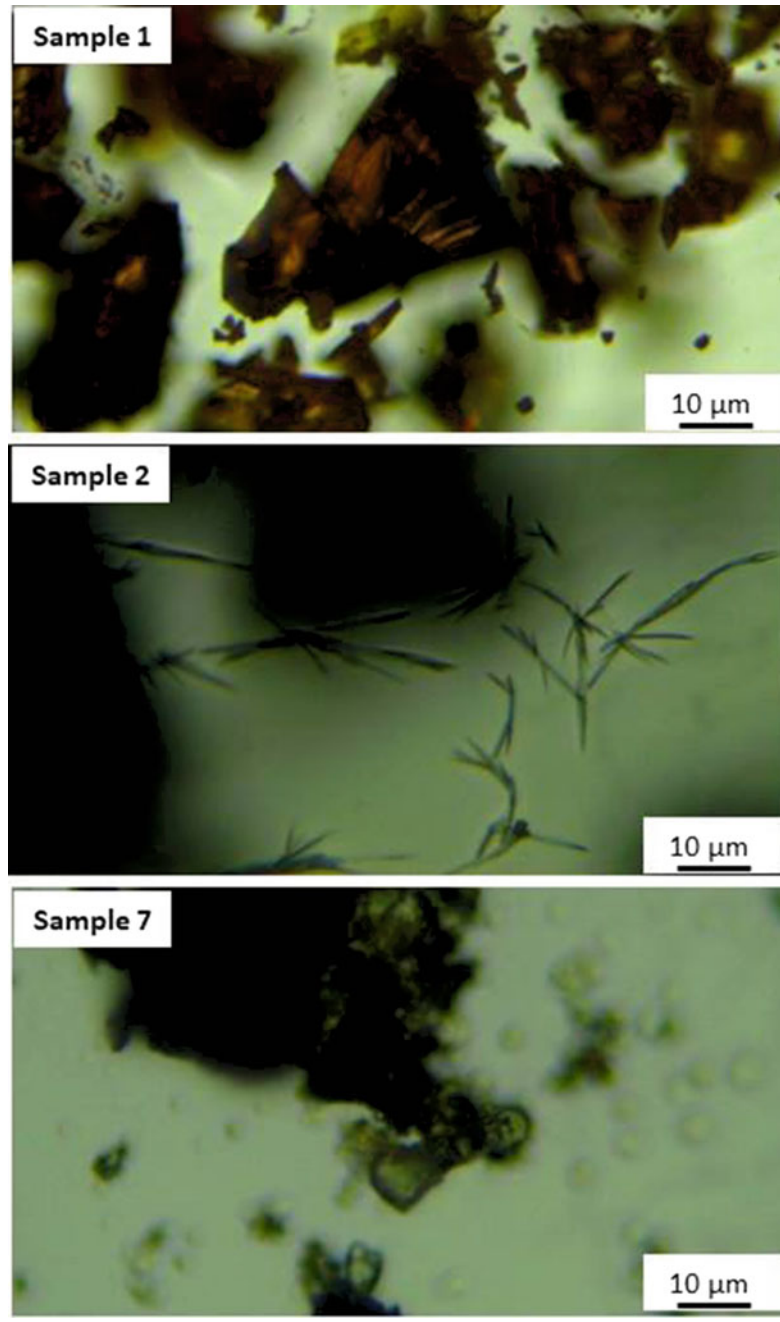

Fig. 3 Polarizing optical micrographs of some of the samples studied as indicated in this work

Thus, the studied Ayurvedic drugs several functional groups typical of organic phase. The presence of organic moieties (i.e. organometallic structural framework) in the drugs has been indicated by the FTIR results [8–10]. However, the confirmation can only be obtained by far-infrared spectroscopy.

Conclusions

Some heavy metal containing Ayurvedic formulations were studied with respect to their structural and morphological features and their

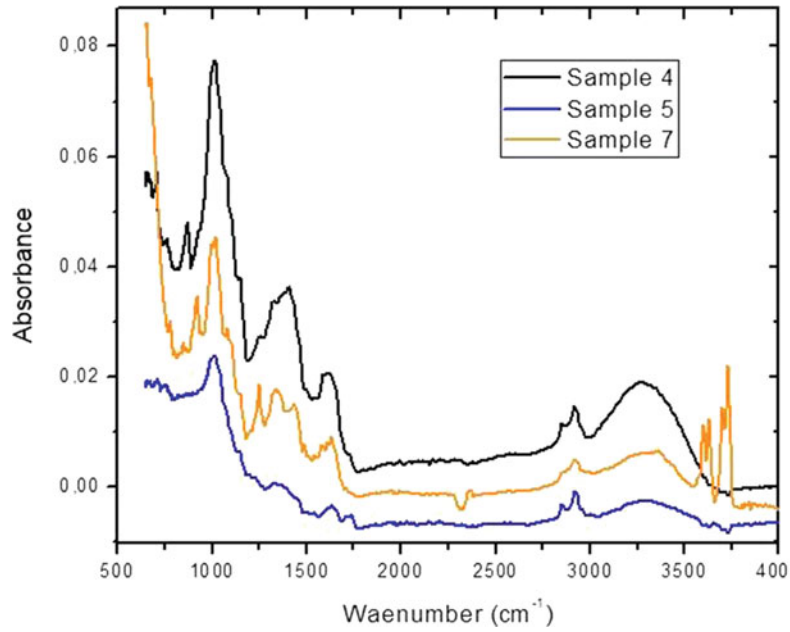

Fig. 4 FTIR spectra of some of the samples studied

antibacterial activity. The results can be summarized as follows:

1. The drugs thus studied did not exhibit pronounced toxicity against the Gram-negative and Gram-positive bacteria. Most of the Ayurvedic formulations studied in this work could form suspensions in lemon extract, which were stable for several hours.
2. The moderate activity of the drugs against Gram-negative bacteria fairly suggests the presence of the small-sized polar molecules which was also supported by the FTIR spectroscopy. The compounds did not show, however, activity against Gram-positive bacteria.
3. The investigated Ayurvedic medicines contain a significant amount of organic groups which might have originated from the herbs used in the formulations.
4. The Ayurvedic compounds containing heavy metals, which are otherwise thought to be strongly poisonous, can have different levels of toxicity than that of free metal ions. Further alteration in toxicity can be expected on the mode of consumption, for example, in combination with milk, honey and/or lemon juice as substrate. Thus, the future works should concentrate on detailed study of the cytotoxicity of the formulations in comparison with non-Ayurvedic heavy metal preparations.

Acknowledgements We would like to acknowledge Universal Science and Engineering College, Chakopat, Lalitpur for providing lab facility for antimicrobial tests, Antonella Esposito (University of Rouen, France) for FTIR measurements and Dr. Bhanu Bhakta Neupane (Central Department of Chemistry, Tribhuvan University, Kathmandu) for microscopic studies.

References

1. Kapoor RC (2010) Some observations on the metal-based preparations in Indian systems of medicine. Indian J Tradit Med
2. Adhikari R (2014) Ayurvedic bhasmas: overview on nanomaterialistic aspects, applications, and perspectives. In: Rameshwar A, Santosh T (eds) Advances in experimental medicine and biology, vol 807. Springer, India, New Delhi, pp 23–32
3. Governmet of India Department of Indian Systems of Medicine and Homeopahty (2003) The ayurvedic pharmacopoeia of India, 2nd edn. The controller of publications, New Delhi
4. Jarup L (2003) Hazards of heavy metal contamination. Br Med Bull 68(1):167–182

5. Saper RB, Kales SN, Paquin J, Burns MJ, Eisenberg DM, Davis RB, Phillips RS, Phillips RS (2004) Heavy metal content of ayurvedic herbal medicine. JAMA J Am Med Assoc 292(23):1–8
6. Chan K (2003) Some aspects of toxic contaminants in herbal medicines. Chemosphere 52(9):1361–1371
7. Tchounwou PB, Yedjou CG, Patlolla AK, Sutton DJ (2012). Heavy metal toxicity and the environment, vol 101. Springer, Basel, pp 133–164
8. Janadri S, Mishra AP, Kumar R, Shanmukh I, Rao N, Kharya M (2015) Preparation and characterization of mercury-based traditional herbomineral formulation: Shwas kuthar rasa. J Ayurveda Integr Med 6(4):268–272
9. Guillen MD, Cabo N (1997) Infrared spectroscopy in the study of edible oils and fats. J Sci Food Agric 75 (111):1–11
10. Silverstein RM, Webster FX, Kiemle DJ, Bryce DL (2014) Spectrometric identification of organic compounds. Wiley
11. Cohen GN (2011) The outer membrane of gram-negative bacteria and the cytoplasmic membrane. Springer, Netherlands, pp 11–16

Application of Metallic Nanomaterials in Nanomedicine

Mahi R. Singh

Abstract

In this chapter, we explain why metallic nanomaterials are used in nanomedicine. We have shown that the electron density in metallic nanomaterials oscillates and creates electron density waves. When laser light falls on metallic nanoparticles, light interacts with electron density waves. According to Einstein, light, which is electromagnetic waves, consists of particles called photons. Similarly, electron density waves are also made of particles called surface plasmons. Therefore, photons from laser light and surface plasmons from metallic nanostructures interact with each other and create new particles called surface plasmon polaritons. These new particles produce an intense light near the surface of metallic nanomaterials. We showed that this intense light is important in the application of metallic nanomaterials in nanomedicine. Further, we have applied metallic nanoparticles, single metallic nanoshells and double metallic nanoshells for treatment of cancer and detection of smaller tumors.

Keywords

Metallic nanomaterials · Nanomedicine

Introduction

Recently, there is considerable interest to study the physical properties of metallic nanomaterials (MNMs) for the application of nanomedicine and nanotechnology [1–14]. Nanotechnology refers to the branch of science and engineering dedicated to the study of materials which have dimensions in the order of nanometres. On the other hand, the branch of science which uses nanomaterials in medical treatment of diseases in humans and animals is called nanomedicine. Nanotechnology has provided the development of new types of nanomaterials for biomedical applications with emphasis in therapy and diagnostics in the nanomedicine. The size of MNMs which are used in nanomedicine range between 10 and 500 nm. The nanosize of these particles allows them to attach to the surfaces of bio-cells. Because of their small size, nanoparticles can readily interact with biomolecules both at the surface and inside cells. This interaction between MNMs and biomolecules produces better signals and can be used for diagnostics and therapeutics treatment.

M. R. Singh (✉)
Department of Physics and Astronomy, The University of Western Ontario, London, Ontario N6G3K7, Canada
e-mail: msingh@uwo.ca

R. Adhikari and S. Thapa (eds.), *Infectious Diseases and Nanomedicine III*,
Advances in Experimental Medicine and Biology 1052, https://doi.org/10.1007/978-981-10-7572-8_8

Metallic nanoparticles (MNPs) fabricated from noble metals are versatile agents with a variety of biomedical applications. For example, they can be used in highly sensitive diagnostic assays, thermal ablation, radiotherapy, as well as drug and gene delivery [1]. It is found that they are nontoxic carriers for drug and gene delivery applications. They have unique characteristics such as high surface-to-volume ratio and broad optical properties suitable for medical treatments. Their optical energy can be easily tunable to desirable wavelengths by changing their sizes, shapes, and composition. These qualities are useful in cancer treatment, imaging of small tumors, and photothermal applications.

MNPs can be functionalized with antibodies, peptides, DNA, and RNA to target bio-cells and can be used for drug and gene delivery applications. Moreover, they can efficiently convert light or radio frequencies into heat, thus enabling thermal ablation of targeted cancer cells. When metallic particles are ejected into animal or human body, they are attached to bio-cells. When external laser light falls on the MNPs, the light is scattered from MNPs. The scattered light emitted from the MNPS has huge intensity. This intense light is converted into heat which in turn is used to kill cancer cells and photothermal applications. Recently, in a series of papers, we have calculated the intensity of scattered light from MNPs [14]. We showed that they produce high intense light due to surface plasmon present at the surface of MNPs and this intense light can be used in as nanomedicine.

We know that according to Einstein, light is made of particles called photons. It is also well known that metallic nanoparticles have high density of electrons on their surfaces. The density of electrons fluctuates with time and surface electron density waves are created on the surface of the MNP. These surface waves of electrons are called surface plasmons. Therefore, when light falls on the MNPs, photons scatter with surface plasmons. We considered that photons couple with surface plasmons and create new particles called surface plasmon polaritons (SPPs) [14]. We further showed that light emitted by MNPs is due to SPPs. We also found that the intensity of light changes with shapes and sizes of MNPs. We also predicted that the intensity of SPP light is enhanced when the wavelength of the laser light is close to the SPP wavelength [14].

It is found that besides MNPs, single metallic nanoshells (SMNSs) are also used for the application of nanomedicine [2–13]. SMNSs are fabricated from a dielectric core coated with a metallic shell. The word “single” is used since they have a single interface between the metallic shell and the dielectric core. MNSs have been fabricated by many groups [2–11] to study the scattering of light and their application to nanomedicine. We have calculated the scattering of light with SMNSs and it was found that SMNSs can be used as contrast agents for enhanced optical coherence tomography imaging [4, 5]. They have also been used for cancer therapeutics [6, 7] due to their nanosize.

It is well known that to have successful treatment for diseases such as cancer in animals and human, an early detection of these diseases is very critical. We know that the traditional diagnostic and imaging techniques cannot detect small size tumors in early developing stages. However, the MNPs and SMNSs can be used as imaging agents to detect smaller tumors. It is found that metallic structures can yield more sensitive and selective imaging of smaller size tumors and other tissues. Further, they can be used as potential carriers for delivering to diseased sites with minimal collateral damage to normal tissues [13].

Further, double metallic nanoshells (DMNSs) are also used for the application of nanomedicine [15–17]. These nanostructures are fabricated from a spherical dielectric core, metallic shell, and a spacer layer coated on the surface of the metallic shell. They have two interfaces. The first is between the core and the metallic shell. The second is located between the metallic shell and the spacer layer. Hence, they have double interfaces and that is why, they are called DMNSs. These nanostructures have been fabricated by several groups [15–17] to study the scattering of light and their application to nanomedicine. We have calculated the light scattering in DMNSs and we showed that these structures have three

types of SPPs [17]. Further, we showed that they can be used for nanomedicine since their optical energy can be easily tunable to desirable wavelengths by changing size and shapes of the dielectric core, metallic shell, and the spacer layer. These qualities are useful in cancer treatment, imaging of small tumors, and photothermal applications.

The study of metallic nanohybrids is a new and a very active research area in nanotechnology and nanomedicine. Metallic nanohybrids are fabricated from quantum emitters and metallic nanomaterials. Examples of the quantum emitters (QEs) are quantum dots, chemical molecules, and biocompatible molecules such as Indocyanine Green, IR800 molecules, and J-aggregate molecules. The main physical properties of QEs are that they have electron and hole pairs. We know that holes have positive charges and electrons have negative charges. An electron and a hole are bound to each other by the Coulomb interaction and form a particle called excitons. Hence, QEs contain excitons. Here are three main types of metallic nanomaterials which are used in the fabrication of metallic nanohybrids. The first type is noble metal nanomaterials (i.e., MNPs, SMSs, and DMSs) which we have discussed in above paragraphs.

The second type of metallic nanomaterials is gapless nanomaterials. Examples of gapless nanomaterials are graphene, germanene, and silicanes. Graphene was invented theoretically by Wallace in 1947 [18]. He considered that graphene is a two-dimensional material and it is made of carbon atoms. Carbon atoms in graphene are arranged in honeycomb unit cells. He predicted that graphene is a gapless semiconductor, and it has indirect band gap. He died in 2005 and missed the Graphene Nobel in 2012. I worked with Wallace and we showed that there are other gapless materials such as Cd_3AS_2 and HgTe, which have direct band gaps [19]. Further, we found that the optical energy absorption/emission is stronger in the direct bands than the indirect band. Recently, graphene like germanene [20] and silicanes [21] have been invented. However, most of the recent research on metallic nanomaterials and their application to nanomedicine has focused predominantly on metallic nanoparticles (MNPs) made of noble metals [22]. We have studied the scattering of light with the graphene and their application to nanomedicine in a series of papers [23].

The third type of metallic nanomaterials is metamaterials. Metamaterials are a new class of artificial materials with unique optical properties [24–30]. The building blocks of metamaterials are called the meta-atom, and they can be arranged into periodic arrays to form one-dimensional (1D) chains, two-dimensional (2D) metasurfaces, and three-dimensional (3D) metamaterials. Using different metamaterial designs, researchers have been able to engineer the material properties with unprecedented degrees of freedom. They possess simultaneously negative dielectric permittivity, magnetic permeability [23–26], and SPPs [26] for a range of frequencies in the electromagnetic spectrum. The broad spectrum of material properties of metamaterials propels the rapid development of plasmonics to manipulate the flow of electromagnetic waves.

In a series of papers, we have studied the scattering of light with metamaterials and photonic crystals and their applications to nanomedicine [29, 30]. It is found that photonic crystals [28] and metamaterials [24] have both photonic band gaps due to the periodic structure. Their plasmonic properties are not well understood and not well investigated. We have developed a compressive theory for the band structure of photon propagation in metallic nanohole array (NHA) metamaterials and showed that the negative electric permittivity in NHAs leads to the formation of SPPs which generates exceptionally strong localized electromagnetic fields. We have studied the role of photonic crystals on metallic nanostructures in the application to nanomedicine and nanotechnology [30].

In this chapter, we will concentrate on nanohybrids fabricated from quantum emitters and noble metal nanomaterials. This is because most of the recent research on metallic nanomaterials and their application to nanomedicine has focused predominantly on noble metal nanoparticles (MNPs) [1–22]. It is known that

light emission rates of quantum emitters in noble metal nanohybrids are significantly enhanced [31–43]. The enhancement of the emission in QEs such as molecular fluorophores is highly useful for improving detection sensitivity and selectivity in many emerging applications. Examples of these applications are DNA screening [35], single molecule detection [36], and image enhancement [37]. The design and development of these nanohybrids for enhancing molecular fluorescence is of broad interest.

There is considerable interest to study nanohybrids made of biocompatible fluorescent molecules and metallic double nanoshells (DNSs). Because they can be used for biomedical imaging and for the detection of disease markers in the near-infrared wavelength region [38]. Further studies showed that the penetration depth of near-infrared light is large in most biological media. It is found that these hybrids have large absorption coefficients and high quantum yields in the far-infrared region [39, 40]. Therefore, these hybrids can be used for imaging deeply into the organs and soft tissues of animals and humans. They can also be used as agents for contrast enhancement and in physiological environments [41].

Fluorescence emission in QE-MNS hybrids has been widely investigated recently [15, 16, 39–41]. We know that the fluorescence imaging has been used in clinical diagnosis and monitoring processes in biological systems [15, 16]. Fluorescent QEs which emit light at wavelengths in the physiologically relevant range 700–900 nm are interesting due to the large penetration depth of near-infrared (NIR) light in most biological media. These QEs have potential to be used for imaging at significant depths in living tissues. However, it is extremely difficult to achieve bright fluorescent emission with photostable and biocompatible near-IR fluorophores. We know that when QEs are near the metallic surface, fluorescence emission of QEs can be enhanced. The presence of nearby MNSs can not only enhance the quantum yield of the fluorescence emission but also stabilize adjacent fluorophores against photobleaching. In new and emerging light-assisted therapeutic applications such as photothermal cancer therapy.

In Ref. [40], we have studied the photoluminescence emission in a quantum emitter (QE) and SMNSs. We considered that the SMNS is made of a dielectric core coated with a thin layer of metal. It is surrounded by biological cells such as cancer cells. Surface plasmon polariton (SPP) resonances in these nanostructures are calculated. It is found that the SMNS has two SPP resonances. Locations of SPP resonances can be modified by changing the size of the core and the metallic shell. It is also found that the PL spectrum of the QE splits from one peak to two or three peaks depending on the locations of two SPP resonances. We showed that these interesting findings may be useful in the fabrication of nanosensors, nanoswitches, and for other applications in medicine.

Further, we calculated light emission from quantum emitter (QE) and double metallic nanoshell (DNS) hybrid systems [41]. Here, the DNS is made of a dielectric core and two outer nanoshells. The first nanoshell is made of metal, and the second one is made of a dielectric material or human serum albumin. The fluorescence emission in a QE-DNS hybrid has been calculated, and we compared our theory with hybrid systems where QEs are taken as the Indocyanine Green (ICG) and IR800 fluorescent molecule. The outer shells of the DNS are taken as silica and human serum albumin whose thicknesses can be changed. We found the enhancement of fluorescence spectra of IR800-DNS and ICG-DNS hybrids. We predicted that as the thickness of the spacer layer is increased the enhancement in the fluorescence is decreased. It is found that the enhancement in the fluorescence depends on the type of the QE, spacer layer, and the DNS. We also showed that the fluorescence spectra can be switched from one peak to two peaks by removing the degeneracy of the QE. We suggested that with these properties, one can use these hybrids as sensing and switching devices as applications in medicine.

The aim of this chapter is to answer the question of why metallic nanomaterials are used in nanomedicine. We will discuss physics of the scattering of light with metallic nanohybrids

made from quantum emitters and metallic nanosystems and their application to nanomedicine. In Sect. 2, we will calculate surface plasmons in metallic nanomaterials and their application to nanomedicine. In Sect. 3, scattering of laser light with metallic nanostructures will be discussed. The creation of surface plasmon polaritons and intensity of the emitted light from metallic nanoparticles will be calculated. The metallic nanomaterials which are considered are metallic nanoparticles, single metallic nanoshells and double metallic nanoshells. In Sect. 4, the extinction coefficient in metallic nanostructures will be evaluated. Finally, in Sect. 5, we will calculate the absorption of the optical energy into metallic nanostructures. The fluorescence emission from quantum emitters in nanohybrids will be evaluated, and its application to nanomedicine will be discussed.

Metallic Nanostructures and Surface Plasmons

In this section, we will discuss the scattering of laser light with metallic nanostructures (MNSs). We will explain why MNSs are used in nanomedicine. To understand the application of MNSs in nanomedicine, we should know some physical terms used in literature.

It is well known that metallic nanoparticles have high density of electrons. The density of electrons fluctuates with time on the surface of an MNP, and surface waves are created on the surface of the MNP. These surface waves of electrons are called surface plasmon. The property of MNP due to surface plasmon polariton is denoted by a physical quantity called dielectric constant. It is denoted as ϵ_m. Using the Drude model, we can calculate the dielectric function of the metallic shell, and it is written as

$$\in_m = \in_\infty - \frac{\omega_p^2}{\omega^2 + i\omega\gamma_m} \tag{1}$$

where ω_p is the plasmon frequency of the metal, and it plays a key role in the application in nanomedicine. Here, ϵ_∞ is its relative permittivity at very large energies ($\omega \gg \omega_p$). Here, γ_m is called the decay rate and represents the thermal energy loss in the metallic shell. This thermal energy loss is well known in metals, and it is due to the electric resistance present in metals. This is also known as ohmic loss. We should note that the dielectric constant of the metals depends on the frequency of the laser light.

The plasmon frequency depends on the concentration of electrons in metals. We know that each metal has its own electron concentration. Hence, the plasmon frequency has different values for different metals. For example, gold (Au) has $\omega_p = 9.0\,\text{eV}$, and copper has $\omega_p = 7.0\,\text{eV}$. It is interesting to note that the dielectric constant of metals has negative values when the frequency of laser light is less than the plasmon frequency of metals. Note that when the laser light frequency is lower than the plasmon frequency, i.e., $\omega < \omega_p$, the dielectric constant has negative value.

We can see from Eq. (1) that all noble metals have negative dielectric constant $\omega < \omega_p$. In nature, there are no other materials which have this fascinating property. As we explained in the introduction, gapless nanomaterials and metamaterials are also metallic nanostructures. Hence, they have also negative dielectric constant. This unique property of MNSs that they have negative dielectric constant is responsible for the application of these materials in nanomedicine. We will explain this point further in later sections.

In this chapter, we will use frequency ω, wavelength λ, and energy E units in the calculation of the intensity of the emitted light. These terms can be exchangeable in this chapter. Hence, we will give the relationship between these quantities in the following equations:

$$\begin{aligned} \omega &= \frac{2\pi c}{\lambda} = \frac{2\pi E}{h} \\ E &= \frac{h\omega}{2\pi} = h\frac{c}{\lambda} \\ \lambda &= \frac{2\pi c}{\omega} = \frac{ch}{E} \end{aligned} \tag{1a}$$

where c is the speed of light, and h is the Planck constant.

Scattering of Light with Surface Plasmons

Laser light is nothing but electromagnetic waves. According to Einstein, light is made of particles called photons. In other words, when laser light falls on MNPs, it means photons are scattering with MNPs. We have shown that MNSs have surface plasmons which are electron density oscillations. The laser light induces new types of oscillations in surface plasmons due to coupling electric field of the laser light and charge density of MNSs. In other words, photons of the laser light couple with surface plasmons and create new types of particles called surface plasmon polaritons. We will calculate the surface plasmon energy and their intensity for metallic nanosphere, single metallic nanoshell and double metallic nanoshell as follows. In this chapter, we will call metallic nanospheres as metallic nanoparticles.

Metallic Nanosphere

We have pointed out in the introduction section that metallic nanoparticles (MNP) have been widely used in nanomedicine. MNPs are fabricated from the noble metals such as Au and Ag. Generally, they have spherical shapes. The typical radius of MNPs is of the order of 100 nm. We have shown that they have surface plasmons and their dielectric constant ϵ_m has negative value for $\omega < \omega_p$. When they are doped in human body, they are surrounded by bio-cells. The optical properties of bio-cells are also characterized by its dielectric constant. Let us denote the dielectric constant of bio-cells as ϵ_b. It is found that the dielectric constant of the bio-cells is a constant quantity and does not depend on the frequency of light. On the other hand, the dielectric constant of MNPs does depend on the frequency of light.

When MNPs are injected into the human body, they are surrounded by bio-cells. Hence, there is a single interface which exists in this system. This interface is located between bio-cells and the surface of MNPS. When the laser light falls at the interfaces it induces new oscillations in surface plasmons due to the coupling of the electric field of the laser light and the charge density of MNSs. Photons of the laser light couple with surface plasmons and create new types of particles called surface plasmon polaritons (SPPs) at the interface.

We have calculated the surface plasmon energy and their intensity for metallic nanosphere in Ref. [42, 43]. The SPP energy is calculated from the physical quantity called polarizability. Let us calculate the polarizability. The wavelength (λ) of light in the visible region is of the order of 600 nm. Hence, the size of the MNPs is much smaller than the wavelength of laser light. We can consider that the amplitude of the laser electric field is constant over the MNP. This is known as the quasi-static approximation [44, 45]. A laser light with energy ω and electric field E_P is applied to the MNP. The MNP is polarized due to the probe field, and its polarization P_{ns} is calculated in Ref. [42, 43]

$$P_{\mathrm{ns}} = \alpha_{\mathrm{ns}} E_P \tag{2}$$

where α_{ns} is called the polarizability.

Solving Maxwell's equations in quasi-static approximation and using the boundary conditions at the interface, the expression for polarizability is derived as [42, 43]

$$\alpha_{\mathrm{ns}} = 4\pi \in_0 \in_b (R_s)^3 \zeta_s \tag{3}$$

Here, ϵ_0 is the dielectric constant of vacuum. Function ζ_s is called the polarizability factor and is found as

$$\zeta_s = \left[\frac{\in_m - \in_b}{(\in_m + 2 \in_b)}\right] \tag{4}$$

It is important to note that polarizability has a huge value (singularity) when ϵ_m has negative value. However, when ϵ_m has positive value the polarizability has very small value. We have pointed in Sect. 2 that ϵ_m has a negative value when $\omega < \omega_p$.

Now, we calculate the surface plasmon polariton (SPP) resonance frequencies (energies) in the MNP. The singularity in the polarizability

gives the locations of SPP energies and can be found by putting the denominator of Eq. (4) equal to zero. Let us rewrite the denominator as follows:

$$\in_m + 2 \in_b = 0 \tag{5}$$

Putting Eq. (1) into Eq. (5) and after solving this equation, we find the following expression of the SPP energy:

$$\omega_{\mathrm{sp}} = \frac{\omega_p}{\sqrt{\in_\infty + \in_b}} \tag{6}$$

Here, ω_{sp} is called SPP resonance frequency. Note that the MNP inside bio-cells has SPP energy given by the above equation, and ω_{sp} depends on the dielectric constant of the surrounding material.

Note that the polarizability has a peak at $\omega = \omega_{\mathrm{sp}}$. This means the SPP resonance frequencies of metallic nanostructures can be calculated from the polarizability.

It is important to note that polarizability has a peak at $\omega = \omega_{\mathrm{sp}}$. This peak is related to the enhancement of emitted light from MNP. This will be discussed in the next section. Note that the SPP frequency is lower than the plasmon frequency, i.e., $\omega_{\mathrm{sp}} < \omega_p$. This means that the dielectric constant at SPP frequency has negative values. We conclude that the polarizability has peaks only because the MNP has negative dielectric constant. Therefore, the enhancement of light occurs in metallic nanomaterials but not in other materials found in nature.

Single Metallic Nanoshells

Single metallic nanoshells (SMNSs) are also used for the application of nanomedicine as we discussed in the introduction section. They are fabricated from a dielectric-core nanoparticle coated with a metallic shell. The word "single" is used since they have a single interface between the metallic shell and the dielectric core. MNSs have been fabricated by many groups to study the scattering of light and their application to nanomedicine. We have calculated the scattering of light with single-MNSs. We have considered that they are doped in human body, and hence, they are surrounded by bio-cells. Due to doping, there is a second interface which exists in these structures, and it is located between the bio-cells and the metallic shell. A schematic diagram of the SMNS is plotted in Fig. 1.

We have calculated the light scattering in single-MNSs and two types of SPPs [40]. The first types of SPPs are present at the interface between core dielectric materials and metal. The second types of SPPs are found at the interface between the bio-cells and metallic shell. The wavelength of SPPs in nanoshells can be controlled through the size and composition of each layer of MNSs. They can be used for nanobiotechnology and nanomedicine due to their convenient surface bio-conjugation with molecular probes. They can also be used for nanomedicine since their optical energy can be easily tunable to desirable wavelengths by changing size and shapes of the dielectric core and metallic shell. These qualities are useful in cancer treatment, imaging of small tumors and photothermal applications.

Here, we present the calculation of SPPs from Ref. [40]. An SMNS is made from a core dielectric nanoparticle and an outer metallic shell. The refractive index of the metallic nanoshell and the core material are denoted as ϵ_{m} and ϵ_{c}, respectively. The radius of the core is denoted as R_c, and the radius of the nanoshell is taken as R_m. We consider that the SMNS is surrounded by bio-cells with dielectric constant ϵ_{b}. Using the quasi-static approximation, the polarizability of the SMNS is calculated as [40]

$$\alpha_{\mathrm{ns}} = 4\pi \in_0 \in_b (R_c + d_m)^3 \zeta_{\mathrm{ns}} \tag{7}$$

Here, $d_m = R_m - R_c$ is the thickness of the outer shell, and ζ_{PS} is called the polarizability factor and is found as [40]

$$\zeta_{\mathrm{ns}} = \left[\frac{(R_c + d_m)^3(\in_m - \in_b)(\in_c + 2\in_m) + 2R_c^3(\in_c - \in_m)(\in_b + \in_m)}{(R_c + d_m)^3(\in_m + 2\in_b)(\in_c + 2\in_m) + 2R_c^3(\in_m - 2\in_b)(\in_c - \in_m)}\right] \tag{8}$$

If we put $R_c = 0$, then the above expression reduces to the polarizability of metallic spherical nanoparticles.

We calculate the SPP resonance frequencies in the SMNS. The singularity in the polarizability gives the locations of SPP energies. By putting the denominator of the polarizability equation (Eq. 8) equal to zero. We get

$$(R_c + d_m)^3(\in_m + 2\in_b)(\in_c + 2\in_m) + 2R_c^3(\in_m - 2\in_b)(\in_c - \in_m) = 0 \tag{9}$$

Note the above expression is second order in ϵ_m and has the two following roots:

$$\in_m = \in_m^+ \qquad \in_m = \in_m^- \tag{10}$$

where

$$\in_m^{\pm} = \left[\frac{(R_c + d_m)^3(\in_c + 4\in_b) + R_c^3(2\in_c + 2\in_b)}{4\left((R_c + d_m)^3 - R_c^3\right)} \pm \frac{\sqrt{\left[(R_c + d_m)^3(\in_c + 4\in_b) + R_c^3(2\in_c + 2\in_b)\right]^2 - 16\left((R_c + d_m)^3 - R_c^3\right)^2 \in_c \in_b}}{4\left((R_c + d_m)^3 - R_c^3\right)}\right] \tag{11}$$

The first term $\in_m^+$ gives the condition for the polariton creation at the interface of the bio-cell/metallic shell. The second term $\in_m^-$ creates SPPs at the interface of the metallic shell/core interface. Putting the expression of Eq. (1) into Eq. (10, 11), we get the following two SPP resonance frequencies:

$$\omega_{\mathrm{sp}}^+ = \frac{\omega_p}{\sqrt{\in_\infty + \in_m^+}} \qquad \omega_{\mathrm{sp}}^- = \frac{\omega_p}{\sqrt{\in_\infty + \in_m^-}} \tag{12}$$

We have plotted a schematic diagram showing the SMNS has two SPP energies at ω_{sp}^- and ω_{sp}^+ in Fig. 1. These two energies can be represented by three energy levels, and the energy difference between two levels gives SPP energies as shown in Fig. 1.

Note that the polarizability has two peaks located at $\omega = \omega_{\mathrm{sp}}^-$ and $\omega = \omega_{\mathrm{sp}}^+$. This means the SPP resonance frequencies of metallic nanostructures can be calculated from the polarizability.

Here, we have considered the gold metallic nanoshell and it is surrounded by the human cancer cell [40]. The MNS made using a gold shell with a gold sulfide (Au_2S) core and this MNS has been studied for medical applications. The dielectric constant of the human cancer cell is found to be approximately $\epsilon_b = 3.0$. The

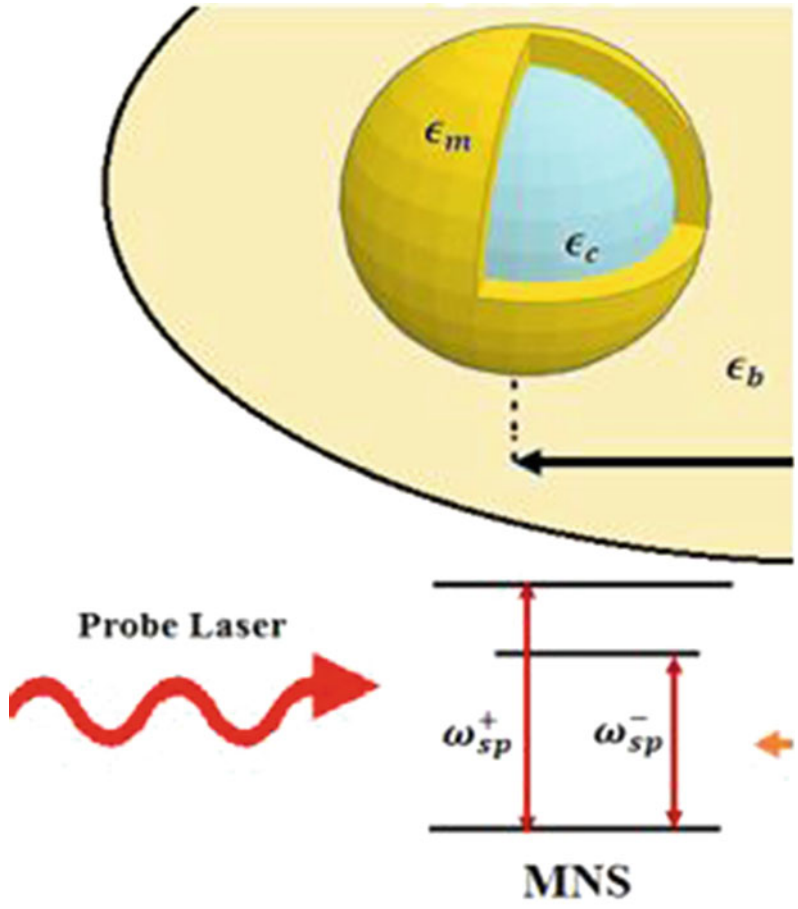

Fig. 1 A schematic diagram showing the SMNS has two SPP energies at ω_{sp}^{-} and ω_{sp}^{+} is plotted

dielectric constant of the Au_2S core is found as $\epsilon_c = 5.4$. We have calculated the SPP resonance energies for this MNS for $R_c/R_m = 0.96$ and $R_m = 50$ nm. The parameters for the gold shell are taken as $\varepsilon_p = 9.0\,\text{eV}$, $\gamma_m = 0.07\,\text{eV}$, and $\epsilon_\infty = 8$.

The SSP frequencies are calculated in Ref. [40]. It is found that SPP resonance energies are located at $\varepsilon_{sp}^{-} = 0.84$ eV and $\varepsilon_{sp}^{+} = 3.3$ eV. We found that the height of the first peak which is due to the shell/bio-cell interface is stronger than the peak due to the shell/core interface.

We found that SMNSs have two surface plasmon polaritons propagating within the two interfaces. By adjusting the shell and core radii, the SPP resonances can vary from UV to IR wavelengths for nanomedicine application.

Double Metallic Nanoshell

We have pointed in the introduction section that double metallic nanoshells (DMNSs) are also used for the application of nanomedicine. They are fabricated from a spherical dielectric core, metallic shell and a spacer layer coated on the surface of the metallic shell. Hence, they have double interfaces and that is why, they are called double-MNSs. The first interface is located between the metallic shell and the dielectric core. The second interface is located between the spacer layer and the metallic shell.

DMNSs have been fabricated by many groups to study the scattering of light and their application to nanomedicine. For example, Bardhan et al. [15] have fabricated DMNSs from a silica

core, Au metallic shell, and the silica space layer. We denote this structure as SiO_2-Au-SiO_2. Further, Bardhan et al. [16] have also fabricated double-MNSs from a silica core, an Au metallic shell. In this case, the space layer is fabricated from human serum albumin (HSA). We denote this structure as SiO_2-Au-HSA.

When DMNSs are doped in a human body, they are surrounded by bio-cells. Hence, there is a third interface present in these structures and it is located between the bio-cells and the spacer layer. We have calculated the light scattering in double-MNSs and three types of SPPs are found. The first types of SPPs are present at the interface between core dielectric materials and metal. The second types of SPPs are found at the interface between the bio-shell and metallic shell.

It is found that the wavelength of SPPs in nanoshells can be controlled through the size and composition of each layer of MNSs. They can also be used for nanomedicine since their optical energy can be easily tunable to desirable wavelengths by changing the size and shapes of the dielectric core, metallic shell and the spacer layer. These qualities are useful in cancer treatment, imaging of small tumors, and photothermal applications.

Here, we present the calculation of SPPs from Ref. [41]. We consider that a DMNS is made from a core dielectric nanoparticle and an outer metallic shell. The nanoshell has a spherical shape. It is coated with another spacer layer such as human serum albumin (HSA). The core, metallic shell, and spacer layer are denoted as 1, 2, and 3, respectively. We denote the dielectric constants for core, metallic shell, and the spacer layer as ϵ_1, ϵ_2, and ϵ_3, respectively. The radii of the core, metallic shell, and DNS are denoted as R_1, R_2, and R_3, respectively. The hybrid is injected into a human or animal cell and it is surrounded by a bio-cell with a dielectric constant ϵ_b. The volume of the core is V_1, metallic shell and core is V_2, and DNS is V_3. A schematic diagram of the DNS is plotted in Fig. 2.

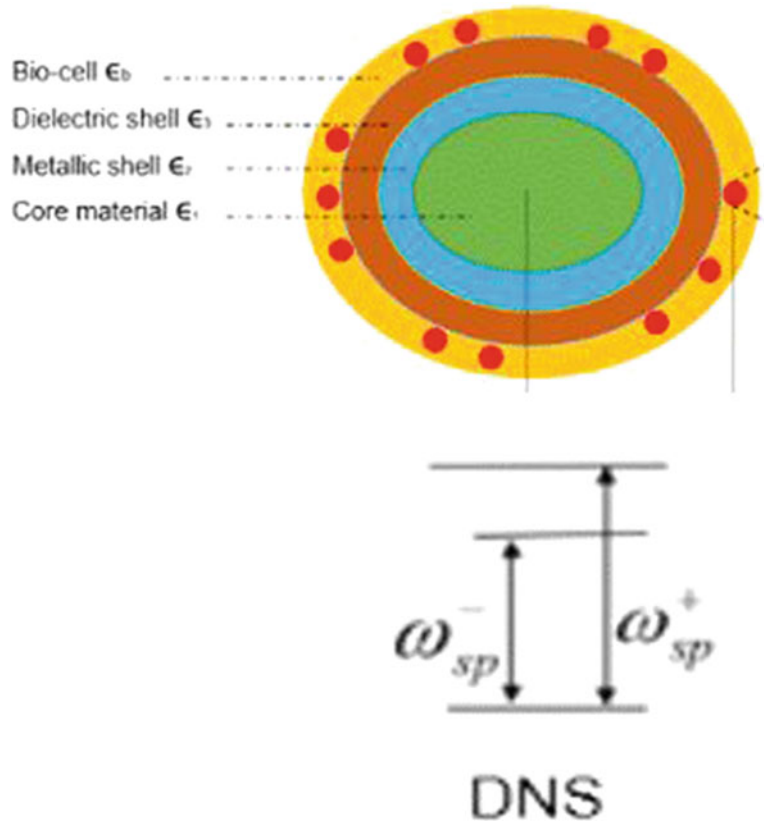

Fig. 2 A schematic diagram showing the an SMNS has two SSP energies at ω_{sp}^{-} and ω_{sp}^{+} is plotted

Using the quasi-static approximation, the polarizability of the α_{NS} of the parabolic DMNS is found as

$$\alpha_{\mathrm{ns}} = 4\pi \in_0 \in_b R_3^3 \zeta_{\mathrm{ns}} \tag{13}$$

where ς_{ns} is calculated as

$$\varsigma_{\mathrm{ns}} = \frac{[\in_{32} - \in_b]}{\in_{32} + 2 \in_b} \tag{14}$$

where

$$\in_{32} = \in_3 \left[\frac{R_3 + 2R_2\varsigma_{32}}{R_3 - R_2\varsigma_{32}}\right], \quad \varsigma_{32} = \frac{[\in_{21} - \in_3]}{\in_{21} + 2 \in_3} \tag{15a}$$

$$\in_{21} = \in_2 \left[\frac{R_2 + 2R_1\varsigma_{21}}{R_2 - R_1\varsigma_{21}}\right], \quad \varsigma_{21} = \frac{[\in_1 - \in_2]}{\in_1 + 2 \in_2} \tag{15b}$$

The singularity in the polarizability gives the locations of SPP frequencies and can be found by putting the denominator of the polarizability factor equal to zero. The DNS structure can have three surface plasmon polaritons propagating within the three interfaces.

Note that the polarizability in Eq. (13) depends on the radii and the dielectric constants of the constituents of the DMNS. This means by adjusting the shape of the parabolic DNS, the SPP resonance wavelengths can be made larger than the size of the DNS. These resonances can vary from UV to IR wavelengths.

The singularity in the polarizability in Eq. (13) will give the SPP resonances. This system is going to have three SPP frequencies. The results for polarizability will have two peaks due to the core–shell and shell–spacer layer interfaces. The SPPs will be not present at the interface space layer and bio-cell since there is no metal present at this interface. The expression of polarizability will be used to calculate the fluorescence in the later section.

We have plotted a schematic diagram showing the DMNS has two SPP energies at ω_{sp}^{-} and ω_{sp}^{+} in Fig. 2. These two energies can be represented by three energy levels and the energy difference between two levels gives SPP energies as shown in Fig. 2.

Extinction Coefficient in Metallic Nanostructures

Similarly, we can also calculate the extinction coefficient which is denoted as σ_{ext}. The extinction coefficient is calculated by adding the ratio of the power scattered from the MNS (σ_{scat}) and the ratio of the power absorbed by MNS (σ_{abs}). Hence, the extinction coefficient is expressed as

$$\sigma_{\mathrm{ext}} = \sigma_{\mathrm{abs}} + \sigma_{\mathrm{scat}} \tag{16}$$

The expressions for absorption and scattering cross sections have been obtained in Ref. [19]. They are written as

$$\sigma_{\mathrm{abs}} = \frac{\omega}{c \in_0} \mathrm{Im}(\alpha_{\mathrm{SP}}), \quad \sigma_{\mathrm{scat}} = \frac{\omega^4}{6\pi c^4 \in_0^2} |\alpha_{\mathrm{SP}}|^2 \tag{17}$$

Single Metallic Nanoshell: Extinction Coefficient

Here, we calculate the extinction coefficient σ_{ext} for the MNP. The extinction coefficient has been calculated in Eq. (16). Putting the expression of polarization from Eq. (3) into Eq. (16), we get the following expression for the extinction coefficient:

$$\sigma_{\mathrm{ext}} = \frac{4\pi \in_b \omega}{c} (R_c)^3 \mathrm{Im}(\varsigma_{\mathrm{ns}}) + \frac{8\pi \in_b^2 \omega^4}{3c^4} (R_c)^6 |\varsigma_{\mathrm{ns}}|^2 \tag{18}$$

Note that the extinction coefficient depends on the polarizability factor ς_{ns} of the MNP.

Single Metallic Nanoshells: Extinction Coefficient

Next, we calculate the extinction coefficient σ_{ext} and PL for the SMNs. The extinction coefficient has been calculated in Eq. (16). Putting the expression of polarization of the SMNs from Eq. (7) into Eq. (16), we get the following expression of the extinction coefficient for polarization for the SMNs:

$$\sigma_{\text{ext}} = \frac{4\pi \in_b \omega}{c}(R_c + d_m)^3 \text{Im}(\varsigma_{\text{sp}}) + \frac{8\pi \in_b^2 \omega^4}{3c^4}(R_c + d_m)^6 |\varsigma_{\text{sp}}|^2 \quad (19)$$

Note that the extinction coefficient depends on the polarizability factor ς_{ns}.

Double Metallic Nanoshell: Extinction Coefficient

Finally, we calculate the extinction coefficient σ_{ext} and PL for the MNS. The extinction coefficient has been calculated in Eq. (16). Putting the expression of polarization of the SMNS from Eq. (13) into Eq. (16), we get the following expression for the extinction coefficient for polarization of the DMNS:

$$\sigma_{\text{ext}} = \frac{4\pi \in_b \omega}{c}(R_3)^3 \text{Im}(\varsigma_{\text{ns}}) + \frac{8\pi \in_b^2 \omega^4}{3c^4}(R_3)^6 |\varsigma_{\text{ns}}|^2 \quad (20)$$

Note that the extinction coefficient depends on the polarizability factor ς_{ns} of the DMNS.

Extinction Coefficient for Single Metallic Shell: Theory and Experiments

In this section, we compare the expression of the extinction coefficient with experimental data. We have mentioned in the introduction section that SMNSs have been fabricated for medical purposes by many groups. For example, Gobin et al. [2] have fabricated an SMNS with a silica core and coated in a gold shell. The radius of the core is taken as R_c = 60 nm and the thickness of the shell is considered as d_m = 12 nm. They have also measured the extinction coefficient for silica–gold metallic nanoshell. We have compared our theory with their experiments, and the results are presented in Ref. [40].

In Ref. [2], the extinction coefficient is measured in terms of the wavelength λ. Therefore, we convert Eq. (19) for the extinction coefficient from frequency to wavelength as

$$\sigma_{\text{ext}} = \frac{8\pi^2 \in_b}{\lambda}(R_c + d_m)^3 \text{Im}(\varsigma_{\text{SP}}) + \frac{64\pi^5 \in_b^2}{3\lambda^4}(R_c + d_m)^6 |\varsigma_{\text{SP}}|^2 \quad (19a)$$

Here, λ is the wavelength of the probe field. In Eq. (19a), the first term is the absorption of light in the SMNS and the second term is the scattering of light from the SMNS.

In Fig. 3, the solid curve represents our theoretical results, and open circles are the experimental data points. In this sample, the MNS is made of gold shell and silica core. The radius of

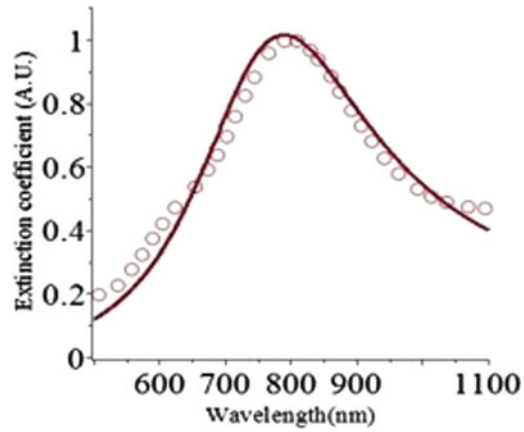

Fig. 3 Plot of the extinction coefficient (A.U.) as a function of wavelength (nm). The solid curve is the theoretical result, and open circles are the experimental data. The MNS is made of gold shell and silica core. The radius of the core is about $R_c = 60$ nm, and the thickness of the shell is $d_m = 12$ nm

the core is about $R_c = 60$ nm and the thickness of the shell is $d_m = 12$ nm. Other parameters are taken as $\varepsilon_p = 9.0\,\text{eV}$ and $\epsilon_\infty = 8.2$. It is found that a good agreement between theory and experiment is found. From the experiment, the SPP resonance wavelength was found to be 800 nm.

We showed that there are two SPP resonances $\varepsilon_{sp}^{+} = \hbar\omega_{sp}^{+}$ and $\varepsilon_{sp}^{-} = \hbar\omega_{sp}^{-}$ present in the SMNS. Note that only one peak appears in Fig. 3. It is due to the first SPP resonance. It seems that the second peak is very weak compared to the first peak.

Nanohybrids: Light Energy Absorptions and Fluorescence

In this section, we study the scattering of light with nanohybrids fabricated from quantum emitters (QEs) and metallic nanostructures (MNSs). We denote these nanohybrids as QE-MNSs. Here, QEs can be taken as quantum dots, chemical molecules and biocompatible molecules (Indocyanine Green, IR800 molecules, and J-aggregate molecules). We have found that the intensity of scattered light from QEs is significantly enhanced in QE-MNSs. The enhancement of the emission in QEs is a highly useful strategy in the application of these nanohybrids in nanomedicine.

Here, we will calculate the light energy absorption and emission rates in nanohybrids. Example of the light energy emission and absorption in fluorescence emission. Therefore, we will calculate the fluorescence emission form nanohybrids fabricated from (1) SMNSs and (2) DMNS. Fluorescent QEs which emit light at wavelengths in the physiologically relevant range 700–900 nm are interesting due to the large penetration depth of near-infrared (NIR) light in most biological media. We know that the fluorescence imaging has been used in clinical diagnosis and monitoring processes in nanomedicine.

Nanohybrids: Power Absorbed and Fluorescence

We discuss the energy absorption from laser light to metallic nanostructures. A laser light with frequency ω and amplitude E_p falls on an MNS. The light induced a polarization in the MNP, and energy is absorbed. Light power absorbed by the MNS has been calculated by us in Ref. [43]. The power absorbed by the MNP from the laser light is found as

$$Q_{\text{ns}} = -\frac{\omega}{2} Im(\alpha_{\text{ns}}) \left|E_p\right|^2 \tag{21}$$

where α_{ns} is the polarizability of the MNS. The expression of α_{ns} for the MNP, SMNS, and DMNS was calculated in a previous section.

The fluorescence is directly related to power absorbed by the MNS. The fluorescence is the power emitted by the MNS. Hence, power absorbed by the MNS and power emitted by MNS are related to each other. The expression for the fluorescence of the QE is found as [41]

$$I_{\text{pl}} = Q_{\text{ns}} W_{\text{ns}} \tag{22}$$

where Q_{ns} is called the PL efficiency factor and generally taken as one. In this case, the fluorescence becomes.

$$I_{\text{pl}} = W_{\text{ns}} \tag{23}$$

Note that the fluorescence intensity is equal to the power absorbed by the MNP.

Single Metallic Nanoshell Nanohybrids: Fluorescence

The SMNSs hybrids are fabricated by depositing quantum emitters near or on the surface of SMNS. We have mentioned in the introduction section that SMNSs have been fabricated for medical purposes by many groups. For example, Gobin et al. [2] have fabricated metallic nanoshells with a silica core and coated it with a gold shell.

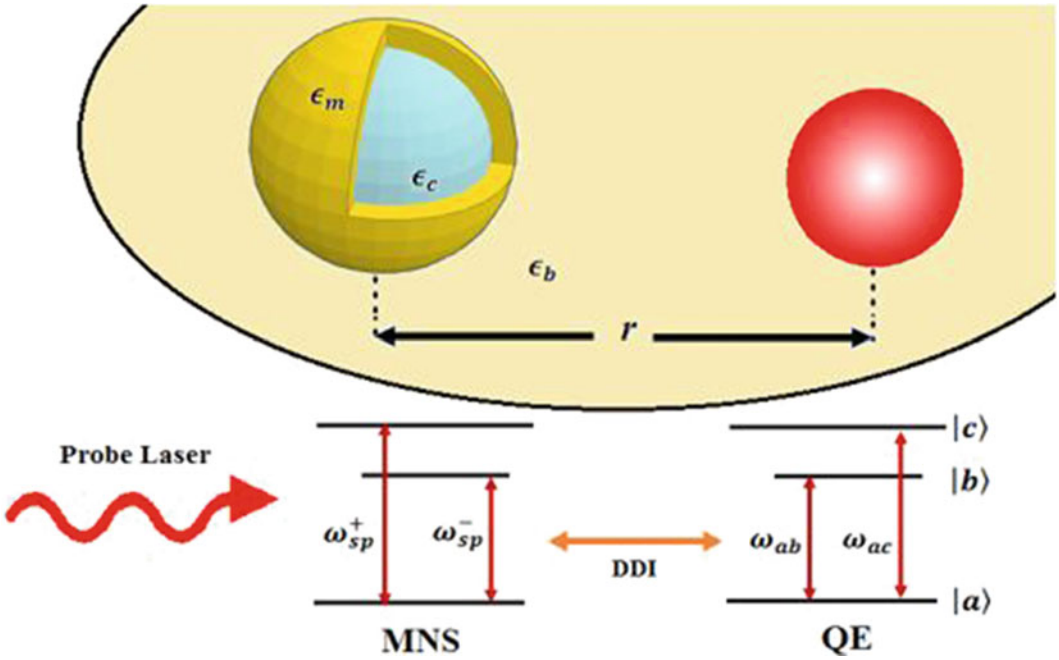

Fig. 4 A schematic diagram of the nanohybrid is shown here. The MNS is doped in a bio-cell with dielectric constant ε_b. The distance between the SMNS and QE is taken as r. The energy levels of the DNS and QE are plotted. The QE has two excitonic states ω_{ab} and ω_{ac}, and DNS has also two localized SPP states ω_{sp}^{+} and ω_{sp}^{-}

In this section, we choose a quantum dot (QD) as a quantum emitter. The quantum dots are made from semiconductors such as GaAs, InAs, and CdS. Their typical radius is about 2 nm. They are called artificial atoms since their energy levels are very similar to an atom. Here, we consider only three levels of the QD. Energy levels are denoted as $|a$, $|b$ and $|c$. Their frequencies are found as ω_a, ω_b, and ω_c. This QD has two excitons and their energies are found as ω_{ab} and ω_{ac} due to transitions $|a \rightarrow |b$ and $|a \rightarrow |c$, respectively. A schematic diagram of the QE is shown in Fig. 4.

Now, we deposit the QE near an SMS to form a nanohybrid. A schematic diagram of this nanohybrid is plotted in Fig. 4. In Fig. 4, the dielectric constants of the core material and outer metallic shell are denoted as R_c and R_m, respectively. The DMNS is doped in a bio-cell with dielectric constant $\in_b$ and is a distance r from the QE. The radius of the core nanoparticle is taken as R_c and the radius of the nanoshell is R_m.

Let us calculate the fluorescence of the SMNS using Eq. (23). For QE with two exciton energies ω_{ab} and ω_{ac} the expression of the FL is modified as follows:

$$I_{QE} = W_{QE} = \frac{(\omega_{ba} + \omega_{ca})}{2} Im(\alpha_{QE}) |E_{QE}|^2 \quad (24)$$

where E is the light falling on the QE and α_{QE} is called the polarizability of the QE. These quantities are evaluated in Ref. [41]. From Ref. [41], we can find the expression of the FL for the SMNS as follows:

$$I_{QE} = I_{QE}^0 Im\left(\frac{4(1+\Lambda)(\delta_k/\gamma - i)}{(\delta_k/\gamma - i)^2 - \omega_{cb}^2/\gamma^2}\right)|1+\Lambda|^2 \quad (25)$$

where

$$I_{\mathrm{QE}}^{0} = \hbar(\omega_{\mathrm{ba}} + \omega_{\mathrm{ca}})\gamma(\Omega/\gamma)^2$$
$$\Lambda = g_l \in_b \left(\frac{(R_c + d_m)^3}{r^3}\right)\varsigma_{\mathrm{ns}}$$
$$\Omega = \frac{\mu E_P}{2\hbar} \tag{26}$$
$$\delta_k = \omega_{\mathrm{ca}} + \omega_{\mathrm{ba}} - 2\omega$$

The constant g_l is called the polarization parameter and it has the values $g_l = -1$ and $g_l = 2$. Here, μ is the dipole moment for the QE and Ω, is the Rabi frequency associated with the intensity of the laser light. Here, δ_k is called the probe detuning parameter.

The physical meaning of the Λ is due to the interaction of the excitons with the SPP electric field. This term is called the dipole–dipole interaction (DDI) between the QE and the SMNS. Note that the Λ term is inversely proportional to r^3 and depends on the DDI between the QE and MNS. For smaller distances, the DDI term has large values. It also depends on the polarizability via term ς_{ns} of SMNS and it has large values at the SPP resonance energies.

Single Metallic Nanoshell Hybrid: Application to Nanomedicine

We study the effect of the DDI due to the gold SMNS on the QE in nanohybrids. The SMNS made using a gold shell with a gold sulfide (Au_2S) core. This type of the MNS has been studied for medical applications [21]. We consider that this nanohybrid is surrounded by the human cancer cell. The dielectric constant of the human cancer cell is taken as ϵ_b = 3.0 and the dielectric constant of the Au_2S core is found as ϵ_c = 5.4. The size of the MNSs is given as R_c/R_m = 0.96 and R_m = 50 nm. The physical parameters for the gold shell are found as $\varepsilon_p = 9.0\,\mathrm{eV}$, $\gamma_m =$ 0.07 eV and ϵ_∞ = 8. For this SMNS, the SPP energies are found as $\varepsilon_{\mathrm{sp}}^{-} = 0.84$ eV and $\varepsilon_{\mathrm{sp}}^{+} = 3.3\,\mathrm{eV}$.

Now, we calculate the PL spectrum of the QE-MNS hybrid. We consider that the resonance energies of the QE are degenerate. This means we have $\hbar\omega_{\mathrm{ab}} = \hbar\omega_{\mathrm{ac}}$. In this case, the QE becomes a two-level QD. We consider that $\varepsilon_{\mathrm{ab}} = \hbar\omega_{\mathrm{ab}}$ lies near the SPP energy $\varepsilon_{\mathrm{sp}}^{+}$ (i.e., $\varepsilon_{\mathrm{ab}} = \varepsilon_{\mathrm{sp}}^{+} = 3.3\,\mathrm{eV}$). The results are plotted in Fig. 5 where the solid and dotted curves are plotted when the distances between the MNS and QE are r = 400 nm and r = 80 nm. Parameters for the MNS are used $\varepsilon_p = 9.0\,\mathrm{eV}$, $\gamma_m = 0.07$, ϵ_b = 3, ϵ_c = 5.4, ϵ_∞ = 8, R_c/R_m = 0.95 and R_m = 50 nm. Parameters for the QE are taken as $\gamma = 0.01\,\mathrm{eV}$, $(\varepsilon_{\mathrm{ab}} + \varepsilon_{\mathrm{ac}})/2 = 3.3\,\mathrm{eV}$, $\varepsilon_{\mathrm{ac}} = 0$. We found that the solid curve has one peak whereas the dotted curve has two peaks. It shows that a single peak of the PL spectrum splits into two peaks as the distance between the QE and MNS is decreased from 400 to 80 nm.

To understand the splitting effect in Fig. 5 (left), we have also plotted a three-dimensional PL spectrum as a function the distance r and energy in Fig. 5 (right). One can see from this figure that the splitting of one peak to two peaks. We found that the reason for this splitting is the DDI effect between the SMNS and QE.

We found that the FL depends directly on the DDI term which in turn depends on the polarizability of the MNS and distance r between the QE and SMNS. We have shown that the DDI term is inversely proportional to the cube of the distance r. Note that as the distance between QE and SMNS decreases the DDI decreases and the intensity of the FL spectrum decreases.

We have found that the number of peaks in the PL spectrum can be modified by changing the frequency of the external laser field. This means that by changing the frequency of the external laser one can switch on and off the thermal energy emitted by these hybrids. This effect can be used to fabricate nanoswitches for medical applications. We have also found that the SPP frequencies depend on the dielectric constant of the bio-cell. Therefore, these hybrids can be used as nanosensors for medical applications.

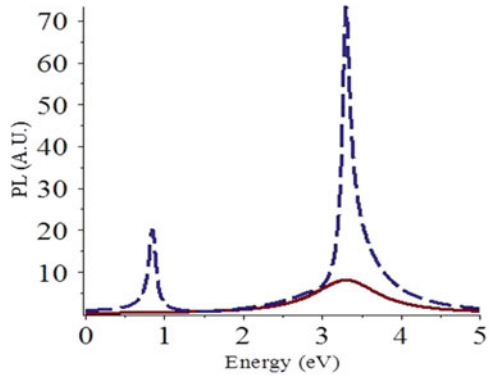

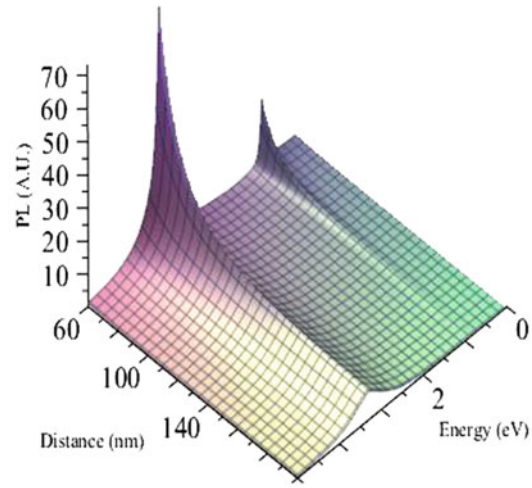

Fig. 5 (left): Plot of the PL spectrum as a function of energy (eV). The solid and doted curves are plotted when the distance between the MNS and QE is 400 and 80 nm. (right) Three-dimensional figure is plot of the PL spectrum as a function of energy (eV) and distance (nm). Here, the following parameters are used: $\varepsilon_p = 9.0\,\text{eV}$, $\gamma_m = 0.07$, $\epsilon_b = 3$, $\epsilon_c = 5.4$, $\epsilon_\infty = 8$, $R_c/R_m = 0.95$ and $R_m = 50$ nm; $\gamma = 0.01\,\text{eV}$, $(\varepsilon_{ab} + \varepsilon_{ac})/2 = 3.3\,\text{eV}$, $\varepsilon_{ac} = 0$

Finally, we discuss the application of QE-MNS hybrid systems in nanomedicine. We have shown that the intensity of the PL spectrum is enhanced many orders of magnitude. Recently, it has been found that energy emitted by metallic nanoparticles is converted to heat energy in the picosecond time domain by rapid electron–phonon and phonon–phonon interaction processes. Therefore, when this hybrid is injected into the human body, the strong PL emission will be emitted. This light emitted by the nanohybrid is converted into heat. This heat can be used for heating bio-cells by using external laser radiation. This property of metallic hybrids is advantageous in the photothermal therapy of cancer and other diseases. This heating can be used for destroying cancer cells by photothermal ablation.

Double Metallic Nanoshell Hybrids: Fluorescence

The DMNSs hybrids are fabricated by depositing quantum emitters near or on the surface of DMNS. We have shown in the introduction that the fluorescence emission in DNMs nanohybrids has been widely investigated. Recently, Bardhan et al. [9] have fabricated these nanohybrid systems to study the near-infrared fluorescence (FL). Here, Indocyanine Green (ICG) is used as a QE and it is a fluorescent molecule. Here, QE is deposited onto the spacer layer of SiO_2-Au-SiO_2 DNS to complete the ICG-DNS hybrid. The distance between ICG molecules and the DNS surface is varied by changing the thickness of the spacer layer.

Further, Bardhan et al. [10] have also investigated the FL emission in IR800 molecules when they are deposited on the spacer layer of an HSA-Au-SiO_2 DNS. The HSA is a large multidomain protein relevant to many physiological functions and it binds to Au by electrostatic attraction between the amine groups of HSA and the negative charge on the gold surface. They have measured the fluorescence enhancement of IR800 molecules and found that the quantum yield of IR800 is enhanced as the thickness of the HSA layer is decreased.

In this section, we choose Indocyanine Green (ICG) and IR800 molecules as a quantum emitter. Here, we consider only three levels of these QEs. Energy levels are denoted as $|a$, $|b$ and $|c$. Their frequencies are found as ω_a, ω_b, and ω_c. This QD has two excitons and their energies are

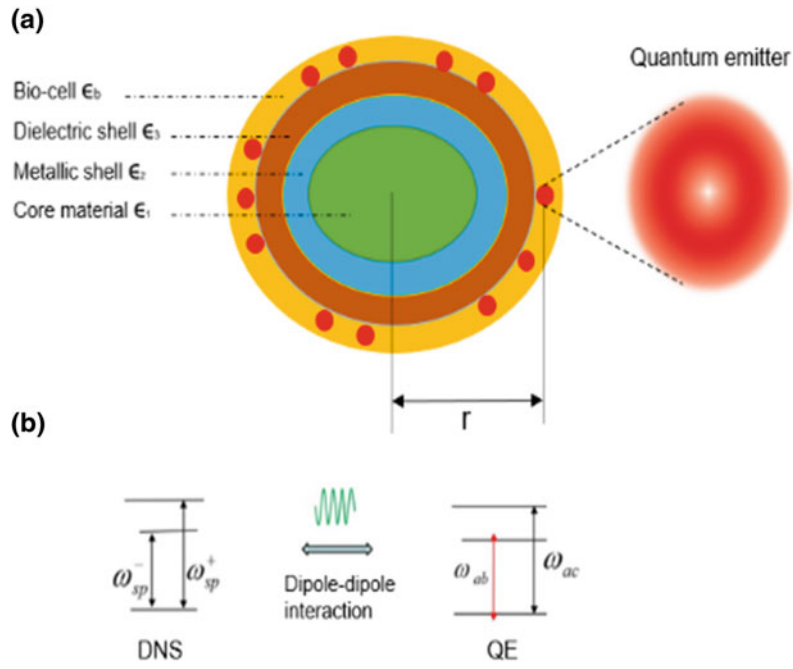

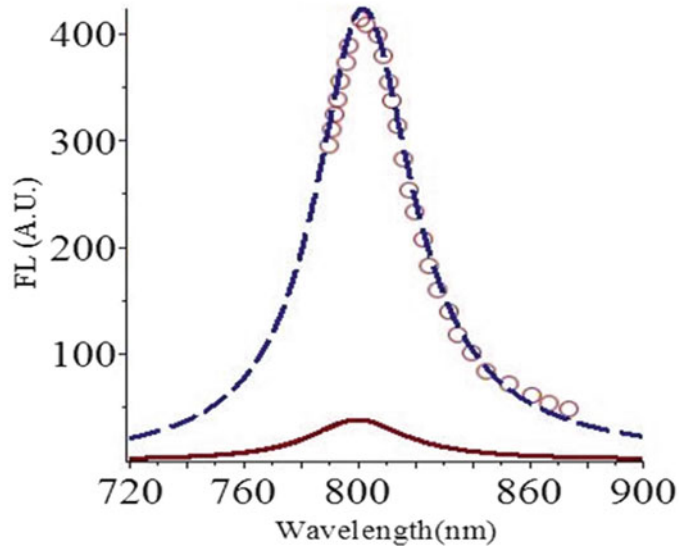

Fig. 6 **a** A schematic diagram of the double nanoshell is plotted. The dielectric constants of the inner core, metallic shell, and the spacer layer are denoted as ϵ_1, ϵ_2, and ϵ_3, respectively. The DNS is injected into a bio-cell with dielectric constant ϵ_b. QEs are deposited on the surface of the DNS. The distance between the DNS and QE is denoted as *r*. **b** The energy levels of the DNS and QE are plotted. The QE has two excitonic states ω_{ab} and ω_{ac}, and the DNS has also two localized SPP states ω_{sp}^{+} and ω_{sp}^{-}. Figure 6 (bottom): Plot of the FL (A.U.) as a function of wavelength (nm) for the IR800-Au-DNS. Here, A.U. stands for the arbitrary unit

found as ω_{ab} and ω_{ac} due to transitions $|a \rightarrow |b$ and $|a \rightarrow |c$, respectively. A schematic diagram of the QE is shown in Fig. 6.

Now, we deposit the QE near an SMS to form a nanohybrid. A schematic diagram of this nanohybrid is plotted in Fig. 6a. The DMNS is doped in a bio-cell with dielectric constant $\in_b$ and is a distance *r* from the QE.

We calculate the FL for the QE in the presence of exciton–SPP interaction. The QE has excitons (electron-hole pairs) and the DNS contains SPPs and they interact with each other via

dipole–dipole interaction (DDI). Let us calculate the fluorescence of the DMNS nanohybrids by using Eq. (23). For the QE with two exciton energies ω_{ab} and ω_{ac}, the expression of the FL is modified as follows:

$$I_{QE} = W_{QE} = \frac{(\omega_{ba} + \omega_{ca})}{2} Im(\alpha_{QE}) |E_{QE}|^2 \quad (27)$$

where E_{QE} is the light falling on the QE and α_{QE} is called the polarizability of the QE. These quantities are evaluated in Ref. [41]. From Ref. [41], we can find the expression of the FL for these nanohybrids as follows:

$$\begin{aligned} I_{QE} = I^b_{QE} Im\left(\frac{4(1+\Lambda_b)}{(\delta_b/\gamma - i)}\right)|1+\Lambda_b|^2 \\ + I^c_{QE} \mathrm{Im}\left(\frac{4(1+\Lambda_c)}{(\delta_c/\gamma - i)}\right)|1+\Lambda_c|^2 \end{aligned} \quad (28)$$

Here, $\delta_b = \omega_{ab} - \omega$ and $\delta_c = \omega_{ac} - \omega$ are called the probe field detunings.

$$\begin{aligned} &I^b_{QE} = \hbar\omega_{ba}\gamma(\Omega/\gamma)^2, \qquad I^c_{QE} = \hbar\omega_{ca}\gamma(\Omega/\gamma)^2 \\ &\Lambda_b = g_l \in_b \left(\frac{V_3}{r^3}\right)\varsigma_{ns}\left(\omega^-_{sp}\right), \qquad \Lambda_c = g_l \in_b \left(\frac{V_3}{r^3}\right)\varsigma_{NS}\left(\omega^+_{sp}\right) \end{aligned} \quad (29)$$

The constant g_l is called the polarization parameter and it has the values $g_l = -1$ and $g_l = 2$. Here, μ is the dipole moment for the QE and Ω is the Rabi frequency associated with the intensity of the laser light. We consider that the SPP frequency ω^+_{SP} lies close to the exciton frequency ω_{ac}. Similarly, the SPP frequency ω^-_{SP} lies close to the exciton frequency ω_{ab}.

Now, we calculate the FL when the two excitons have the degenerate states. This means they have $\omega_{ca} \approx \omega_{ba}$. In this case, the FL expression reduces to

$$\begin{aligned} &I_{QE} = I^0_{QE} Im\left(\frac{4(1+\Lambda_b+\Lambda_c)(\delta_k/\gamma - i)}{(\delta_k/\gamma - i)^2 - \omega^2_{cb}/\gamma^2}\right)|1+\Lambda_b+\Lambda_c|^2 \\ &I^0_{QE} = \hbar\omega_{ba}\gamma(\Omega/\gamma)^2 \end{aligned} \quad (30)$$

where δ_k is called the probe detuning and is defined as $\delta_k = \omega_{ca} + \omega_{ba} - 2\omega$.

The physical meaning of the Λ term is due to the interaction of the excitons with the SPP electric field. This term is called the dipole–dipole interaction (DDI) between the QE and the DMNS. Note that the Λ term is inversely proportional to r^3 and depends on the DDI between the QE and DMNS. For smaller distances, the DDI term has large values. Note that the FL depends on Λ which is inversely proportional to r^3. This means the FL depends on the DDI between the QE and DMNS. For smaller distances, the DDI term has large values. It also depends on the polarizability factor $\varsigma^{\pm}_{NS}$ which has large values at the SPP resonance energies.

Double Metallic Nanoshell Hybrid: Application to Nanomedicine

We plot the theoretical results with the experimental work of Bardhan et al. [9] where they have fabricated the IR800 fluorophore (QE) and Au-DNS (IR800-DNS) hybrid system. The core of the Au-nanoshell is made of the silica (SiO_2) with radius 63 nm and it is coated with Au-shell and its radius is 76 nm. Next, Au-nanoshell is coated with human serum albumin (HSA). This serves as a spacer layer to construct the DNS. After that, they fabricated nanohybrid by absorbing the IR800 fluorophore molecules onto the DMNS.

We plot theory and above experimental data in Fig. 6 (bottom). In our calculation, we have considered that the core of the Au-nanoshell is made of the silica (SiO2) with radius 63 nm and the Au-shell with radius 76 nm. Au-nanoshell is coated with human serum albumin (HSA) with thickness 8 nm. The solid diamonds denote the experimental data. The solid curve is theoretical results for when the exciton wavelength and SPP wavelength are not in resonance ($\lambda_{sp} \neq \lambda_{ab}$). Similarly, the dotted curve is plotted when the exciton wavelength and SPP wavelength are in resonance ($\lambda_{sp} = \lambda_{ab}$). Other parameters are taken as $\hbar\omega_p = 9$ eV and $\epsilon_\infty = 8$, $\gamma_m = 0.3$ eV. The dielectric constants for the silica and HAS are taken as $\epsilon_1 = 1.3$ and $\epsilon_3 = 1.35$, respectively.

We consider that the IR800 fluorophore molecules have two excitonic states with wavelength λ_{ab} and λ_{ac} and both states are degenerate ($\lambda_{ab} = \lambda_{ac}$). The SPP wavelength of the Au-DNS is $\lambda_{sp} = 805$ nm. The solid diamonds denote the experimental data when the thickness of the HSA is 8 nm and the solid curve is plotted when the exciton wavelength and SPP wavelength are not in resonance ($\lambda_{sp} \neq \lambda_{ab}$). The dotted curve is plotted when the exciton wavelength and SPP wavelength are in resonance with the exciton wavelength ($\lambda_{sp} = \lambda_{ab}$). There is a dramatic enhancement in the FL in the dotted curve. A good agreement between theory and experiment is found.

Further, we investigate experimental work of Bardhan et al. [16] where authors have fabricated the ICG-DMNS hybrid. They have taken ICG molecules to act as a QE. The core of the DMNS is made of silica (SiO2) with radius 60 nm and it is coated with an Au-shell and its radius is 72 nm. After that, the Au-shell is coated with varying thicknesses of silica to complete the DNS. Finally, the nanohybrid system was fabricated by absorbing the ICG molecules onto the DNS surface electrostatically to complete the ICG-DMNS hybrid. The outer silica shell acts as the spacer layer and it changes the distance between the ICG and Au-shell in the DMNS.

We compare our theory with the experimental data of ICG-DNS hybrid [2]. In the calculation, we have considered that the exciton wavelength and SPP wavelength are in resonance with each other ($\lambda_{sp} = \lambda_{ab}$). We have considered that the radius of the core and metallic shell are taken as 60 nm and 72 nm, respectively. Other parameters are taken as $\hbar\omega_p = 9\,\text{eV}$ and $\epsilon_\infty = 8$, $\gamma_m = 0.7$ eV. The dielectric constant for the silica is taken as $\epsilon_1 = \epsilon_3 = 1$. We consider that ICG molecules act as QE and have two degenerate excitonic states with wavelength λ_{ab}. The SPP wavelength of the Au-DNS is found as $\lambda_{sp} = 810$ nm. We found a good agreement between theory and experiment is found. The figures are shown in Ref. [41].

In summary, we found that as the thickness of the spacer layer is increased, the enhancement in the FL is decreased. We predicted that the enhancement in the FL depends on the type of the QE, spacer layer, and DNS. We showed that the FL spectra can be switched from one peak to two peaks by removing the degeneracy of the QE. Therefore, using these properties, one can use these hybrids as sensing and switching devices for applications in medicine. The enhancement of the FL emission of QEs will improve the detection limits of the near-infrared fluorescence-based imaging. These hybrids can also detect significantly smaller tumors.

Conclusions

In this chapter, we have answered the question of why metallic nanomaterials are used in nanomedicine. We have calculated surface plasmons in metallic nanomaterials and their application to nanomedicine. Next, we have studied the scattering of laser light with metallic nanostructures. The creation of surface plasmon polaritons and intensity of the emitted light from metallic nanoparticles has been calculated for metallic nanoparticles, single metallic nanoshells and double metallic nanoshells. Further, the extinction coefficient of metallic nanostructures has been evaluated. Finally, we have calculated the absorption of the optical energy into metallic nanostructures. The fluorescence emission from quantum emitters in nanohybrids has been evaluated, and its application to nanomedicine has been discussed.

Acknowledgements The author (MRS) is thankful to the Natural Sciences and Engineering Research Council of Canada (NSERC) for their research grant. The author also thanks full my graduate students Mr. Kevin Black for editing English of the paper and Mr. Jiaohan Guo for converting the figures into the JPG format.

References

1. Conde J, Doria G, Baptista P (2012) J Drug Deliv
2. Gobin AM, Lee MH, Halas NJ, James WD, Drezek RA, West JL (2007) Nano Lett 7, 1929
3. Oldenburg SJ, Averitt RD, Westcott SL, Halas NJ (1998) Chem Phys Lett 288:243

4. Loo C, Lowery A, Halas N, West J, Drezek R (2005) Nano Lett 5:709
5. Loo CH, Lin A, Hirsch L, Lee M, Barton JK, Halas NJ, West JL (2004) Technol Cancer Res Treat 3:33
6. Hirsch LR, Stafford RJ, Bankson JA, Sershen SR, Rivera B, Price RE, Hazle JD, Halas NJ, West JL (2003) Proc Natl Acad Sci USA 100:13549
7. O'Neal DP, Hirsch LR, Halas NJ, Payne JD, West JL (2004) Cancer Lett 209:171
8. Shi W, Sahoo Y, Swihart MT, Prasad PN (2005) Langmuir 21:1610
9. Kim J-H, Bryan W, Lee TR (2008) Langmuir 24:1147
10. Nikolai G, Khlebtsov AD (2010) J Quant Spectrosc Radiat Trans 111, 1. (J Franck, Chem Rev 115, 10407, 2015)
11. Fofang NT, Park T, Neumann O, Mirin NA, Nordlander P, Halas NJ (2008) Nano Lett 8:3481
12. Wersall M, Cuadra J, Antosiewicz TJ, Balci S, Shegai T (2017) Nano Lett 17:551
13. Erickson TA, Tunnell JW (2010) Online library. wiley.com. Wiley–VCH Verlag
14. Singh MR et al (2015) J Appl Phys 117:103102
15. Bardhan R, Grady NK, Cole JR, Joshi A, Halas NJ (2009) ACS Nano 3:744
16. Bardhan R, Grady NK, Halas NJ (2008) Small 4:1716
17. Singh MR et al (2017) J Appl Phys 121:094303
18. Wallace PR (1947) Phys Rev 71:622
19. Singh M, Wallace PR (1987) J Phys C 20:2169
20. Acun A, et al (2015) Germanene. J Phys Condens Matter 27, 443002
21. Vogt P et al (2012) Phys Rev Lett 108:155501
22. Cao A et al (2010) Adv Mater 22:103
23. Singh M et al (2017) Plasmonics 12:1021
24. Marques R, Martin F, Sorolla M (2006) Metamaterials with negative parameters. Wiley, New Jersey
25. Meinzer N et al (2014) Nat Photonics 8:889
26. Singh M et al (2015) J Appl Phys 117:184302
27. Temnov VV (2012) Nat Photonics 6:728
28. Yablonovitch E (1987) Phys Rev Lett 58:2059
29. Singh M et al (2015) J Appl Phys 117:184302
30. Cox JD, Singh MR et al (2011) Nano Lett 11:5284
31. Artuso RD, Bryant GW (2010) Phys Rev B 82:195419
32. Sadeghi SM, Deng L, Li X, Huang WP (2009) Nanotechnology 20:365401
33. Cox JD, Singh MR, Gumbs G, Anton MA, Carreno F (2012) Phys Rev B 86:125452
34. Singh M et al (2017) J Appl Phys 121:094303
35. Pease AC, Solas D, Sullivan EJ, Cronin MT, Holmes CP, Fodor SPA (1994) Proc Natl Acad Sci USA 91:5022
36. Weiss S (1999) Science 283:1676
37. Weinberger AW, Kirchhof B, Mazinani BE, Schrage NF (2001) Graefe's Arch Clin Exp Ophthalmol 239:388
38. Adams KE, Ke S, Kwon S, Liang F, Fan Z, Lu Y, Hirschi K, Mawad ME, Barry MA, Sevick-Muraca EM (2007) J Biomed Opt 12:024017
39. Houston JP, Ke S, Wang W, Li C, Sevick-Muraca EM (2005) J Biomed Opt 10:0540101
40. Singh MR, Chandra Sekhar M, Balakrishnan S, Masood S (2017) J Appl Phys 122:034306
41. Singh MR, Guo J, Jorge Cid JM, Martínez JEH (2017) J Appl Phys 121:094303
42. Singh MR (2014) Electronic, photonic, polaritonic and plasmonic materials. Wiley Custom, Toronto
43. Singh MR (2014) Excitonic and photonic processes in materials. Springer, New York, p 30. (J Singh, T Williams (eds))
44. Novotny L, Hecht B (2006) Principle of nano-optics. Cambridge University Press
45. Sarid D, Challener WA (2010) Modern introduction to surface plasmons: theory, mathematica modeling, and applications. Cambridge University Press

Challenges in Malaria Management and a Glimpse at Some Nanotechnological Approaches

Adrian Najer, Cornelia G. Palivan, Hans-Peter Beck and Wolfgang Meier

Abstract

Malaria is a devastating infectious disease transmitted by mosquitoes, affecting millions of people and killing about half a million children each year. Despite tremendous progress in the control and elimination of malaria within the past years, there are still considerable challenges to be solved. To name a few, drug-resistant parasites, insecticide-resistant mosquitoes and the difficulty to formulate a potent malaria vaccine need to be addressed with new strategies to achieve the final goal of malaria eradication. Nanotechnology—researching and designing innovative structures at the nanoscale—is a promising contemporary technology that is being applied to a vast number of biomedical problems. In the case of malaria, nanotechnology provides tools to design strategies to target drug molecules to specific stages of the parasite, treat drug-resistant parasites, resolve severe malaria, increase vaccine efficacies and combinations thereof. This chapter introduces malaria, discusses current challenges of malaria control and relates these challenges to some potential solutions provided by the nanotechnology field.

Keywords

Malaria · Nanotechnology · Drug delivery
Vaccine delivery

Malaria

Malaria is an infectious disease caused by *Plasmodium* spp. parasites, which are mainly prevalent in developing countries, due to the habitat of their arthropod vector: female *Anopheles* mosquitoes. Several *Plasmodium* species are known to infect humans: *P. falciparum, P. vivax, P. ovale, P. malariae* and *P. knowlesi.* The most aggressive and life-threatening species is *P. falciparum*, which accounts for most of the malaria-related deaths, and is the main form occurring in sub-Saharan African countries. *P. vivax* is more prevalent in Asia and South America. This parasite species is less life-threatening, but the liver stage of this parasite can remain latent as hypnozoites, which

A. Najer · C. G. Palivan · W. Meier (✉)
Department of Chemistry, University of Basel, 4056 Basel, Switzerland
e-mail: wolfgang.meier@unibas.ch

A. Najer · H.-P. Beck
Swiss Tropical and Public Health Institute, University of Basel, 4002 Basel, Switzerland

R. Adhikari and S. Thapa (eds.), *Infectious Diseases and Nanomedicine III*,
Advances in Experimental Medicine and Biology 1052, https://doi.org/10.1007/978-981-10-7572-8_9

can release pathogens even months or years after infection and cause a relapse of the disease. Of an estimated 198 million malaria cases, about 584'000 ended fatally in 2013 [1]. About 90% of all the malaria deaths occurred in sub-Saharan Africa and 78% were children aged below 5 years [1]. These numbers highlight the large burden malaria still puts on public health in less developed countries.

Life Cycle of *Plasmodium falciparum*

Plasmodium spp. parasites—belonging to parasitic protists of the phylum Apicomplexa—undergo very complex life cycles, which include arthropod (*Anopheles* mosquito) and human host. Various extracellular (sporozoites, merozoites and ookinetes) and intracellular (intra-erythrocytic and intra-hepatocytic schizonts) forms of the parasite are involved in the life cycle (Fig. 1).

Only part of the life cycle of *P. falciparum* is briefly summarised herein. More information on the mosquito-based stages and gametogenesis needed for transmission from the human host back to the mosquito vector can be found elsewhere [2]. Multiplication within the human host exclusively occurs by mitosis, whereas meiosis is restricted to the replication within the mosquito host [4]. First, infected female *Anopheles* mosquitoes inject from a few dozens up to a few hundred sporozoites into the bloodstream of humans, whilst taking their blood meal. This extracellular sporozoite form travels through the bloodstream, passes through Kupffer cells in the liver and finally infects and reproduces within hepatocytes. Each infected hepatocyte releases thousands of merozoites into the bloodstream, after they were formed through asexual cell division. Merozoites are polarised pear-shaped cells with a length of only about 1.5 µm; merozoites belong to the smallest known eukaryotic cells [5]. Merozoites are equipped and primed to attach to and invade red blood cells (RBCs). Therein, this parasite form undergoes schizogeny for about 48 h to yield about 16–32 fresh

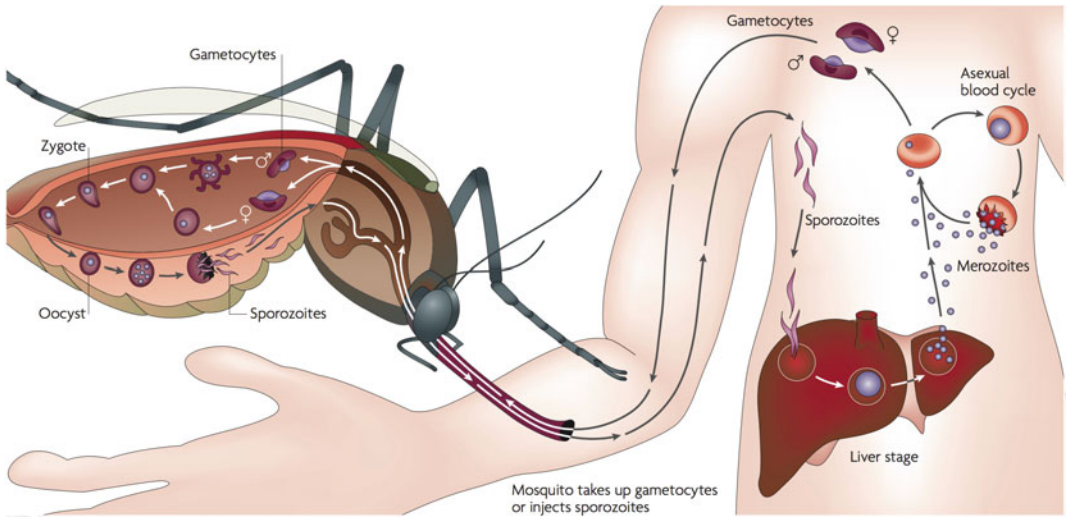

Fig. 1 Malaria parasite life cycle. During the blood meal, *Anopheles* mosquitoes can inject sporozoites into the bloodstream of humans or take up gametocytes from infected humans. Info on the life cycle in the mosquito vector and gametogenesis can be found elsewhere [2]. Sporozoites asexually reproduce within hepatocytes in the liver, which release thousands of merozoites back into the bloodstream. Merozoites invade red blood cells (RBCs) where they asexually divide to form more parasites (schizogeny). After about 48 h (*P. falciparum*), all infected RBCs burst and release the freshly generated parasites that rapidly invade more RBCs. This erythrocytic cycle is responsible for malaria pathogenesis. Reprinted with permission from Ref. [3]. Copyright (2007) Nature Publishing Group

daughter merozoites within each infected RBC (iRBC) in the case of *P. falciparum* [6]. Daughter merozoites egress from iRBCs to rapidly infect more RBCs. This erythrocytic asexual life cycle of the parasite continues and is finally responsible for malaria pathogenesis as discussed in the next subchapter [4].

Pathogenesis of Malaria

Pathogenesis is solely related to the blood stage cycle of malaria. Symptoms, which usually appear about 10–15 days after infection, and potential establishment of severe malaria, are all attributed to the multiplication and residence of parasites within RBCs. Laboratory manifestations of severe malaria include severe anaemia, acidosis, hyperlactatemia and hypoglycemia, pulmonary edema and acute kidney injury [4]. Severe *P. falciparum* malaria is responsible for most malaria-related deaths and is mainly caused by sequestration of iRBCs and subsequent dysfunction of various vital organs [4]. So-called cerebral malaria, which is a syndrome that frequently leads to death, is also related to sequestration, in this case within the brain microvasculature [7]. Sequestration, also called cytoadherence, relates to the adhesion of *P. falciparum* iRBCs (about 12–15 h post-invasion) to endothelial cell surfaces in veins and capillaries via knob structures on iRBCs. Sequestration leads to interference with microcirculatory flow leading to malfunctioning of the affected organ and ultimately to death, if not treated [4].

The major adhesion protein in these knob structures of the iRBC surface is *P. falciparum* erythrocyte membrane protein 1 (*Pf*EMP1), which is in fact the main responsible molecule for the disease pathogenesis. Intracellular parasites have the astonishing ability to dramatically change the RBC physicochemical properties during the 48 h intracellular cycle of, e.g. *P. falciparum*. In fact, the intracellular parasite exports about 10% of all its proteins to the host cell cytosol, where a parasite-derived membranous sorting machinery, termed Maurer's clefts, further sends certain proteins, including *Pf*EMP1, to the iRBC surface [8]. Even more astonishing is the fact that the parasite has 60 different *var* genes, which all encode for one specific type of *Pf*EMP1, whereas only one is mutually exclusively expressed at each time point [9]. This allows the parasite to vary cytoadherence by binding to another receptor, which changes pathogenesis and helps the parasite to evade the immune system. Important members of host receptors for different *Pf*EMP1 are chondroitin sulphate A in the placenta, ICAM1 in the brain, and CD36 in many other organs [4, 7].

Another important modification of the host cell is the large increase of the membrane permeability towards certain small solutes [10]. The activity of so-called new permeation pathways (NPPs) on iRBCs, which were related to reactivation of endogenous dormant protein channels, has been proposed to cause this increase in permeability [10]. Nevertheless, access of even larger proteins and nanoparticles up to 80 nm diameter to the intracellular parasite, without passing the host cytosol, suggests another yet unclear modification of the host cell to increase permeability; one possibility being a duct pathway that originates from unsuccessful closure of the merozoite entry site [11–15]. Detailed review of other host cell alterations through exported proteins leading to modification of the host's cytoadherence, permeability and rigidity can be found elsewhere [8, 16].

Malaria Prophylaxis, Treatment and Control Strategies

Malaria can be treated using different combination therapies. The first-line treatment options include the very effective drugs of the artemisinin class in combination with other partner drugs. These drug combinations are also used for prophylaxis in travellers. The current drugs act on the intracellular parasites, no drug is on the market that can inhibit RBC invasion, for example [17]. Similar to other antimicrobials, antimalarials constantly lose their efficacy due to the development and spread of drug resistance. Recently, drug resistance against the

artemisinin-based drug combinations emerged in South East Asia [18] is spreading westwards [19] and has already led to treatment failures [20]. This explains the constant need for novel antimalarials. Furthermore, there is an urgent need to develop drugs to reduce the high mortality of severe malaria [21]. For final elimination of malaria, it will also be necessary to develop drugs that kill gametocytes, therefore blocking transmission, and drugs to eliminate dormant hypnozoites of *P. vivax* to inhibit relapse of the disease months after the infection [21, 22].

There is no malaria vaccine on the market yet. Several are in various stages of clinical trials. The most advanced being RTS,S/AS01 (Mosquirix^{TM}), for which a phase 3 clinical trial finished in 2015 [23] and the European Regulators have approved the use of the vaccine in July 2015. Nevertheless, the vaccine efficacy for this particular vaccine in children and infants was only about 30% after four vaccinations [23], which is one of the reasons why WHO has only recommended usage in pilot implementation studies; no countrywide implementation has been recommended as yet [24]. In recent years, the whole pathogen vaccination strategy has become more attractive again, especially the attenuated sporozoite vaccine approach, which has regained attention due to new, larger scale production possibilities and remarkable protection in small studies [25]. However, a very recent study with this sporozoite-based vaccine revealed a protection of about 50% for homologous challenge in adults for at least 1 year [26], which is again similar to protection achieved in adults using the RTS,S subunit vaccine [27]. Larger studies are needed to evaluate the sporozoite-based vaccination, especially heterologous challenge to demonstrate clone-independent protection. Nevertheless, issues regarding affordable large-scale production, dosing, administration, storage, distribution and safety remain questionable at the moment [28, 29].

Global control measures for malaria, which mainly helped to cut the mortality of malaria by half during the last decade, are the extended use of long-lasting insecticide-impregnated bed nets and indoor residual spraying of insecticides [30]. However, these efforts are also greatly challenged by insecticide-resistant mosquitoes that are already prevalent in many malaria endemic areas [31].

In the following subchapters, the focus is shifted from the current challenges in malaria control to novel possibilities provided by nanotechnology to design future tools necessary in the fight against malaria.

Nanotechnological Approaches for Malaria

The current problems associated with malaria discussed in the first subchapter demand for innovative strategies for future control of this disease. Nanotechnology is increasingly acknowledged as a valuable tool to design novel diagnostic [32], therapeutic [33–36], and prophylactic [37, 38] approaches for malaria. For detailed examples, readers are referred to the above-mentioned extensive reviews on this topic. Herein, only a few examples regarding malaria therapy and prophylaxis—diagnostic approaches are not covered—are highlighted to demonstrate the broad applicability of nanotechnology to design new tools with the potential to be implemented in the future malaria control arsenal.

Antimalarial Drug Delivery

Similar to anticancer drug delivery, antimalarials are other valuable carrier molecules to be incorporated within nanoparticles for drug delivery to parasitised cells. In case of malaria, nanoparticle-based drug delivery is being evaluated to reduce drug-related toxicities, fight drug resistance development, increase drug performance, treat severe malaria and block transmission as exemplified below. Up to now, the main carriers evaluated for antimalarial drug delivery have been liposomes, solid lipid nanoparticles, polymeric nanoparticles, cyclodextrins and dendrimers [35].

Currently, blood stage parasites are the main target of antimalarial drug delivery. Increasing

the drug concentration within intracellular parasites through targeted nanostructure-based drug delivery is thought to be a valuable tool to fight the establishment of drug resistance and treatment of drug-resistant parasites [15, 39]. However, it is an ongoing controversy through which mechanism nanostructures deliver antimalarials to iRBCs. The two main proposed mechanisms are a direct access of nanoparticles (<80 nm diameter) to intracellular parasites via the 'leakiness' of iRBCs [12, 13, 15, 40] and membrane fusion of, e.g. drug-loaded liposomes with iRBC membranes (iRBCM) [41–43]. The main difference between these two mechanisms is the role of the host cell cytosol. With the first mechanism, the drug delivery system (DDS) bypasses the host cytosol (Fig. 2B, C), whereas membrane fusion demands subsequent crossing of the host cytosol by the drug molecule (Fig. 2A). Possible explanations for these pathways are summarised in Fig. 2.

The increased permeability of iRBCs to small solutes has been attributed to new permeation pathways (NPP) appearing on iRBC membranes (Fig. 2A) [10]. However, the size of these channels does not provide a pathway for nanoparticles. Possible sites for the entry of sub-80 nm nanoparticles into iRBCs are the sites where the iRBCM is in close proximity to the parasitophorous vacuole membrane (PVM) and parasite plasma membrane (PPM) (Fig. 2B-a) [44]. Uptake of nanoparticles could also occur via the tubovesicular membrane (TVM) that fuses with the iRBCM (Fig. 2B-b). Alternatively, the merozoite entry site might never completely close and therefore provide a parasitophorous duct that allows direct entry from the serum site (Fig. 2C) [44].

The second pathway, delivery via membrane fusion, calls for a membranous nanostructure, such as liposomes, and active targeting to iRBCs. iRBC-targeting antibodies and polysaccharides presented on liposome surfaces were demonstrated to increase fusion of the nanocarrier with membranes of infected cells [41, 42, 45]. This strategy reduced the amount of drug needed to kill the intracellular parasites in vitro by more than 10-fold compared to free drug, but parasitemia could not completely be eliminated from the cultures [42]. In contrast, targeting liposomes to all RBCs, including non-infected RBCs, also yielded some beneficial effect due to the residence of the antimalarial chloroquine (CQ) already before entry of the parasite [43, 46]. Dendrimers have been investigated for antimalarial delivery as well [15, 39]. Poly(amidoamine) dendrimers loaded with CQ were much more effective in an in vivo model of malaria

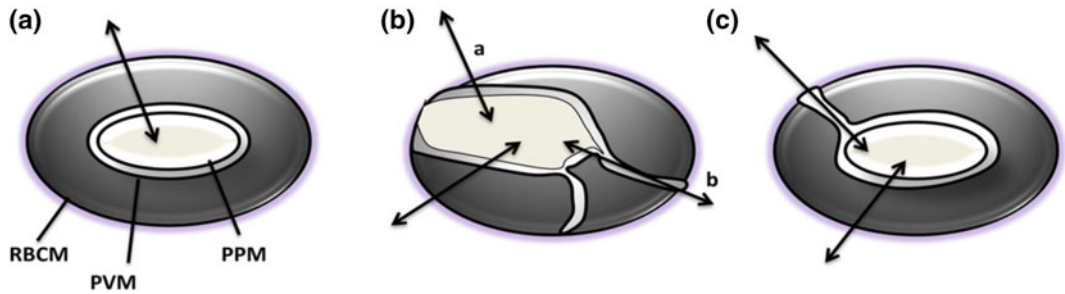

Fig. 2 Schematic representation of proposed iRBC morphology causing increased permeability of iRBCs compared to RBCs. **A** Traditional sequential pathway: solutes sequentially cross red blood cell membrane (RBCM), parasitophorous vacuole membrane (PVM), and parasite plasma membrane (PPM) to reach the parasite. **B**, **C** Alternative models 'parallel pathways' for solute transport that does not involve the host cytosol: **B** (a) PVM and PPM are close to RBCM to facilitate solute uptake or (b) tubovesicular membrane (TVM) fuses with RBCM, which allows entry of solutes from extracellular medium. **C** Parasitophorous duct originating from merozoite entry connects the intracellular parasite with the external medium. This scheme is based on Ref. [44]. Reprinted with permission from Ref. [35]. Copyright (2013) Elsevier

compared to the free drug [15]. This was attributed to the targeting effect of these dendrimers to iRBCs, which specifically take up these drug-loaded nanocarriers. Another type of dendrimers, amphiphilic dendrimers, were also loaded with CQ and primaquine (PQ), which yielded similar beneficial effects as the first example when tested in vitro and in vivo against malaria [39]. Targeted delivery of high drug concentrations to iRBCs is considered a valuable strategy to tackle development of drug resistance [15, 39].

Another avenue for antimalarial delivery via DDS is the optimisation of drug performance of existing antimalarials. Nanostructure-based artemisinin delivery was evaluated in a malaria mouse model using PEGylated liposomes via parenteral administration. Delivery by this specific carrier showed the highest efficiency compared to free artemisinin and conventional liposomal formulation of artemisinin [47, 48]. The artemisinin-loaded liposomes yielded much longer blood-circulation times and more stable drug concentration levels in the blood compared to free artemisinin [47, 48]. Furthermore, the liposomal formulations had an immediate effect on the parasites, whereas free artemisinin decreased parasitemia not before 7 days after the treatment start [48]. In conclusion, the efficacy of an existing drug could be optimised using liposomal nanocarriers [48].

A further strategy is the development of DDS to reduce the high mortality associated with severe malaria [49]. Liposomes have been tested in a model of a severe pathological event, cerebral malaria [49, 50]. In contrast to previous examples, the DDS used in this case did not deliver an antimalarial, but a toxic glucocorticoid prodrug. This DDS reduced cerebral inflammation when administered to mice with experimental cerebral malaria. By first reducing the adverse effects related to the cerebral syndrome using this steroidal nano-drug, the time window for subsequent anti-parasite treatment with conventional antimalarial drugs was significantly increased [49, 50]. This sequential treatment completely cured mice with cerebral malaria. The authors conclude that this is a valuable treatment option for this severe form of malaria, even if patients would arrive at a late stage of disease.

Stimuli-responsive nanoparticles that release their cargo upon a change in pH, temperature, redox potential or concentration of a specific enzyme [51, 52], have only recently been applied for potential antimalarial drug delivery. The highly reducing cytosol of intracellular malaria parasites [53] provides an endogenous trigger to initiate intracellular nanoparticle disassembly and drug release [54]. This strategy is comparable to reduction-triggered anticancer drug release from DDS within the reducing cytosol of cancer cells [55]. We demonstrated that reduction-triggered drug delivery of an experimental antimalarial compound to iRBCs can be achieved [54]. This nanoparticle type successfully solubilised and delivered the experimental, metabolically unstable antimalarial drug candidate, serine hydroxymethyltransferase (SHMT) inhibitor (±)−1 [54, 56]. This opens up the possibility to use non-optimised antimalarial drug candidates with solubility and metabolic stability issues before chemical optimisation using a suitable nanocarrier system. The cytosol of drug-resistant parasite strains (CQ-resistant) was previously found to be even more reducing (higher glutathione (GSH) levels and glutathione S-transferase activity) compared to drug-sensitive strains [57]. More recent data also revealed the same elevated GSH levels within parasite cytosols of artemisinin- and mefloquine-resistant strains [58]. This reduction of drug-sensitivity might be overcompensated by delivery of high local concentrations of drugs using reduction-triggered nanoparticles. These triggered carriers might release their payload faster and more effectively within the highly reducing cytosol of drug-resistant parasites.

Other parasite stages that are currently being addressed using nanostructure-based delivery systems are the mosquito stages [59]. One possible way would be the administration of these drug-loaded nanoparticles to humans, which would subsequently delivery the nanoparticles from their blood to the mosquito during their blood meal [59].

Nanostrategies for Malaria Vaccines

Various nanostructures have been proposed and tested as delivery vehicles for malaria vaccines [37, 38]. In the context of vaccines, nanostructures are delivery platforms in a cocktail of antigens (or DNA encoding for antigens), adjuvants and immunomodulatory molecules. This complex design helps to generate and modulate the immune response [60]. The most advanced malaria vaccine candidate RTS,S/AS01 from GSK can be considered a nanovaccine; the antigen is formulated as virus-like particle and combined with a liposomal adjuvant system (AS01) [61]. RTS,S/AS01 is an example of a subunit protein/peptide vaccine, containing part of the circumsporozoite protein (CSP) of the pre-erythrocytic sporozoite form of *P. falciparum* formulated with an adjuvant to induce strong cellular and humoral immune response. The clinical outcome of this vaccine is discussed above.

Another nanotechnological vaccination example is the use of viral envelopes, called virosomes, for targeted delivery of incorporated antigens [62]. This strategy was, e.g. used to successfully induce production of parasite growth-inhibitory antibodies against apical membrane antigen 1 (AMA1) of blood stage malaria parasites [62]. In even more advanced formulations, epitopes are integrated into designer proteins that self-assemble into 'virus-like' nanoparticles themselves [38]. This combines the high immunogenicity of virus-like nanoparticles with the purity of designer proteins; such a self-assembled nanoparticle—based on CSP epitopes—will enter human clinical trials in 2017 [38].

DNA vaccination is another alternative. In this case, DNA encoding for certain antigens is used for vaccination. Unfortunately, free DNA suffers from insufficient cellular uptake and low stability in biological fluids. This is circumvented by protection and delivery of the DNA via nanocarriers. However, the perfect carrier in combination with the best route of administration has not yet been found [37].

In general, malaria blood stage protein-based vaccines are challenging to design, due to the difficulty to select and prioritise the antigen or combination of antigens that can induce a maximum protective response. Future protein-based malaria vaccine development to achieve a highly effective vaccine, which can either prevent death, disease or transmission, will need to include new strategies for identification, selection and formulation of the vaccine [63]. Conserved and essential antigens, which are not necessarily the main targets of naturally acquired immunity, should be selected in the future and most beneficial antigen combinations for protective efficacy should be found [63]. Furthermore, finding improved protein vaccine delivery platforms (nanotechnology) and adjuvants to significantly fine-tune and enhance humoral and cellular immunity is another priority [63]. Overall, we have learned that formulation of an effective subunit protein vaccine for malaria is extremely challenging. For final eradication of malaria, a combination of subunit protein vaccines and whole parasite vaccines (see previous subchapters) might be the solution [64].

We developed a different nanotechnological approach that is designed to provide a mixed drug- and 'vaccine-like' activity [65]. This approach is based on first inhibiting *Plasmodium* merozoite invasion into RBCs (drug activity). In a second step ('vaccine-like' activity), the immune response against extracellular parasites will be fine-tuned by targeting the merozoite–nanoparticle complex—obtained during the 'drug activity' in the first step—to immune cells to potentially induce protective immunity. We finalised the first step of this approach by creating nanostructures (termed nanomimics) based on polymer vesicles (polymersomes) functionalised with a molecule found on RBCs and known to be important for malaria parasite invasion [65]. These nanomimics bound to *P. falciparum* merozoites after egress from their host RBCs and inhibited subsequent invasion (Scheme, Fig. 3, left). Highly potent invasion inhibition by these nanostructures was found in vitro, which is explained by strong multivalent interactions between nanomimics and parasites (Fig. 3, right) [65, 66].

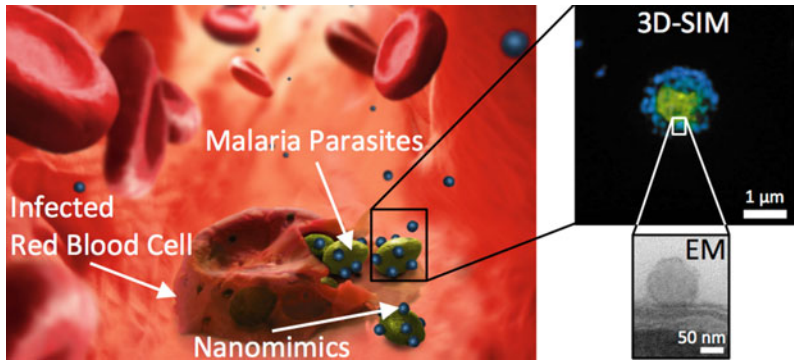

Fig. 3 Left: Schematic representation of the first step of the nanomimic approach; nanomimics (blue) bind to egressing *Plasmodium* merozoites (yellow) to inhibit subsequent invasion of healthy RBCs. Right: Super-resolution 3D structured illumination microscopy (3D-SIM) of a single *P. falciparum* merozoite (DNA stain, yellow) with surface-bound nanomimics (fluorescent dye-loaded, blue) and below, an excerpt of a transmission electron micrograph (TEM) of an ultrathin slice of the nanomimic–merozoite complex; a single nanomimic tightly sticking to the outer membrane of a

Conclusions

The challenges we face with respect to malaria control, elimination and finally eradication demand for the establishment of innovative tools to be added to the current antimalarial arsenal. Nanotechnology is a rapidly expanding field that provides advanced solutions to biomedical problems including malaria. The potential impact of nanotechnological approaches could be the treatment of drug-resistant parasites, resolving the features of severe malaria, improving properties of experimental antimalarial drug candidates, targeting and inhibiting transmission stages of the parasite, formulation of vaccines with increased efficacy and innovative combinations of various functions within a single formulation.

Acknowledgements This work was supported by the Swiss National Science Foundation and by the NCCR Molecular Systems Engineering, which is gratefully acknowledged.

References

1. World Health Organization. World Health Statistics (2015) World Health Organization, Geneva, 1–164
2. Josling GA, Llinás M (2015) Sexual development in Plasmodium parasites: knowing when it's time to commit. Nat Rev Micro 13:573–587
3. Su X, Hayton K, Wellems TE (2007) Genetic linkage and association analyses for trait mapping in Plasmodium falciparum. Nat Rev Genet 8:497–506
4. White NJ, Pukrittayakamee S, Hien TT, Faiz MA, Mokuolu OA, Dondorp AM (2014) Malaria. Lancet 383:723–735
5. Cowman AF, Berry D, Baum J (2012) The cell biology of disease: the cellular and molecular basis for malaria parasite invasion of the human red blood cell. J Cell Biol 198:961–971
6. Cowman AF, Crabb BS (2006) Invasion of red blood cells by malaria parasites. Cell 124:755–766
7. Cooke B, Coppel R, Wahlgren M (2000) Falciparum malaria: sticking up, standing out and out-standing. Parasitol Today 16:416–420
8. Mundwiler-Pachlatko E, Beck H-P (2013) Maurer's clefts, the enigma of Plasmodium falciparum. Proc Natl Acad Sci USA 110:19987–19994
9. Voss TS, Healer J, Marty AJ, Duffy MF, Thompson JK, Beeson JG et al (2006) A var gene promoter controls allelic exclusion of virulence genes in Plasmodium falciparum malaria. Nature 439:1004–1008
10. Ginsburg H, Stein WD (2004) The new permeability pathways induced by the malaria parasite in the membrane of the infected erythrocyte: comparison of results using different experimental techniques. J Membrane Biol 197:113–134
11. Pouvelle B, Spiegel R, Hsiao L, Howard RJ, Morris RL, Thomas AP et al (1991) Direct access to serum macromolecules by intraerythrocytic malaria parasites. Nature 353:73–75
12. Goodyer ID, Pouvelle B, Schneider TG, Trelka DP, Taraschi TF (1997) Characterization of macromolecular transport pathways in malaria-infected erythrocytes. Mol Biochem Parasitol 87:13–28
13. El Tahir A, Malhotra P, Chauhan VS (2003) Uptake of proteins and degradation of human serum albumin

by Plasmodium falciparum-infected human erythrocytes. Malar J 2:1–8
14. Bergmann-Leitner ES, Duncan EH, Angov E (2009) MSP-1p42-specific antibodies affect growth and development of intra-erythrocytic parasites of Plasmodium falciparum. Malar J 8:183–195
15. Urbán P, Valle-Delgado JJ, Mauro N, Marques J, Manfredi A, Rottmann M et al (2014) Use of poly (amidoamine) drug conjugates for the delivery of antimalarials to Plasmodium. J Control Release 177:84–95
16. Spillman NJ, Beck JR, Goldberg DE (2015) Protein export into malaria parasite-infected erythrocytes: mechanisms and functional consequences. Annu Rev Biochem 84:813–841
17. Kappe SHI, Vaughan AM, Boddey JA, Cowman AF (2010) That was then but this is now: malaria research in the time of an eradication agenda. Science 328:862–866
18. Dondorp AM, Nosten F, Yi P, Das D, Phyo AP, Tarning J et al (2009) Artemisinin resistance in *Plasmodium falciparum* malaria. N Engl J Med 361:455–467
19. Tun KM, Imwong M, Lwin KM, Win AA, Hlaing TM, Hlaing T et al (2015) Spread of artemisinin-resistant Plasmodium falciparum in Myanmar: a cross-sectional survey of the K13 molecular marker. Lancet Infect Dis 15:415–421
20. Amaratunga C, Lim P, Suon S, Sreng S, Mao S (2016) Dihydroartemisinin–piperaquine resistance in Plasmodium falciparum malaria in Cambodia: a multisite prospective cohort study. Lancet Infect Dis 16:357–365
21. Miller LH, Ackerman HC, Su X-Z, Wellems TE (2013) Malaria biology and disease pathogenesis: insights for new treatments. Nat Med 19:156–167
22. Wells TNC, van Huijsduijnen RH, Van Voorhis WC (2015) Malaria medicines: a glass half full? Nat Rev Drug Discov 14:424–442 Nature Publishing Group
23. Rts SCTP (2015) Efficacy and safety of RTS, S/AS01 malaria vaccine with or without a booster dose in infants and children in Africa: final results of a phase 3, individually randomised, controlled trial. Lancet 386:31–45 Elsevier Ltd.
24. World Health Organization (2016) Malaria vaccine: WHO position paper-January 2016. Wkly Epidemiol Rec 91:33–51
25. Seder RA, Chang LJ, Enama ME, Zephir KL, Sarwar UN, Gordon IJ et al (2013) Protection against malaria by intravenous immunization with a nonreplicating sporozoite vaccine. Science 341:1359–1365
26. Ishizuka AS, Lyke KE, DeZure A, Berry AA, Richie TL, Mendoza FH, et al (2016) Protection against malaria at 1 year and immune correlates following PfSPZ vaccination. Nat Med 1–13. Nature Publishing Group
27. Kester KE, Cummings JF, Ofori Anyinam O, Ockenhouse CF, Krzych U, Moris P et al (2009) Randomized, Double-Blind, Phase 2a Trial of Falciparum Malaria Vaccines RTS, S/AS01B and RTS, S/AS02A in Malaria-Naive Adults: Safety, Efficacy, and Immunologic Associates of Protection. J Infect Dis 200:337–346
28. Richards JS, Beeson JG (2009) The future for blood-stage vaccines against malaria. Immunol Cell Biol 87:377–390
29. Hoffman SL, Billingsley PF, James E, Richman A, Loyevsky M, Li T et al (2010) Development of a metabolically active, non-replicating sporozoite vaccine to prevent Plasmodium falciparum malaria. Hum Vaccines 6:97–106
30. Tanner M, Greenwood B, Whitty CJM, Ansah EK, Price RN, Dondorp AM et al (2014) Malaria eradication and elimination: views on how to translate a vision into reality. BMC Med 13:167
31. Hemingway J, Ranson H, Magill A, Kolaczinski J (2016) Averting a malaria disaster: will insecticide resistance derail malaria control? Lancet 387:1785–1788
32. Lukianova-Hleb EY, Campbell KM, Constantinou PE, Braam J, Olson JS, Ware RE et al (2014) Hemozoin-generated vapor nanobubbles for transdermal reagent- and needle-free detection of malaria. Proc Natl Acad Sci USA 111:900–905
33. Santos-Magalhães NS, Mosqueira VCF (2010) Nanotechnology applied to the treatment of malaria. Adv Drug Deliver Rev 62:560–575. Elsevier B.V
34. Dennis E, Peoples VA, Johnson F (2015) Utilizing Nanotechnology to Combat Malaria. J Infect Dis Ther 3:1–6
35. Aditya NP, Vathsala PG, Vieira V, Murthy RSR, Souto EB (2013) Advances in nanomedicines for malaria treatment. Adv Colloid Interfac 201–202:1–17
36. Kuntworbe N, Martini N, Shaw J, Al-Kassas R (2012) Malaria intervention policies and pharmaceutical nanotechnology as a potential tool for malaria management. Drug Dev Res 73:167–184
37. Tyagi RK, Garg NK, Sahu T (2012) Vaccination Strategies against Malaria: novel carrier(s) more than a tour de force. J Control Release 162:242–254
38. Burkhard P, Lanar DE (2015) Malaria vaccine based on self-assembling protein nanoparticles. Expert Rev Vaccines 14:1525–1527
39. Movellan J, Urbán P, Moles E, la Fuente de JM, Sierra T, Serrano JL, et al (2014) Amphiphilic dendritic derivatives as nanocarriers for the targeted delivery of antimalarial drugs. Biomaterials 35:7940–7950
40. Pouvelle B, Gormley JA, Taraschi TF (1994) Characterization of trafficking pathways and membrane genesis in malaria-infected erythrocytes. Mol Biochem Parasitol 66:83–96
41. Urbán P, Estelrich J, Cortés A, Fernàndez-Busquets X (2011) A nanovector with complete discrimination for targeted delivery to Plasmodium falciparum-infected versus non-infected red blood cells in vitro. J Control Release 151:202–211. Elsevier B.V
42. Urbán P, Estelrich J, Adeva A, Cortés A, Fernàndez--Busquets X (2011) Study of the efficacy of antimalarial

drugs delivered inside targeted immunoliposomal nanovectors. Nanoscale Res Lett 6:620–630
43. Moles E, Urbán P, Jiménez-Díaz MB, Viera-Morilla S, Angulo-Barturen I, Busquets MA et al (2015) Immunoliposome-mediated drug delivery to Plasmodium-infected and non-infected red blood cells as a dual therapeutic/prophylactic antimalarial strategy. J Control Release 210:217–229
44. Kirk K (2001) Membrane transport in the malaria-infected erythrocyte. Physiol Rev 81:495–537
45. Marques J, Moles E, Urbán P, Prohens R, Busquets MA, Sevrin C et al (2014) Application of heparin as a dual agent with antimalarial and liposome targeting activities toward Plasmodium-infected red blood cells. Nanomed-Nanotechnol 10:1719–1728
46. Moles E, Fernàndez-Busquets X (2015) Loading antimalarial drugs into noninfected red blood cells: an undesirable roommate for Plasmodium. Future Med Chem 7:833–835
47. Isacchi B, Arrigucci S, Marca GL, Bergonzi MC, Vannucchi MG, Novelli A et al (2011) Conventional and long-circulating liposomes of artemisinin: preparation, characterization, and pharmacokinetic profile in mice. J Lipos Res 21:237–244
48. Isacchi B, Bergonzi MC, Grazioso M, Righeschi C, Pietretti A, Severini C, et al (2012) Artemisinin and artemisinin plus curcumin liposomal formulations: Enhanced antimalarial efficacy against Plasmodium berghei-infected mice. Eur J Pharm Biopharm 80:528–534. Elsevier B.V
49. Waknine-Grinberg JH, Even-Chen S, Avichzer J, Turjeman K, Bentura-Marciano A, Haynes RK, et al (2013) Glucocorticosteroids in nano-sterically stabilized liposomes are efficacious for elimination of the acute symptoms of experimental cerebral malaria. PLoS ONE 8:e72722. Coban C (ed)
50. Guo J, Waknine-Grinberg JH, Mitchell AJ, Barenholz Y, Golenser J (2014) Reduction of experimental cerebral malaria and its related proinflammatory responses by the novel liposome-based β-Methasone nanodrug. Biomed Res Int 2014:1–8
51. Mura S, Nicolas J, Couvreur P (2013) Stimuli-responsive nanocarriers for drug delivery. Nat Mater 12:991–1003
52. Palivan CG, Goers R, Najer A, Zhang X, Car A, Meier W (2016) Bioinspired polymer vesicles and membranes for biological and medical applications. Chem Soc Rev 45:377–411
53. Kasozi D, Mohring F, Rahlfs S, Meyer AJ, Becker K (2013) Real-time imaging of the intracellular glutathione redox potential in the malaria parasite plasmodium falciparum. PLoS Pathog 9:e1003782. Ginsburg H (ed)
54. Najer A, Wu D, Nussbaumer MG, Schwertz G, Schwab A, Witschel MC et al (2016) An amphiphilic graft copolymer-based nanoparticle platform for reduction-responsive anticancer and antimalarial drug delivery. Nanoscale 8:14858–14869
55. Schafer FQ, Buettner GR (2001) Redox environment of the cell as viewed through the redox state of the glutathione disulfide/glutathione couple. Free Radic Biol Med 30:1191–1212
56. Witschel MC, Rottmann M, Schwab A, Leartsakulpanich U, Chitnumsub P, Seet M et al (2015) Inhibitors of Plasmodial Serine Hydroxymethyltransferase (SHMT): cocrystal structures of pyrazolopyrans with potent blood- and liver-stage activities. J Med Chem 58:3117–3130
57. Dubois VL, Platel DF, Pauly G, Tribouley-Duret J (1995) Plasmodium berghei: implication of intracellular glutathione and its related enzyme in chloroquine resistance in vivo. Exp Parasitol 81:117–124
58. Vega-Rodríguez J, Pastrana-Mena R, Crespo-Lladó KN, Ortiz JG, Ferrer-Rodríguez I, Serrano AE (2015) Implications of glutathione levels in the plasmodium berghei response to chloroquine and artemisinin. PLoS ONE 10:e0128212. Carvalho LH (ed)
59. Paaijmans K, Fernàndez-Busquets X (2014) Antimalarial drug delivery to the mosquito: an option worth exploring? Future Microbiol 9:579–582
60. Reed SG, Orr MT, Fox CB (2013) Key roles of adjuvants in modern vaccines. Nat Med 19:1597–1608
61. Vekemans J, Leach A, Cohen J (2009) Development of the RTSS/AS malaria candidate vaccine. Vaccine 27S:G67–G71
62. Mueller MS, Renard A, Boato F, Vogel D, Naegeli M, Zurbriggen R et al (2003) Induction of Parasite Growth-Inhibitory Antibodies by a Virosomal Formulation of a Peptidomimetic of Loop I from Domain III of Plasmodium falciparum Apical Membrane Antigen 1. Infect Immun 71:4749–4758
63. Draper SJ, Angov E, Horii T, Miller LH, Srinivasan P, Theisen M et al (2015) Recent advances in recombinant protein-based malaria vaccines. Vaccine 33:7433–7443 Elsevier Ltd.
64. Vaughan AM, Kappe SH (2012) Malaria vaccine development: persistent challenges. Curr Opin Immunol 24:324–331 Elsevier Ltd
65. Najer A, Wu D, Bieri A, Brand F, Palivan CG, Beck H-P et al (2014) Nanomimics of host cell membranes block invasion and expose invasive malaria parasites. ACS Nano 8:12560–12571
66. Najer A, Thamboo S, Duskey JT, Palivan CG, Beck H-P, Meier W (2015) Analysis of molecular parameters determining the antimalarial activity of polymer-based nanomimics. Macromol Rapid Commun 36:1923–1928. Lendlein A, Pandit A (eds)

Author Index

R. Adhikari and S. Thapa (eds.), *Infectious Diseases and Nanomedicine III*,
Advances in Experimental Medicine and Biology 1052, https://doi.org/10.1007/978-981-10-7572-8

Subject Index

R. Adhikari and S. Thapa (eds.), *Infectious Diseases and Nanomedicine III*,
Advances in Experimental Medicine and Biology 1052, https://doi.org/10.1007/978-981-10-7572-8